

https://dspace.org/

The fatty acid analysis of microalgae for biodiesel production

Maepa, Mpho

2018

https://hdl.handle.net/10539/26963

Maepa, Mpho (2018) The fatty acid analysis of microalgae foe biodiesel production, University of the Witwatersrand, Johannesburg, <http://hdl.handle.net/10539/26963>

Downloaded from a DSpace repository. https://dspace.org/



UNIVERSITY OF THE
WITWATERSRAND,
JOHANNESBURG

THE FATTY ACID ANALYSIS OF MICROALGAE FOR BIODIESEL PRODUCTION

Mpho Maepa

A dissertation submitted to the Faculty of Engineering and the Built Environment, University of the Witwatersrand, Johannesburg, in fulfillment of the requirements for the degree of Master of Science in Engineering.

Johannesburg, November 2018

DECLARATION

I declare that this dissertation is my own, unaided work. It is being submitted for the degree of Master of Science in Engineering at the University of the Witwatersrand, Johannesburg. It has not been submitted before for any other degree or examination at any other University.

_____ _____

Signature of candidate Date

ABSTRACT

Current biodiesel feedstocks are food crops, which are an added strain to the food market. However, algae are not a primary food source for humans, and can accumulate a high lipid yield. The suitability of *Acutodesmus obliquus* and *Chlamydomonas* CC125 as lipid feedstock was investigated by studying their fatty methyl ester content in the esterified oil (*i.e.* biodiesel) extracted from algae grown under different conditions of light and stirring regime. Algae cells were grown in pure CO_2 for 12 days, harvested and dried. Lipid extraction followed the Bligh and Dyer method, while fatty esters were derived via transesterification. A 5% phenyl polysilphenylene-siloxane GC column was used to identify the fatty esters. Their quantities were used to predict biodiesel quality from equations in literature. The condition with the light intensity of I = 80 μmol.m^{-2}.s^{-1} and an agitation speed of S = 100 rpm was the most suitable of all tested. Under this condition, *A. obliquus* was 0.17 g.L^{-1}.d^{-1} more productive in biomass than *Chlamydomonas*. Both algae yielded lipid extracts above 80% dwt., under all conditions. This confirms literature reports, that green microalgae are able to accumulate high amounts of storage lipids (*e.g.* triacylglycerides). Both algae species contained more methyl linolelaidate (C18:2) than any other fatty ester: 94.0% in *A. obliquus* and 66.6% in *Chlamydomonas*. For comparison, waste cooking oil fatty ester content contained 71.4% methyl linolelaidate. Algae fuel resembled a good cold-filter plugging point (*CFPP* = -17^{o}C). That is, it can be used in cold climates. *A. obliquus* produced the most suitable combustion quality (*CN* = 0.54) than *Chlamydomonas* (*CN* = 0.013). Therefore, it is the most suitable candidate than *Chlamydomonas*, for further improvements to the algae biodiesel process.

DEDICATION

To my late grandfather,

Ntate Ramailane,

and my beloved grandmother,

Ma'Ramailane

ACKNOWLEDGEMENTS

I would like to thank my supervisors, Professor Kevin Harding and Dr. Michelle Low, for the insightful advice, encouragement, constructive criticism, expertise and guidance they gave me during the course of this work.

Also, I wish to express my gratitude for the assistance I received from the School of Chemical and Metallurgical Engineering (and its workshop team) and the Industrial and Mining Water Research Unit (IMWaRU), Professor Vincent Gray of the School of Molecular and Cell Biology (MCB), Professor Stuart Sym of the School of Animal, Plant and Environmental Sciences (APES) and Dr. Pierre Durand of the Evolutionary Studies Institute (ESI). In addition, I thank the South African National Phycology Culture Collection (SANPCC) for the algae culture used.

I am indebted to the National Research Foundation (NRF) and TATA Africa Post-graduate Scholarship for giving me financial assistance for the entire period during which I was working on this dissertation.

Lastly, I appreciate my family for both encouragement and moral support during the course of this project.

CONFERENCE PRESENTATIONS

M Maepa, M Low and K G Harding, (2018) Fatty methyl esters in biodiesel: Comparison between two microalgae, *Bioresource Technology for Bioenergy, Bioproducts & Environmental Sustainability (BIORESTECH) 2nd International Conference, Sitges BCN Spain, 18 September 2018. (Abstract, Oral presentation*)

TABLE OF CONTENTS

DECLARATION ii
ABSTRACT iii
DEDICATION iv
ACKNOWLEDGEMENTS v
CONFERENCE PRESENTATIONS vi
LIST OF TABLES x
LIST OF FIGURES xi
NOMENCLATURE xiii

CHAPTER ONE - 1 -
1. INTRODUCTION - 2 -
1.1. Background and motivation - 2 -
1.2. Problem statement - 5 -
1.3. Aim and objectives - 5 -
1.4. Research questions - 6 -
1.5. Chapter overview - 7 -

CHAPTER TWO - 8 -
2. LITERATURE REVIEW - 9 -
2.1. Advantages of utilizing algae biomass - 9 -
2.2. Cultivation of algae: via photosynthesis - 11 -
2.2.1. Light intensity - 12 -
2.2.2. Stirring - 13 -
2.2.3. Carbon dioxide - 14 -
2.3. Algae lipids: synthesis and different types - 15 -
2.3.2. Type of algae lipids - 20 -
2.4. Extraction of lipids from algae biomass: using solvents - 23 -
2.4.1. Types of lipid extraction methods - 23 -
2.4.2. Solvents used in lipid extraction - 25 -
2.5. Biodiesel production: using transesterification - 25 -
2.6. Biodiesel properties: with focus on combustion and cold-flow - 29 -
2.6.1. Combustion quality: cetane number - 29 -
2.6.2. Cold-flow quality: viscosity and cold-filter plugging point - 33 -

CHAPTER THREE ..... - 35 -
3. MATERIALS AND METHODS ..... - 36 -
3.1. Reagents ..... - 36 -
3.2. Species selection ..... - 36 -
3.3. Stock culture maintenance ..... - 37 -
3.4. Cultivation conditions ..... - 37 -
3.4.1. Carbon dioxide ..... - 37 -
3.4.2. Light ..... - 38 -
3.4.3. Absorbance and dry biomass weight ..... - 39 -
3.4.4. Baseline experiment: Condition 0 ..... - 40 -
3.5. Monitoring ..... - 41 -
3.5.1. pH-monitoring ..... - 41 -
3.5.2. Dissolved oxygen ..... - 42 -
3.5.3. Nitrate testing ..... - 42 -
3.6. Lipid accumulation and extraction process ..... - 43 -
3.6.1. Accumulation: using $NaHCO_3$ ..... - 43 -
3.6.2. Lipid extraction: using Bligh and Dyer ..... - 43 -
3.6.3. Waste cooking oil ..... - 45 -
3.7. Methyl ester derivation: using transesterification ..... - 45 -
3.8. FAME identification: using GC-MS ..... - 47 -
3.9. FAME quantification: theoretical estimation of $\%FAME_i$ from GC-MS area proportions ..... - 48 -
3.9.1. Conversion of area values to FAME concentrations (in $mg.ml^{-1}$) ..... - 48 -
3.9.2. Conversion of FAME concentrations (in $mg.ml^{-1}$) to $\%FAME_i$ ..... - 49 -
3.10. Prediction of fuel properties: using $\%FAME_i$ values ..... - 49 -

CHAPTER FOUR ..... - 53 -
4.1. Cultivation conditions ..... - 54 -
4.1.1. Growth curves ..... - 54 -
4.1.3. Dissolved oxygen ..... - 61 -

CHAPTER FIVE ..... - 65 -
5. RESULTS AND DISCUSSION [ALGAE LIPID] ..... - 66 -
5.1. Lipid extract yield ..... - 66 -
5.2. Lipid productivities ..... - 69 -
5.3. FAME profile of esterified lipid ..... - 71 -

5.4. Selection of the most suitable cultivation condition based on: biomass and lipid production ..... - 75 -

5.5. Theoretical prediction of biodiesel properties: using *%FAME$_m$* values from Condition 4 (*I* = 80; *S* = 100) ..... - 76 -

5.5.1. FAME concentration: comparison between A. obliquus and Chlamydomonas ... - 77 -

5.5.2. FAME concentration: comparison between A. obliquus and waste cooking oil .. - 78 -

5.5.3. Biodiesel quality: comparison between A. obliquus and Chlamydomonas ..... - 78 -

5.5.4. Biodiesel quality: comparison between A. obliquus and waste cooking oil ..... - 80 -

5.5.5. A. obliquus in relation to reported values ..... - 81 -

CHAPTER SIX ..... - 86 -

6.1. Conclusions ..... - 87 -

6.2. Recommendations ..... - 89 -

REFERENCES ..... - 91 -

APPENDICES ..... - 104 -

APPENDIX A: Algae cultivation ..... - 104 -

A.1. Beijerinck medium recipe ..... - 104 -

A.2. Calibration curves ..... - 105 -

APPENDIX B: GC-MS compound tables and chromatograms ..... - 106 -

B.1. Condition 0 (I = 35; S = 150) ..... - 106 -

B.2. Condition 1 (I = 60; S = 250) ..... - 107 -

B.3. Condition 2 (I = 60; S = 100) ..... - 111 -

B.4. Condition 3 (I = 80; S = 250) ..... - 113 -

B.5. Condition 4 (I = 80; S = 100) ..... - 115 -

APPENDIX C: Calculations ..... - 119 -

C.1. Effects of cultivation on algae lipid yield ..... - 119 -

C.2. Cetane number and viscosity of biodiesel ..... - 121 -

C.3. Carbon mass analysis ..... - 122 -

LIST OF TABLES

Table 1: Growth conditions and productivity of microalgae ..... - 16 -
Table 2: FAME profile of lipid from various microalgae feedstock ..... - 22 -
Table 3: Utilization of organic solvents and assisted-extraction in lipid recovery..... - 26 -
Table 4: Various feedstock in biodiesel production: Edible and non-edible..... - 30 -
Table 5: Set of experiments conducted in this study ..... - 41 -
Table 6: GC-MS program modified from Mandotra *et al*. (2016) ..... - 47 -
Table 7: FAME concentrations from Botineştean *et al*. (2012)..... - 48 -
Table 8: FAME profile of all cultivation conditions (0, 1, 2, 3 & 4) ..... - 74 -
Table 9: Biodiesel quality from microalgae and waste cooking oil under Condition 4 (I = 80; S = 100)…..... - 80 -
Table B1: Complete list of compounds identified in *A. obliquus* (Condition 0) ..... - 106 -
Table B2: Complete list of compounds identified in *Chlamydomonas* (Condition 0) .. - 107 -
Table B3: Complete list of compounds identified in (Condition 1)..... - 108 -
Table B4: Complete list of compounds identified in *Chlamydomonas* (Condition 1) .. - 110 -
Table B5: Complete list of compounds identified in *A. obliquus* (Condition 2) ..... - 111 -
Table B6: Complete list of compounds identified in *Chlamydomonas* (Condition 2) .. - 112 -
Table B7: Complete list of compounds identified in *A. obliquus* (Condition 3) ..... - 113 -
Table B8: Complete list of compounds identified in *Chlamydomonas* (Condition 3) .. - 114 -
Table B9: Complete list of compounds identified in *A. obliquus (*Condition 4) ..... - 115 -
Table B10: Complete list of compounds identified in *Chlamydomonas* (Condition 4) - 116 -
Table B11: Complete list of compounds identified in waste cookin oil..... - 117 -
Table C1: Total sum values for calculation of the effect of algae cultivation on lipid yield. ..... - 120 -
Table C2: Cetane number and viscosity values of individual FAME molecules identified..... .- 121 -

LIST OF FIGURES

Figure 1. Simplified diagram of photosynthesis (Reece, *et al.*, 2009) ..... - 15 -
Figure 2. Simplified diagram of the Kennedy pathway (Lenka, *et al*., 2016) ..... - 20 -
Figure 3. Transesterification reaction (Mutanda, *et al*., 2011)..... - 28 -
Figure 4. Batch cultivation set-up (Replicate 1 = *x*, Replicate 2 = *y* & Replicate 3 = *z*) . - 38 -
Figure 5. Dry weight of *A. obliquus* and *Chlamydomonas* under Condition 0 (*I*: 35; *S*: 150). Error bars represent *SD*. ..... - 54 -
Figure 6. Dry weight of *A. obliquus* under two different light intensities and agitation of *S* = 250 rpm (Condition 1 & 3). Error bars represent *SD*..... - 55 -
Figure 7. Dry weight of *Chlamydomonas* under two different light intensities and agitation of *S* = 250 rpm (Condition 1 & 3). Error bars represent *SD*. ..... - 55 -
Figure 8. Dry weight of *A. obliquus* and *Chlamydomonas* under two different light intensities and agitation of *S* = 100 rpm (Condition 2 & 4). Error bars represent *SD*... - 56 -
Figure 9. Maximum growth rate of *A. obliquus* and *Chlamydomonas* under different conditions (0, 1, 2, 3 & 4)..... - 58 -
Figure 10. Maximum biomass productivity of *A. obliquus* and *Chlamydomonas* under different conditions (0, 1, 2, 3 & 4) ..... - 60 -
Figure 11. Maximum rate of O_2 production of *A. obliquus* and *Chlamydomonas* under different conditions (0, 1, 2, 3 & 4) (RO_2 = 0 is ideal)..... - 64 -
Figure 12. Percentage lipid extracts of *A. obliquus* and *Chlamydomonas* under different conditions (0, 1, 2, 3 & 4). Error bars represent *SD*. ..... - 66 -
Figure 13. Maximum lipid productivities of *A. obliquus* and *Chlamydomonas* under different conditions (0, 1, 2, 3 & 4) ..... - 70 -
Figure 14. *%FAME* composition of microalgae and waste cooking oil under Condition 4 (*I* = 80; *S* = 100). The most common area value amongst a triplicate set (*n* = 3) was used to determine *%FAME* (Section *3.9.1.*)..... - 79 -
Figure 15. Summary of the carbon flow through the processes involved in studying *A. obliquus* FAMEs under Condition 4 (*I* = 80; *S* = 100)..... - 85 -
Figure A1. Calibration curve of absorbance (λ = 680 nm) and *AD* dry weight..... - 105 -
Figure A2. Calibration curve of absorbance (λ = 680 nm) and *CR* dry weight..... - 105 -

Figure B1. Chromatogram (Abundance vs Retention time) of *A. obliquus* under Condition 1 ..... - 107 -
Figure B2. Chromatogram (Abundance vs Retention time) of *Chlamydomonas* under Condition 1 ..... - 110 -
Figure B3. Chromatogram (Abundance vs Retention time) of *A. obliquus* under Condition 2 ..... - 111 -
Figure B4. Chromatogram (Abundance vs Retention time) of *Chlamydomonas* under Condition 2 ..... - 112 -
Figure B5. Chromatogram (Abundance vs Retention time) of *A. obliquus* under Condition 3 ..... - 113 -
Figure B6. Chromatogram (Abundance vs Retention time) of *Chlamydomonas* under Condition 3 ..... - 114 -
Figure B7. Chromatogram (Abundance vs Retention time) of *A. obliquus* under Condition 4 ..... - 115 -
Figure B8. Chromatogram (Abundance vs Retention time) of *Chlamydomonas* under Condition 4 ..... - 116 -
Figure B9. Chromatogram (Abundance vs Retention time) of waste cooking oil – which underwent the same transesterification procedure as algae oil (Section *3.6.3.*) ..... - 117 -

NOMENCLATURE

Greek symbols

μ	growth rate (s^{-1})
λ	wavelength (nm)

Variables

F	carbon dioxide flow rate ($ml.min^{-1}$)
I	light intensity ($\mu mol.m^{-2}.s^{-1}$)
S	agitation speed during growth stage (rpm)
S_t	agitation speed during transesterification reaction (rpm)
T	temperature (^oC)

Abbreviations

ACP	acyl carrier protein
AD	*Acutodesmus obliquus*
ADP	adenosine diphosphate
ASP	Aquatic Species Program
ASTM	American Society for Testing and Materials International Standard
ASW	artificial seawater
ATP	adenosine triphosphate
BBM	Bold's Basal Medium
BF_3	boron trifluoride
BG11	blue-green medium
BP	biomass productivity
C16	16-carbon chain length
C18	18-carbon chain length
$C_6H_{12}O_6$	glucose
CaO	calcium oxide
CFPP	cold-filter plugging point
CH_3ONa	sodium methoxide
CN	cetane number
CoA	coenzyme A
CO	carbon monoxide
Conc.	concentration
CO_2	carbon dioxide
CR	*Chlamydomonas* CC125
db	double bond
DCN	dichloromethane
dH_2O	distilled water
DMSO	dimethyl sulfoxide
DO	dissolved oxygen
DU	degree of unsaturation
DUFAs	di-unsaturated fatty acids
DW	dry biomass weight
e^-	electron

EI	ionization energy
EN	Européen de Normalisation
ESI	Evolutionary Studies Institute
ETC	electron transport chain
EtOH	ethanol
exp.	experiment
FAAEs	fatty acid acyl esters
FAs	fatty acids
FAME	proportion of fatty acid methyl ester
FAMEs	fatty acid methyl esters
%FAME	percentage of fatty acid methyl ester
FAS	fatty acid synthetase
FFAs	free fatty acids
G3P	glyceraldehyde 3-phosphate
GC-MS	gas chromatography mass spectrophotometry
GHGs	greenhouse gases
H^+	proton
H_2O	water
hv	sunlight
IN	iodine number
KOH	potassium hydroxide
LC	proportion of lipid content
%LC	percentage of lipid content
LCSF	long-chain saturated factor
LP	lipid productivity
MeOH	methanol
MFC	mass flow controller
min	minute
MUFAs	mono-unsaturated fatty acids
NaCl	sodium chloride
$NADPH/NADP^+$	nicotinamide adenine dinucleotide phosphate
$NaHCO_3$	sodium carbonate
NaOH	sodium hydroxide
N-limitation	nitrate limitation
NO_3^-	nitrate
NOAA	National Oceanic and Atmospheric Administration
N_{PUFA}	number of poly-unsaturated fatty acids produced
NTNU	Norwegian University of Science and Technology
O_2	oxygen
P_i	inorganic phosphate
PS1	photosystem 1
PS2	photosystem 2
PO_4^{3-}	phosphate
PTA	phosphotungstic acid
PUFAs	poly-unsaturated fatty acids
RO_2	rate of oxygen production
rpm	revolution per minute

SCO_2	supercritical carbon dioxide
SD	standard deviation
sER	smooth endoplasmic reticulum
SFAs	saturated fatty acids
SO_x	sulfates
SQDG	sulfoquinovosyldiacylglycerol
SV	saponification value (or acid value)
SWES	Soil, Water and Environmental Science (The University of Arizona)
TAGs	triacylglycerides
UFAs	unsaturated fatty acids
UHP	ultra-high purity
V	viscosity
WCO	waste cooking oil

CHAPTER ONE

1. INTRODUCTION

1.1. Background and motivation

It is estimated that most fossil fuel reserves, including oil, are to be depleted by 2050 (Ho, *et al*., 2013; Maity, *et al*., 2014; Mandotra, *et al*., 2016). This is a major problem in particular for the transportation sector because it is the largest consumer of crude oil (ExxonMobil, 2017). The majority of the world's transport systems run on liquid fuels, which are difficult to replace (Shay, 1993). Therefore renewable, carbon neutral and economically viable sources of fuel energy are being investigated and this is one of the most pressing challenges of today (Mata, Martins, & Caetano, 2010).

The "Outlook for Energy" reference scenario predicted that biofuels (including bioethanol and biodiesel) will supply 4.3% of road fuels by 2020, with a potential of up to 7% under an alternative policy scenario (ExxonMobil, 2017). These are seen as replacements for petrol and diesel respectively (Antizar-Ladislao & Turrion-Gomez, 2008).

Biodiesel is a mixture of fatty acid methyl esters (FAMEs) produced by the transesterification of oils or fats. Transesterification of oil to biodiesel decreases viscosity and generally improves fuel properties (Bamgboye & Hansen, 2008). Biodiesel has become increasingly attractive because it is biodegradable, non-toxic and can be used in most diesel engines without the need for modification. It results in lower emissions of carbon dioxide (CO_2), CO, SO_x, hydrocarbons and particulate matter than petroleum diesel, although emissions of NO_x can be higher (Shay, 1993; Meher, *et al*., 2006; Tong, *et al*., 2010).

The total carbon dioxide emission from the use of pure biodiesel is 78.45% lower than that of petroleum diesel (Sheehan, *et al*., 1998; Harding, *et al*., 2008; Nascimento, *et al*., 2013).

Biodiesel is currently being produced from oil seeds such as soybean, sunflower, rapeseed and palm oil (Miao & Wu, 2006). These first generation sources are edible and their increased demand will affect their price in the food market and compete directly in the agricultural system with food crops for land and water (Scott, *et al*., 2010). This additional burden on the food market is the main limitation to widespread commercialization of first generation biodiesel. Moreover, deforestation of natural habitats to increase the availability of arable land to supply biodiesel demands also occurs (Ma & Hanna, 1999).

Despite the aforementioned issues, biodiesel continues to be used and promoted around the world. It is seen as a way to create employment opportunities in rural areas and increase the supply of energy (Mata, Martins, & Caetano, 2010). Non-edible sources of biodiesel oil (second generation) such as microalgae feedstock and waste cooking oil (WCO) have been receiving much attention over the years (Sheehan, 1998; Pulz & Gross, 2004; Christi, 2007; Scott, *et al*., 2010; Piker, *et al*., 2016). The use of these cheaper suitable lipid feedstock can reduce the final price of biodiesel (Francisco, *et al*., 2010).

Biodiesel components (*i.e.* FAMEs) tend to crystallize in cold climates. This causes clogged fuel lines and loss of engine power (Sinha & Murugavelh, 2010), as experienced by Scandinavian vehicle owners (NTNU, 2015). Poor quality biodiesel becomes uneconomical and combustion and cold-flow properties of the lipid feedstock should be investigated to avoid precipitation in vehicle engines. These properties are standardized.

The most widely used biodiesel standards are the American Society for Testing and Materials (ASTM) (ASTM D 6751) and European Union standards (EN 14214) (Ramos, *et al*., 2009; Francisco, *et al*., 2010).

Extracted algae lipids are a promising source of biodiesel feedstock. A compelling reason to use algae is because they are not a primary food source for humans. They can be grown on arid and excessively saline land, thereby not competing for agricultural land (Mata, Martins, & Caetano, 2010). Additionally, algae can be grown in waste- and brackish water, since they are found in a wide range of habitats: including salt and freshwater, as well as unusual and extreme environments such as the Arctic Ocean, desert and snow (Barsanti & Gualtieri, 2006).

As a consequence of their diversity, algae continue to be investigated for various applications. Certain oleaginous species such as chlorophytes, haptophytes, and diatoms (Mutanda, *et al*., 2011), have been reported to accumulate high lipid yields in the absence of some essential nutrients, *e.g.* nitrogen and silicon (Sheehan, *et al*., 2008). Algae have been investigated as a source of energy in many different contexts, from direct combustion to hydrogen production (Miao, *et al*., 2004). They are even said to be able to remediate contaminated water (Cai, Park, & Li, 2013). Wastewaters can provide nutrients necessary to accumulate algae biomass (Wu, *et al*., 2012; Maity, *et al*., 2014), and this can potentially reduce high costs associated with large-scale cultivation (Ullah, *et al*., 2014).

Algae are photoautotrophs and are able to use the prevailing CO_2 as a source of carbon during growth. As a consequence of their lack of roots, leaves, vascular systems and

sexual organs; they are capable of doing this faster and more efficiently than higher plants (Ullah, *et al*., 2014). This is advantageous since regulations such as the Copenhagen Accord of 2009 (Rogelj, *et al*., 2010) and Paris Agreement of 2015 demand that countries reduce their fossil fuel consumption and greenhouse gas (GHG) emissions to mitigate climate change, in particular those countries that have CO_2 levels above 350 ppm (NOAA, 2016).

1.2. Problem statement

First generation biofuel sources are edible and require large areas of arable land. This causes direct food competition and price hikes. Algae have been proposed as promising replacement candidates as they are non-edible, grow almost anywhere and accumulate higher lipid yields than other energy crops under conditions of stress (Griffiths, van Hille, & Harrison, 2012).

1.3. Aim and objectives

The purpose of this work was to study and understand the suitability of two freshwater Chlorophyte algae species as biodiesel feedstock. Therefore their growth robustness, lipid content and productivity under various light and agitation conditions were investigated. Additionally, their FAME content was used to predict fuel properties, which are a representation of biodiesel quality.

The specific objectives of this research were to:

1) Determine the amount of lipid content (%*LC*) accumulated from different cultivation conditions of microalgae;
2) Investigate the synergistic effect of light intensity (*I*) and agitation speed (*S*) on the lipid content of $NaHCO_3$-fed batch cultures of microalgae;
3) Determine the FAME composition of the lipid content (%*LC*) through a GC-MS profile;
4) Theoretically predict the following biodiesel properties: cetane number (*CN*), saponification value (*SV*), iodine number (*IN*), viscosity (*V*) and cold-filter plugging point (*CFPP*) to determine the character of the biodiesel in relation to common standards (ASTM D-6751 and the European Standard - EN14214).

1.4. Research questions

This study sought to answer the following questions:

1) Which algae species (*Acutodesmus obliquus* or *Chlamydomonas* CC125) is more productive in biomass and lipids? Under which condition?
2) How much lipid can be extracted from $NaHCO_3$-fed algae?
3) What is the synergistic effect of light and agitation on lipid content (%*LC*)?
4) What type of fatty acid methyl esters (FAMEs) are present in the extract?
5) How do these compare with those present in waste cooking oil (WCO)?
6) What quality of biodiesel can be expected from these FAMEs?

1.5. Chapter overview

This section briefly indicates content in the chapters for this dissertation.

CHAPTER 1: A background of the research study and the motivation behind it. The problem, main aim and research questions are introduced.

CHAPTER 2: A review of the importance of light, stirring, CO_2, *N*-limitation, and an alkaline-pH in algae cultivation and lipid production. Solvent extraction, esterification and biodiesel properties are further reviewed.

CHAPTER 3: A detailed outline of the approaches used in algae cultivation, lipid production and extraction, esterification, FAME analysis and the prediction of biodiesel quality.

CHAPTER 4: A statement and discussion of outcomes of algae cultivation, lipid extraction, esterification, FAME analysis and the prediction of biodiesel quality. The most suitable cultivation condition and algae species are selected. Algae FAMEs are compared with FAMEs present in WCO feedstock.

CHAPTER 5: A summary of each objective and brief recommendations for further research.

CHAPTER TWO

2. LITERATURE REVIEW

This chapter reviews aspects of: algae cultivation, lipid production, solvent extraction, and FAME components of biodiesel.

2.1. Advantages of utilizing algae biomass

Microalgae can be unicellular or colonial, and usually not more than 2000 μm in diameter (Griffiths, *et al*., 2011). These species lack roots, leaves, vascular systems, and sexual organs; and therefore have the potential to grow faster than higher plants (Ullah, *et al*., 2014). The main types of algae grown are known to be *Spirulina* (half of worldwide algae production), *Chorella*, *Dunaliella* and *Haematococcus*. These are chlorophytes (*i.e.* green algae). Green algae, together with diatoms (*Bacillariophyta*) are the most studied algae on lab- or pilot-scale for the purpose of application in biodiesel production (Liu, Wang, & Zhou, 2008; Damiani, *et al*., 2010; Fakhry & El Maghraby, 2013).

Microalgae can grow in non-terrestrial ecosystems and do not necessarily require large areas of land (Mata, Martins, & Caetano, 2010). Some species colonize the Earth's poles and others cause blooms in the tropics (Mutanda, *et al*., 2011). Algae inhabit the most divergent environments, and because of this, are a favorable candidate to investigate as biodiesel feedstock. It is estimated that there are 30,000 species that have been studied (Richmond, 2004; Mata, Martins, & Caetano, 2010), with more than 10,000 species available as feedstock for the accumulation of lipid used for biodiesel production (Mutanda, *et al*., 2011).

Algae biomass as a source of transportation fuel has long been recognized, and research in this field has been carried out since the 1950s (Spolaore, *et al*., 2006). The first large-scale culture of microalgae started in Japan, in the early 1960s, with the cultivation of *Chlorella* (Spoloare, *et al*., 2006).

Publicly-funded research programs were also established in the USA and Australia during the first lipid crisis in the 1970s (Regan & Gartside, 1983; Sheehan, *et al*., 1998). The Aquatic Species Program (ASP) had an investment of more than US$ 25 million from the US Department of Energy from 1978 until 1996 to develop the production of biodiesel from high-lipid producing species grown in open ponds, while using CO_2 from coal-fired power plants (Sheehan, *et al*., 1998). A total of about 3000 species was screened for lipid content ($\%LC$).

A key factor for choosing microalgae as a lipid feedstock for purposes of producing biodiesel remains to be their minimal nutritional requirements (Leite, *et al*., 2013), although results from the ASP highlighted the high cost associated with producing algae biomass. Algae can remove PO_4^{-3} and NO_3^- as nutrients from various wastewater streams (Wu, *et al*., 2012; Maity, *et al*., 2014) and accumulate increased lipid yields as a result of nutrient starvation. Sometimes referred to as "microfactories", microalgae can accumulate lipid quantities of 60% of their dry weight and contain up to 30 times more fuel than equivalent amounts of other sources (Ullah, *et al*., 2014).

2.2. Cultivation of algae: via photosynthesis

Lipids that are fed into the biodiesel process can be extracted from dry biomass weight (*DW*) of algae. Biomass accumulation occurs as a result of cell maturation and division. Microalgae grow heterotrophically, where they are able to utilize organic carbon as the energy source; or mixotrophically, where they are able to utilize both light and organic carbon as energy sources (Kiran, Kumar, & Deshmukh, 2014). For instance, *Chlamydomonas* sp. can also grow on acetate (Tris-Acetate-Phosphate), although organic carbon sources may also promote the growth of contaminating bacteria (Yang, *et al*., 2015).

However most microalgae utilize light as the energy source and CO_2 as the carbon source. These species are photoautotrophs and propagate via the process of photosynthesis (Figure 1). *Acutodesmus obliquus* (investigated in this study) is a photoautotroph. In photosynthesis, H_2O is also required to produce glucose and O_2 (Eq. 1). Algae biomass production can be decreased by a lack of essential nutrients (*e.g*. NO_3^- and PO_4^{3-}), extreme pH, and high salinity (for freshwater species) (Solovchenko, *et al*., 2014). Predation and competition for nutrients with other algae, spores of which can be present in the air, also decrease growth.

$$6CO_2 + 6H_2O + h\nu\ (\text{catalyst}) \rightarrow C_6H_{12}O_6 + 6O_6 \qquad (1)$$

Experiments such as those conducted by Popovich *et al*. (2012) highlight the influence of abiotic factors. Popovich *et al*. (2012) exposed *Neochloris oleoabundans*, a high lipid content algae, to a light intensity of 168 $\mu mol.m^{-2}.s^{-1}$ for 16 hours daily and 1 % CO_2 to obtain an

estimated biomass productivity (*BP*) of 1.08 $g.L^{-1}.d^{-1}$. On the other hand, Nascimento *et al*. (2013) grew *Chlamydomonas* sp. under a light intensity of 140 $\mu mol.m^2.s^{-1}$ for 12 hours daily and 2% CO_2, resulting in a productivity of 0.24 $g.L^{-1}.d^{-1}$. The influence of light intensity (*I*), stirring (*S*), and CO_2 on algae growth is reviewed in the following subsections.

2.2.1. Light intensity

Light intensity strongly influences the growth and cell composition (*e.g.* FAME) of microalgae (Hu, *et al*., 2008; Ho, *et al*., 2012). Light penetrates only a few centimeters into dense cultures as algae biomass begins to shade other cells from receiving sufficient light energy (Richmond, 2004). It is important to agitate the algae culture to ensure exposure of individual cells to sufficient light (Sáncheza, *et al*., 2013). The level of light intensity can either limit, saturate or inhibit algae growth (Ho, *et al*., 2012).

A high light intensity can result in reduced growth because of light inhibition (Wahidin, Idris, & Shaleh, 2013). Before the stage of light inhibition, an increase in the light intensity increases growth (Barsanti & Gualtieri, 2006). Nascimento *et al*. (2013) studied the growth rate of *Chlamydomonas* sp. (Table 1) and *Desmodesmus brasiliensis* to be 0.3- and 0.28 d^{-1} under a light intensity of 140 $\mu mol.m^{-2}.s^{-1}$. In the study by Liu *et al*. (2012), they increased the light intensity five-fold and found that the productivity of *Scenedesmus* sp. increased from 0.26 to 0.45 $g.L^{-1}.d^{-1}$ (Ho, *et al*., 2014).

Solovchenko *et al*. (2014) showed that *Nannochloropsis oceania* grown under a high light intensity of 700 $\mu mol.m^{-2}.s^{-1}$ (higher than midday sunlight) reached a productivity of 0.82 $g.L^{-1}.d^{-1}$. This is higher than most algae species (shown in Table 1) grown under lower

light intensities. Ho *et al*. (2012) found a three-fold increase in the productivity of *Scenedesmus obliquus* after a seven-fold increase in light intensity.

Higher productivity has been reported under continuous illumination rather than a light-dark cycle. Krzeminska *et al*. (2014) reported a productivity of 0.12 $g.L^{-1}.d^{-1}$ for *Botryococcus braunii*, while Aslanbay *et al*. (2016) found *Haematococcus pluvialis* to have a productivity of 0.08 $g.L^{-1}.d^{-1}$ (Table 1). Both green algae species were grown in the presence of ambient air (0.04% CO_2) and a light intensity range of between 60-65 $\mu mol.m^{-2}.s^{-1}$.

2.2.2. Stirring

Mixing is important to expose the algae cells to sufficient light and prevent the settling of biomass. The exposure of light and transfer of CO_2 throughout the algae culture can be enhanced through stirring (Karemore, *et al*., 2015). Nascimento *et al*. (2013) used an agitation speed of 90 rpm to mix the culture of *Chlamydomonas* sp., whereas Xia *et al*. (2015) used 150 rpm for the culture of *Desmodesmus* sp. NMX451. Furthermore, microalgae (*e.g. Platychrysis* sp.) adhere to the surface of the reactor and increased stirring can prevent this (Christi, 2007). Gas sparging as a mechanism of mixing is preferred over mechanical mixing to avoid the premature rapture of algae cells (Christi, 2007). Popovich *et al*. (2012) used continuous air sparging with a flow between 500-700 $ml.min^{-1}$.

2.2.3. Carbon dioxide

Microalgae can reach a higher photosynthetic efficiency provided that both CO_2 and light are non-limiting (Ullah, *et al*., 2014). Algae can grow 20–30 times faster than food crops (Ullah, *et al*., 2014) under such conditions, as light also influences the rate of CO_2 fixation (Ho, *et al*., 2012). CO_2 requires that it be dissolved in water (Eq. 1) in order for efficient absorption by the algae cells (Griffiths, *et al*., 2011). Additional CO_2 should be provided to achieve a high dry biomass weight (Wang, *et al*., 2008). The CO_2 available in ambient air (0.04% CO_2) is not sufficient for producing a highly dense algae biomass (Pulz, 2001).

Most commonly studied algae (mentioned under Section 2.1.) cannot thrive under highly concentrated CO_2 environments. *Scenedesmus* sp. was shown to be able to grow under 80% CO_2, but the maximum dry biomass weight was observed when the CO_2 concentration was 10-20% (Hanagata, *et al*., 1992). A *Chlorella* sp. T-1 strain was found to be capable of growth under pure CO_2, but the highest growth rate was observed under 10% CO_2 concentration (Maeda, *et al*., 1995). In other instances, *Chlamydomonas* sp., *N. oceania* and *S. obliquus* have been grown in 2% CO_2 and reached productivities of 0.24-, 0.82- and 0.16 $g.L^{-1}.d^{-1}$ respectively.

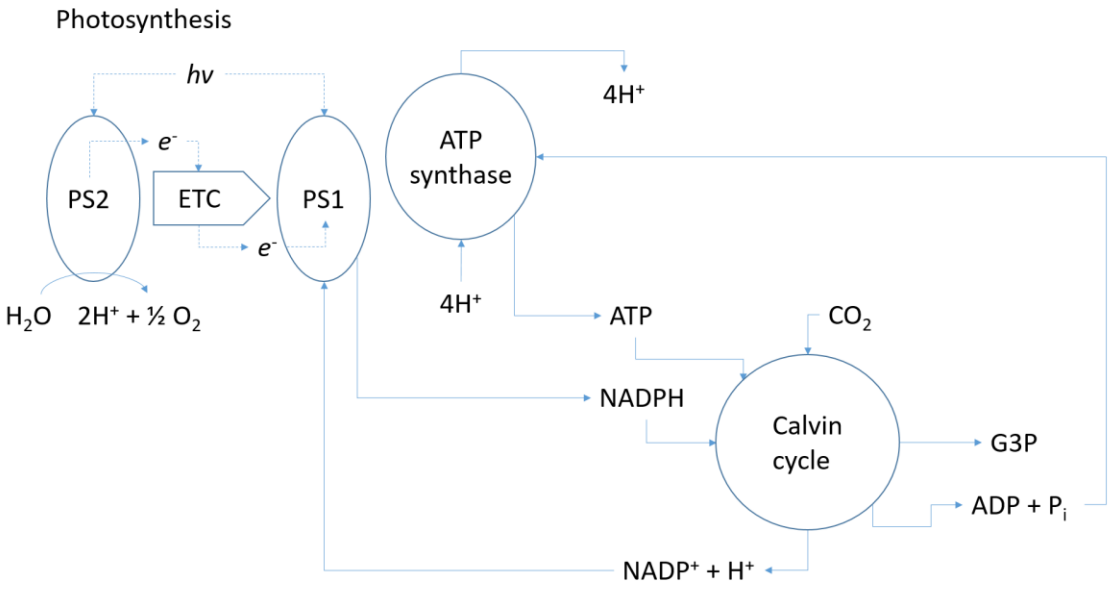


Figure 1. Simplified diagram of photosynthesis (Reece, *et al.*, 2009)

2.3. Algae lipids: synthesis and different types

Algae naturally produce lipids as part of the cell structure (*e.g.* phospho- and glycolipids) and as a dense form of carbon and energy storage (Tsukahara & Sawayama, 2005). Lipid biosynthesis in microalgae has been demonstrated to occur under conditions of stress. Commonly used stress conditions include nitrogen limitation (*N*-limitation) and alkaline pH. Silicon starvation has been used in the case of diatoms (Popovich, *et al.*, 2011). Lipid content can increase to between 60-80% dwt., mostly storage lipids in the form of triacylglycerides (TAGs) (Becker, 1994; Peña, 2007).

Table 1: Growth conditions and productivity of selected microalgae

Strain	Medium	Illumination ($\mu mol.m^{-2}.s^{-1}$)	CO_2/Air (%)	Biomass productivity ($g.L^{-1}.d^{-1}$)	Reference
I. galbana	f/2	36.3	Air	0.03	(Lee, *et al*., 2011)
N. oleoabundans UTEX 1185	SWES (control condition)	168	1% CO_2	1.08	(Popovich, *et al*., 2012)
Chlamydomonas sp.	LC Oligo	140	2% CO_2	0.24	(Nascimento, *et al*., 2013)
C. Vulgaris (CCAP 211/79) (high-density)	3N-BBM+V	250 (red light)	Air	0.12	(Mohsenpour & Willoughby, 2013)
N. oceanica CCALA 804	ASW (zero-saline, N-replete)	700	2% CO_2	0.82	(Solovchenko, *et al*., 2014)
B. braunii SAG 30.81	Kessler's	60	Air	0.12	(Krzeminska, *et al*., 2014)
S. obliquus	BG11	100	2% CO_2	0.16	(Wu, Xu, & Hu, 2015)
Desmodesmus sp. NMX451 [outdoor experiments]	BG11 (N-deplete)	184	Air	0.03	(Xia, *et al*., 2015)
H. pluvialis Flotow EGE MACC-32	BG11	65	Air	0.08	(Aslanbay, Demirel, & Imamoglu, 2016)
Desmodesmus sp.	Beijerinck Medium	81	100% CO_2	0.26	(Kativu, *et al*., 2012)

Griffiths and Harrison (2009) reviewed the lipid parameters of 55 species and reported that *S. obliquus* and *Chlamydomonas applanata* increased their dry weight lipid content (*%LC*) almost two-fold under nitrogen deficient conditions. Algae allocate their carbon molecules to energy-rich lipids (*i.e.* TAGs) under stress (Athensaedt & Daum, 2006).

Alkaline pH conditions have been shown to increase the content of storage lipids in some microalgae (Mandotra, *et al*., 2016). These conditions decrease the growth rate (Gardner, *et al*., 2011; Breuer, *et al*., 2013). Xia *et al*. (2015) showed that the addition of 25 g of $NaHCO_3$ to nutrient medium of 0.3 g $NaNO_3$ resulted in a little over 50% dwt. of lipid after 15 days of *Desmodesmus* sp. NMX451 cultivation. A similar approach is adopted in this work (Section *3.6.1*).

2.3.1. Fatty acid biosynthesis

Microalgae contain fatty acids (FAs) ranging from C8 to C28, often with C16 and C18 unsaturates. Some species contain significant amounts of polyunsaturated fatty acids (PUFAs) (Stansell, Sym, & Gray, 2012). TAGs are produced through a sequential transfer of acyl groups from acyl-CoA to different positions of the glycerol-3-phosphate backbone, by acyltransferases (Li-Beisson. *et al*., 2013). This is the Kennedy pathway (Figure 2). It is the primary pathway for TAG synthesis in microalgae (Lenka, *et al*., 2016).

It is generally accepted that FAs are synthesized from an acyl-CoA-derived compound, acetyl-CoA (Griffiths, *et al*., 2011). The flux of FA biosynthesis is controlled by photosynthetic efficiency because the carbon precursor (acetyl-CoA), energy (ATP), and

reducing power (NADH and NADPH) are provided by light and dark reactions of photosynthesis (Jaworski & Cahoon, 2003).

The priming step of FA biosynthesis involves the transfer of the acetyl group of acetyl-CoA to an acyl carrier protein (ACP) of the fatty acid synthetase (FAS). This is catalyzed by the multifunctional acetyl-CoA carboxylase (ACCase) (Cronan & Waldrop, 2002), and occurs in the cytosol where FAS is located (Campbell & Farrell, 2012). The conversion of acetyl-CoA to malonyl-CoA is the first committed step in lipid biosynthesis (Figure 2) (Livne & Sukenik, 1992).

In a reaction that produces an acetyl-synthetase and an ACP-thiol compound, the acetyl group is transferred to a β-ketoacyl-ACP synthetase. The ACP-thiol compound reacts with malonyl-CoA (Hu, *et al*., 2008), in a reaction that is catalyzed by an ACP-malonyltransferase and produces malonyl-ACP and coenzyme A (CoA). In a condensation reaction catalyzed by a β-ketoacyl-ACP synthetase, the malonyl-ACP reacts with the acetyl-synthetase to produce an acetoacetyl-ACP and CO_2^- (Jaworski & Cahoon, 2003).

Thereafter, NADPH reduces acetoacetyl-ACP to β-hydroxybutyryl-ACP, with $NADP^+$ being generated, and β-hydroxybutyryl proceeds to undergo dehydration to produce a crotonyl-ACP which NADPH further reduces to butyryl-ACP (Campbell & Farrell, 2012). As acetyl-ACP in the first round, butyryl-ACP plays the same role in the second round of FA biosynthesis (Campbell & Farrell, 2012).

In the condensation reaction of the second round, a β-ketoacyl-ACP is produced, and as before, all the other reactions proceed to produce hexanoyl-ACP. This series of reactions is repeated to elongate the FA chain and produce C16- or C18-ACP. FA elongation and desaturation are covered in detail by Bellou *et al*. (2014).

Elongation of the FA chain terminates due to the action of two enzymes: acyl-ACP thioesterase (hydrolyzes acyl-ACP to release the free FAs) and chloroplast acyltransferase (removes the acyl group from ACP and the FA is transferred from ACP to glycerol-3-phosphate (G3P)) (Lenka, *et al*., 2016). The FAs synthesized on the chloroplast envelopes are excreted into the cytosol via the binding of CoA (Joyard, *et al*., 2010), and are reactivated to acyl-CoA to form TAGs (Figure 2) (Ohlrogge & Browse, 1995; Jaworski & Cahoon, 2013). The fatty acid chain length and degree of unsaturation (*DU*) affect properties such as the viscosity (*V*), cold-flow plug point (*CFPP*), iodine number (*IN*) and cetane number (*CN*) of the fuel (Ramos, *et al*., 2009). Hence TAG content and an appropriate FA profile are important for biodiesel production.

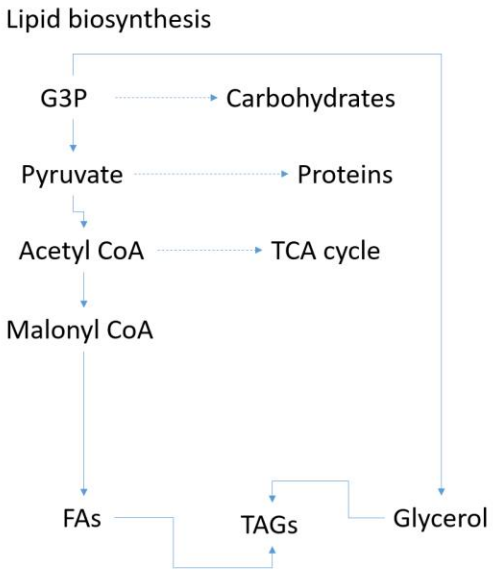


Figure 2. Simplified diagram of the Kennedy pathway (Lenka, *et al.*, 2016)

2.3.2. Type of algae lipids

In some microalgae (*e.g. Synechocystis* sp.), FAs bind to an ACP instead. As mentioned under Section 2.3., C16- or C18-ACP thioesterase catalyzes the hydrolysis of C16- or C18-ACP to palmitate or oleate and ACP before elongation and differentiation to form longer chain FAs, unsaturated FAs (UFAs), TAGs, glycolipids, and phospholipids, using other enzyme systems located in the cytosol, smooth endoplasmic reticulum (sER), and mitochondrion (Kunst & Samuels, 2009; Joyard, *et al.*, 2010). TAGs are preferable for biodiesel as they lack sulfur and phosphates (Athenstaedt & Daum, 2006; Sharma, Singh, & Upadhyay, 2008).

In addition to enhancing the lipid accumulation, stress conditions strongly influence the FA profile in many microalgae. Santos *et al*. (2012) demonstrated that alkaline pH stress also enhances lipid quality. Under a pH of 10, *N. oleoabundans* produced palmitic (C16:0), stearic (C18:0), oleic (C18:1), and linoleic acid (C18:2), all of which are suitable as biodiesel feedstock (Ho, *et al*., 2014). Siaut *et al*. (2011) showed that nitrogen depletion leads to increases in the proportions of saturated (SFAs) and mono-unsaturated (MUFAs) fatty acids, both of which are primary substrates for biodiesel production.

Algae lipid composition is species-specific. Palmitic and oleic acid are the most common fatty acids in nature. Together with linoleic acid, they are common among algae; followed by palmitoleic-, stearic-, C16:2 and C16:3 acid, as seen in Table 2. It is necessary to maintain a balance between combustion and cold-flow properties. Knothe (2005) and Shenk *et al*. (2008) suggest that the ideal mixture of FAs has to be C16:1, C18:1 and C14:0 in the ratio 5:4:1.

Yeo *et al*. (2011) demonstrated that *Chlamydomonas moewusii* tends to accumulate long-chain, polyunsaturated fats (PUFAs). Highly unsaturated fatty acids (*i.e.* PUFAs) are undesirable for biodiesel. Wu & Miao (2014) found that *S. obliquus* has an affinity for SFAs, MUFAs and di-unsaturated fats (DUFAs), as opposed to PUFAs. Hu *et al.* (2014) detected similar fatty acids in *Chlorella vulgaris* (but with C16:3 also present).

Table 2: FAME profile of lipid from various microalgae feedstock

FAME	***Chlamydomonas moewusii*** (Yeo, *et al*., 2011)	***Phaeodactylum tricornutum*** (Breuer, *et al*., 2013)	***Chlorella vulgaris*** (Hu, *et al*., 2014)	***Isochrysis galbana*** (Sample- 1) (O'Neil, *et al*., 2014)	***Scenedesms obliquus*** (Wu & Miao, 2014)
Saturated fatty acid (SFA)					
Methyl myristate (C14:0)	-	✓	✓	✓	✓
Methyl palmitate (C16:0)	✓	✓	✓	✓	✓
Methyl margarate (C17:0)	-	-	✓	-	✓
Methyl stearate (C18:0)	-	✓	✓	✓	✓
Mono-unsaturated fatty acid (MUFA)					
Methyl palmitoleate (C16:1)	-	✓	✓	✓	✓
Methyl oleate (C18:1)	✓	✓	✓	✓	✓
Polyunsaturated fatty acid (PUFA)					
(C16:2)	-	✓	✓	✓	✓
(C16:3)	✓	✓	✓	✓	
Methyl linoleate (C18:2)	✓	✓	✓	✓	✓
Methyl linolenate (C18:3)	✓	✓	-	✓	-
Methyl stearidonate (C18:4)	✓	-	-	✓	-

A high *DU* lowers viscosity and improves the ability of a fuel to flow in cold climates (*e.g.* Scandinavian weather), but this can decrease *CN* and thereby impart poor combustion properties in a fuel (Knothe, 2009). *CN* and other biodiesel properties that are dependent on the FA profile are reviewed in Section 2.6.

2.4. Extraction of lipids from algae biomass: using solvents

Stress conditions are required to accumulate a high content of storage lipids. Limiting the concentration of nitrogen (*N*-limitation) is the most preferred approach to initiate lipid accumulation. In most cases the lipids are extracted after the accumulation stage, although direct processing of wet algae biomass has also been demonstrated by Griffiths *et al*. (2010). Direct processing (also known as *in situ* transesterification) involves no extraction step. The two-step strategy remains the common approach (Taher, *et al*., 2014).

2.4.1. Types of lipid extraction methods

A study by Demirbas and Demirbas (2011) lists three options for the extraction of this lipid from algae biomass:

1. solvent extraction (used in this study),
2. pressing the biomass (pestle and mortar); or
3. supercritical fluid extraction.

Solvent extraction remains the most preferred method (Soares, et al., 2014), although supercritical fluid extraction using liquefied carbon dioxide produced from pressurizing the gas is reported to be the most efficient process (Islam, *et al*., 2015). Halim *et al*. (2011) used supercritical carbon dioxide (SCO_2) at higher pressures and lower temperatures to demonstrate an improved lipid extraction process. Issues of safety remain a concern for researchers adopting the supercritical extraction process because high-pressure conditions are used (Shirazi, Karimi-Sabet, & Ghotbi, 2017).

In addition to solvent- and supercritical fluid extraction, Mercer and Armenta (2011) reviewed ultrasonic-assistance, although they concluded that scaling up this process was going to be difficult. Lin and Lin (2015) demonstrated that microwave-assisted extraction results in 9.08 wt% more lipid than a traditional Soxhlet apparatus. Solvent extraction can be conducted in a reflux set-up such as a Soxhlet apparatus and used with the assistance of radiation including ultra-sonic and microwaves to achieve a high extract yield (Soares, *et al*., 2014; Taher, *et al*., 2014).

Furthermore, a patented step developed by OriginOil (American water technology company) (OriginOil, 2018) combines dewatering, cell disruption and lipid extraction without the use of solvents (Halim, *et al*., 2012). This is advantageous because the residual biomass can be used as animal feed. This bio-refinery approach has been said to improve the costs associated with the algae biodiesel process, by reducing waste (Halim, *et al*., 2012).

2.4.2. Solvents used in lipid extraction

Bligh and Dyer (1959) and Folch *et al*. (1957) use mixtures of chloroform/methanol/water (2:1:1, *v*/*v*/*v*) and chloroform/methanol (2:1, *v*/*v*), respectively for lipid extraction. Various solvents, *e.g*. dichloromethane (DCN) or dimethyl sulfoxide (DMSO), are employed to replace the hazardous chloroform (which can convert to phosgene in presence of oxygen). Soares *et al*. (2014) used DCM/methanol on *Chlorella* to get a slightly higher extract yield than that from *Spirulina* powder extracted by Martínez *et al*. (2017) using Folch *et al*. (1957) method.

Singh and Mallick (2014) and Cancela *et al*. (2016) also used Folch *et al*. (1957) method, to obtain high yields (40% and above), with no extraction-assistance used in the case of Singh and Mallick (2014) (Table 3). Additionally, Zhu *et al*. (2015) employed DMSO/methanol on *Chlorella zofingiensis* to get a yield comparable to Bligh and Dyer (1959) and Folch *et al*. (1957) (Table 3). Folch *et al*. (1957) method often results in the extraction of higher yields (30% and above) (Table 3) and remains the preferred method.

2.5. Biodiesel production: using transesterification

Microalgae lipid cannot be used directly as a fuel because usually it has a higher viscosity and lower volatility than diesel fuel. It is also characterized by polyunsaturated fatty acids (PUFAs), which means it is susceptible to oxidation, which results in engine deposition (Pandey, Rehman, & Sarviya, 2012). Lipid, containing FAs, can be converted to biodiesel, containing the less viscous FAMEs, via the transesterification reaction (Figure 3) (Rawat, *et al*., 2013).

Table 3: Utilization of organic solvents and assisted-extraction in lipid recovery from microalgae

Strain	Type of solvent	Assisted-extraction technique	Extraction yield (% dwt.)	Reference
Nannochloropsis sp.	Chloroform/methanol mixture (1:2 *v*/*v*)	Microwave	31	(Wahidin, Idris, & Shaleh, 2013)
S. obliquus	Chloroform/methanol mixture (2:1 *v*/*v*)	-	40	(Singh & Mallick, 2014)
Chlorella sp.	DCM/methanol mixture	-	10	(Soares, *et al*., 2014)
Scenedesmus sp. (freeze-dried)	*n*-hexane	Soxhlet	21	(Taher, *et al*., 2014)
Scenedesmus sp. (oven-dried)	Chloroform/ethanol mixture (1:1 *v*/*v*)	Microwave	30	(Guldhe, *et al*., 2014)
C. zofingiensis (freeze-dried)	DMSO/methanol mixture (10% solution)	-	35	(Zhu, *et al*., 2015)
I. galbana	*n*-hexane/isopropanol mixture (2:1 *v*/*v*)	Microwave	11	(Lin & Lin, 2015)
M. dybowskii	Chloroform/methanol mixture (1:2 *v*/*v*)	Soxhlet	35	(Yang, He, & Hu, 2015)
P. lutheri (frozen)	Chloroform/methanol mixture (2:1 *v*/*v*)	Ultrasonication	44	(Cancela, *et al*., 2016)
Spirulina sp. LEB 18 powder	Chloroform/methanol mixture (2:1 *v*/*v*)	Sonication	7	(Martínez, *et al*., 2017)

FAs contained in the lipid is reacted with an alcohol (ethanol, isopropanol or methanol) to obtain acyl esters (FAAEs) and glycerol in a stepwise process (Figure 3), and this lowers viscosity (Stansell, Sym, & Gray, 2012). In the work by Shirazi *et al*. (2017), they obtained a 99% FAME yield from the direct transesterification of *Spirulina platensis* (green algae) under high temperature (and a short reaction time). This is comparable to other feedstock (Table 4), although Kim *et al*. (2014) directly transesterified *Scenedesmus* sp. to obtain a 55% FAME yield (under a long reaction time). In addition, methanol is often preferred, due to its relatively low cost (Yang, He, & Hu, 2015).

Transesterification occurs in the presence of an alkali, acid or enzymatic catalyst (*e.g.* lipase). Narula *et al*. (2017) used potassium hydroxide (KOH) on an algae/*Jatropha* lipid blend and obtained an 82% FAME yield (Table 4). Kim *et al*. (2014) used sodium hydroxide (NaOH). However, alkaline transesterification is not suitable for lipid with a high free fatty acid (FFA) content because FFAs react with the alkali-catalyst causing soap formation known as saponification.

On the other hand, Bala *et al*. (2017) used acid transesterification whereby they loaded phosphotungstic acid (PTA) on KIT-5 in order to obtain a 93% FAME yield (from used cooking lipid). This was contradictory to that reported by Um and Kim (2009) where acid transesterification had slow conversion rates. Acid transesterification can be used as a pre-treatment of lipid with high FFA content before alkaline transesterification (Sharma, Singh, & Upadhyay, 2008). After treatment with an acid catalyst, the FFA content can be reduced to less than two percent (Fukuda, *et al*., 2001), therefore, making alkaline transesterification feasible.

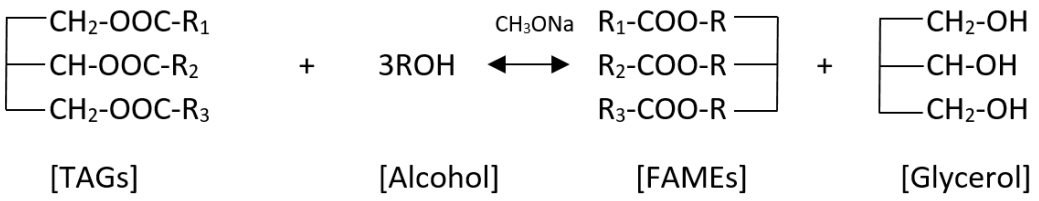


Figure 3. Transesterification reaction (Mutanda, *et al.*, 2011)

On the other hand, lipases have also been investigated and the following FAME yields are of interest from the following authors because they are high. Amini *et al*. (2017) and Santin *et al*. (2017) immobilized lipase (Novozym 435) and achieved high FAME yields (88- and 95% respectively), but from plant lipids. However, lipases are expensive and often do not result in complete transesterification; or require long reaction times as in Santin *et al*. (2017).

Several operational parameters, such as alcohol-to-lipid ratio, affect the efficiency of transesterification (Sharma, Singh, & Upadhyay, 2008). Ehimen *et al*. (2010) investigated the influence of alcohol volume, moisture content, temperature, reaction time, and mixing on an acid-catalyzed *in situ* (direct) transesterification process. It was found that water content in the reaction was greater than 115% w/w (based on lipid weight) and this inhibited the reaction.

Water hydrolyzes the lipid to produce FFAs, which react with the catalyst and counter transesterification. Algae lipid should be dried before. Alternatively, Griffiths *et al*. (2010) used a water scavenger such as the 2,2,-dimethoxypropane to reduce the water content in

the algae lipid feedstock before transesterification. This water scavenger was also used in this study (Section 3.8.).

2.6. Biodiesel properties: with focus on combustion and cold-flow

Biodiesel properties such as *CN*, *V*, *CFPP*, *IN*, and *SV*, play a significant role in the combustion process and the flow of fuel during cold weather. As such, every biodiesel produced should be tested before it can be used in an engine (Sinha & Murugavelh, 2016). Biodiesel can have negative environmental effects due to poor quality (Patel & Sankhavara, 2017). The quality of the algae biodiesel depends on the type of FAs that are present in the lipid extract (Tong, *et al*., 2010), which in turn are influenced by the cultivation conditions.

2.6.1. Combustion quality: cetane number

The cetane number (*CN*) is a commonly used indicator for the determination of diesel fuel quality, especially the ignition quality (Knothe, 2009). It measures the readiness of the fuel to auto-ignite when injected into the engine. The structure of the FAME components present in the lipid extract influence the ignition quality (Knothe, 2005). A lower limit of 47 is specified for *CN* by the ASTM standard (Table 9).

Table 4: Various feedstock in biodiesel production: Edible and non-edible – Part 1

Feedstock	Type of alcohol reagent	Oil: alcohol molar ratio	Catalyst	Reaction temperature (°C)	Duration (h)	Fatty acid acyl ester (FAAE) yield (% dwt.)	Reference
Scenedesmus sp. (direct trans-esterification)	MeOH	1:15	NaOH	70	10	55	(Kim, *et al*., 2014)
Pongamia Pinnata (Karanja) oil	MeOH	1:10	KOH	67	1.5	91	(Verma & Sharma, 2016)
Refined, bleached and deodorized palm oil (RBD oil)	MeOH	1:12	Flyash from wood pellet	60	3	100	(Uprety, *et al*., 2016)
Waste cotton seed oil	MeOH	1:12	Egg shell-derived CaO	60	0.8	92	(Sinha & Murugavelh, 2016)
Hevea brasiliensis (rubber) oil	MeOH	1:9	NaOH	60	1.5	85	(Silitonga, *et al*., 2016)
Ricinus communis (castor) oil						98	

Table 4: Various feedstock in biodiesel production: Edible and non-edible – Part 2

Feedstock	Type of alcohol reagent	Oil: alcohol molar ratio	Catalyst	Reaction temperature (°C)	Duration (h)	Fatty acid acyl ester (FAAE) yield (% dwt.)	Reference
Waste cooking oil (WCO) (without pre-treatment esterification)	MeOH	1:6	Egg shell-derived CaO	25	0.2	97	(Piker, *et al*., 2016)
Jatropha curcas-Ceiba pentandra oil (J50C50)	MeOH	1:3	KOH	60	2	93	(Dharma, *et al*., 2016)
Soybean oil	MeOH	1:23	CH_3ONa	250	0.3	97	(Zeng, Yang, & Fang, 2017)
Spirulina platensis (direct trans-esterification) (supercritical conditions)	MeOH	1:8	KOH	300	0.5	99	(Shirazi, Karimi-Sabet, & Ghotbi, 2017)
Soybean oil	EtOH	1:3	Immobilized lipase (Novozym 435)	70	4	88	(Santin, *et al*., 2017)
Pongamia Pinnata (Karanja) oil	MeOH	1:6	KOH	65	2	97	(Patel & Sankhavara, 2017)

Table 4: Various feedstock in biodiesel production: Edible and non-edible – Part 3

Feedstock	Type of alcohol reagent	Oil: alcohol molar ratio	Catalyst	Reaction temperature (°C)	Duration (h)	Fatty acid acyl ester (FAAE) yield (% dwt.)	Reference
Cotton seed oil (refined)	MeOH	1:6	KOH	55	1	96	(Onukwuli, *et al*., 2017)
Palm oil	MeOH	1:20	GR-SO_3H	100	14	98	(Nongbe, *et al*., 2017)
Algae and *Jatropha curcas* oil blend	MeOH	1:60	KOH	50	3	82	(Narula, *et al*., 2017)
Mucor circinelloides (filamentous fungus) (direct trans-esterification)	EtOH	1:120	H_3PMo/Al_2O_3	200	4	97	(Carvalho, *et al*., 2017)
Used cooking oil (UCO)	MeOH	1:2	Phosphotungstic acid (PTA) loaded on KIT-5	70	4	93	(Bala, Misra, & Chidambaram, 2017)
Ocimum basilicum (sweet basil) L. seed oil	MeOH	1:10	Immobilized lipase (Novozym 435)	47	68	95	(Amini, *et al*., 2017)

Islam *et al*. (2015) determined the *CN* of the algae *Crypthecodinium cohnii* and waste cooking oil (WCO) biodiesel to be 46.5 and 58.6 respectively. The longer the FA carbon chains and the more saturated the molecules, the higher the *CN* (Onukwuli, *et al*., 2017). Ramírez-Verduzco *et al*. (2012) discusses that fuels with low *CN* tend to increase gaseous and particulate exhaust emissions because of incomplete combustion.

2.6.2. Cold-flow quality: viscosity and cold-filter plugging point

Other quality indicators are cold-flow properties associated with the fluidity of the fuel during cold weather conditions (Francisco, *et al*., 2010). Biodiesel components have been reported to crystallize during winter, causing problems such as clogged fuel lines, filters, and injectors (Knothe, 2005; Meher, *et al*., 2006; Demirbas, 2011). Transesterification is widely used as a technique to reduce the highly viscous algae lipid (Kiran, *et al*., 2014). Viscosity (*V*) is a fuel property that influences injection (Fakhry & Maghraby, 2013). The EN 14214 specification for viscosity is 3.5–5 $mm^2.s^{-1}$ at 40°C (Stansell, Sym, & Gray, 2012).

Islam *et al*. (2015) found that pure biodiesel of *C. cohnii* has a viscosity of 5.06 $mm^2.s^{-1}$, slightly higher than that of WCO at 4.82 $mm^2.s^{-1}$. This is due to the higher amount of very long chain FAs (*e.g.* C22:5 and C22:6) in the algae. Like *CN*, viscosity increases with increasing FA chain length and degree of saturation (Fakhry & Maghraby, 2013). A higher degree of saturation is a reflection of a lower iodine number (*IN*) (Francisco, *et al*., 2010). Viscosity increases with a decrease in *IN*. Haik *et al*. (2011) found that other microalgae species such as *Ankistrodesmus braunii* and *Nannochloropsis* sp., with 78% SFAs, have a

viscosity of 4.19 $mm^2.s^{-1}$. The viscosity range required by the ASTM standard is 1.9-6.0 $mm^2.s^{-1}$ (Francisco, *et al*., 2010).

The cold filter plugging point (*CFPP*) is closely related to the cloud point (*CP*) which is the temperature at which the lower melting FAs start to crystallize out of the fuel (Dunn & Bagby, 1995; Lopes, *et al*. 2008). Francisco *et al*. (2010) investigated the biodiesel properties of six microalgae species. *S. obliquus* biodiesel had the highest *CFPP* at 21°C. A high *CFPP* is undesirable because clogging of engine lines can occur easily (Sinha & Murugavelh, 2016). *Phaeodactylum tricornutum* biodiesel had the lowest *CFPP* at -12°C. The ASTM standard sets a summer and winter maximum limit: 0 and -15°C respectively (Francisco, *et al*., 2010).

CHAPTER THREE

3. MATERIALS AND METHODS

This chapter details the experimental and theoretical approaches used to answer the research questions set out in Chapter 1.

3.1. Reagents

All reagents used in this study were of analytical grade (GC grade), and sourced from Merck, South Africa (unless stated otherwise). These were used as obtained, without further purification. Ultra-high-purity (UHP) grade N3.0 CO_2 gas was supplied by AFROX South Africa.

3.2. Species selection

Two green microalgae were chosen for comparison. *Acutodesmus obliquus* (*AD*) was used because it was available in the laboratory and very scarcely studied for FAMEs. *Chlamydomonas* CC125 (*CR*) was chosen because it is a widely accepted model organism that is used to understand biochemical processes in other microalgae (Kim, *et al*., 2016).

AD was obtained from the Biochemical Laboratory (School of Chemical & Metallurgical Engineering, University of the Witwatersrand, Johannesburg). *CR* was donated by The Evolutionary Studies Institute (School of Geosciences, University of the Witwatersrand, Johannesburg) already identified as *Chlamydomonas* (CC125).

3.3. Stock culture maintenance

AD and *CR* algae cells were exposed to 80 μmol.m^{-2}.s^{-1} of light intensity using Osram F36/33-640 cool white fluorescent tubes (Sylvania Gro lux, Germany). Growth bottles (capped) were shaken for two minutes each day. Beijerinck medium (APPENDIX A.1.) was used as the standard medium throughout, and 750 ml was added every fortnight to dilute the cells (250 ml). This was done after removing 750 ml of culture and storing it in the fridge (4^{o}C). This whole procedure was to maintain cells in exponential phase. Zero CO_2 gas was fed into the stock culture.

3.4. Cultivation conditions

This section details the cultivation conditions investigated and the equations used to determine growth rate and biomass productivity. The results are discussed in Chapter 4.

The experimental cultures were exposed to a fixed CO_2 flow rate (20 ml.min^{-1}) and room temperature (25^{o}C). A volume of 250 ml of stock culture containing *AD* or *CR* was inoculated into 1L Erlenmeyer flasks containing 750 ml of Beijerinck medium for each experiment.

3.4.1. Carbon dioxide

Algae cells were fed pure CO_2 (100% *v*/*v*) daily for a period of 2 h (4.8 g CO_2). For pure CO_2, prolonged CO_2 supply may become harmful for the cells. Furthermore, since only two CO_2 tanks were available (as shown in Figure 4) and each replicate had to be fed CO_2 for photosynthesis, CO_2 feed time had to be short. This was done during the dark phase of photosynthesis, because CO_2 is only required then. A Brooks Smart mass flow

controller (MFC) (Brooks® Instrument B.V, Netherlands) was used to purge CO_2 gas into the culture (Figure 4), through air stones to disperse the gas bubbles. The same number of replicates (n = 3) was used in all conditions tested.

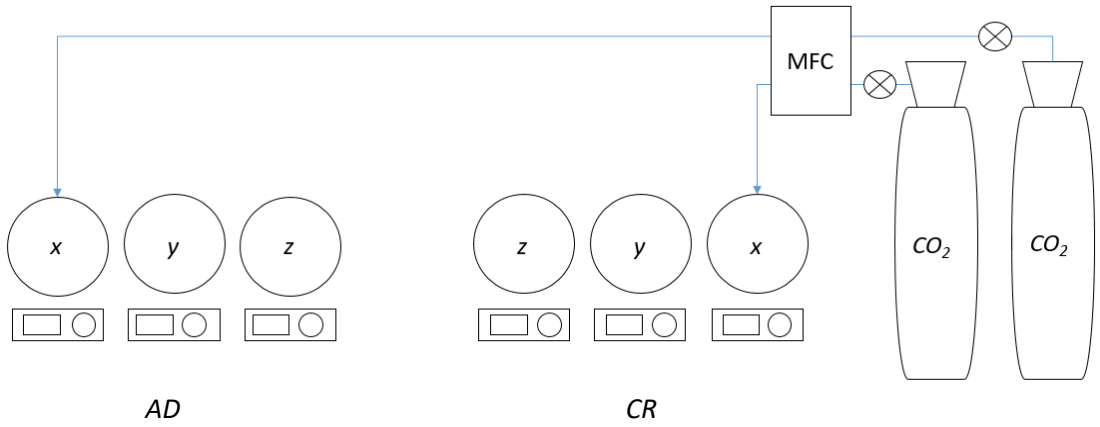


Figure 4. Batch cultivation set-up (Replicate 1 = *x*, Replicate 2 = *y* & Replicate 3 = *z*)

3.4.2. Light

Algae cells were exposed to light intensities of 80 and 60 µmol.m^{-2}.s^{-1} provided by F36/Gro-T8 fluorescent tubes which emit a high level of blue and red radiation (Sylvania Gro lux, Germany) for a period of 12 h (12:12 light-dark cycle) and continuous agitation of 250 and 100 rpm for 12 days. The light intensity (µmol.m^{-2}.s^{-1}) was measured using a LI-250A light meter (LI-COR® Biosciences, Lincoln, Nebraska). One µmol.m^{-2}.s^{-1} reading is equivalent to 0.208 W.m^{-2}. The cultures were kept in constant motion by magnetic stirrers and the change in absorbance in the culture was measured using a PRIM High-Resolution UV/VIS spectrophotometer (Topac Inc., Cohasset, MA).

3.4.3. Absorbance and dry biomass weight

The absorbance (*Abs*) readings were related to dry biomass weight (*DW*) using Eq. (2) for *AD* and Eq. (3) for *CR* from calibration curves (APPENDIX A.2.):

$$\boldsymbol{DW = 0.1957(Abs) + 0.3586} \quad (2)$$

$$\boldsymbol{DW = 1.2749(Abs) - 0.003} \quad (3)$$

Where:

DW = dry biomass weight ($g.L^{-1}$)

Abs = Absorbance

Then the natural logarithm of each dry weight biomass was calculated and used to determine the growth rate for each day using Eq. (4) below:

$$\boldsymbol{\mu = \frac{(\ln DW_2 - \ln DW_1)}{(t_2 - t_1)}} \quad (4)$$

Where:

μ = growth rate (d^{-1})

DW_1 = initial dry biomass weight ($g.L^{-1}$)

DW_2 = final dry biomass weight ($g.L^{-1}$)

t_1 = initial time (d)

t_2 = final time (d)

The biomass productivity (*BP*) was determined from the dry biomass weight (*DW*) and the growth rate (μ) using Eq. (5) shown below (Griffiths, van Hille, & Harrison, 2012):

$$\boldsymbol{BP\ (g.L^{-1}.d^{-1}) = \mu DW} \quad (5)$$

Where:

BP = biomass productivity ($.L^{-1}.d^{-1}$)

μ = growth rate (d^{-1})

DW = dry biomass weight ($g.L^{-1}$)

In order to construct the calibration curves (from whence Eq. (2) and (3) are derived), nitrocellulose filter membranes (0.45 µm pore diameter) were used to filter the biomass from the rest of the medium using a vacuum filter. Beijerinck medium was used as the standard medium throughout.

3.4.4. Baseline experiment: Condition 0

A baseline experiment, Condition 0 (I = 35; S = 150), (see Table 5 for the shorthand notation) was conducted. It can be viewed as the basis for the study (*i.e.* the origin of a Cartesian plane). Under this condition, no CO_2 gas (F = 0 $ml.min^{-1}$) was fed and light was kept to the lowest possible intensity (I = 35 $\mu mol.m^{-2}.s^{-1}$, only one fluorescent tube used).

Table 5: Set of experiments conducted (Notes: Experiments were triplicated = 15 in total)

Condition	Light intensity (I, µmol.m^{-2}.s^{-1})	Agitation speed (S, rpm)	Notation
Baseline exp.			
0	35	150	(I: 35; S: 150)
Core exp.			
1	60	250	(I: 60; S: 250)
2	60	100	(I: 60; S: 100)
3	80	250	(I: 80; S: 250)
4	80	100	(I: 80; S: 100)

3.5. Monitoring

Although the CO_2 flow (F) and temperature (T) were fixed overall, and the light intensity (I) and agitation speed (S) were the parameters of interest in the cultivation stage of this study, the following variables were considered and therefore monitored: pH, dissolved oxygen (DO) and nitrate concentration. Oxygen is a product of photosynthesis (Eq. 1) and can be used to further understand growth. The pH and nitrate concentration are used as triggers for lipid accumulation, as mentioned under Section 2.3.

3.5.1. pH-monitoring

A three-point calibration was performed daily on a Starter 3100 pH meter (OHAU, Switzerland) using pH = 4.00, pH = 7.00 and pH = 10.00 standards to measure the pH. An electrode was inserted into the agitated algae culture (1L growth flask) and, once the reading stabilized, it was recorded. The electrode was rinsed with deionized water before and after use, and then dried with a paper towel and stored in a 3M KCl solution.

3.5.2. Dissolved oxygen

An AL15 Electrochemistry Meter (AQUALYTIC®, Germany) was calibrated using oxygen in ambient air (typically 20.9% (v/v)). Five min were allowed to lapse before readings stabilized with no fluctuation. Dissolved oxygen values were taken daily for 12 days.

3.5.3. Nitrate testing

A NI-11 Model Nitrate Test Kit (Hach, Loveland, CO) was used to determine nitrate concentration colorimetrically (0-40 $mg.L^{-1}$) every 4 days for a 12-day growth period for each algae. A Color Viewing Tube was filled with 5 ml dilute algae sample and inserted into the left opening of a comparator.

A second tube was filled to the 5 ml mark with the same algae sample and NitraVer 5 Nitrate Reagent (color reagent) Powder Pillow was added to this tube and shaken vigorously for 1 min. The presence of nitrates was detected by an amber color. The tube was then inserted into the right opening of the comparator and the comparator held against cool white light directly behind the tubes.

A color disc was used to match the colors of the tubes by rotating the disc, at which point the nitrate concentration was recorded. This value was multiplied by 4 as instructed in the user's manual.

3.6. Lipid accumulation and extraction process

This section details the strategy of lipid accumulation, the method of extracting lipid from the algae biomass, and the equations used to determine lipid extract and productivity. The results are seen in Chapter 5.

3.6.1. Accumulation: using $NaHCO_3$

A "trigger" strategy modified from Xia *et al*. (2015) was adopted. A weight of 25 g of sodium bicarbonate ($NaHCO_3$) was added to the algae cells on the 8th day of growth to achieve an alkaline pH for accumulation of storage lipids (*e.g.* TAGs). This was not done for the baseline experiment (*I*: 35; *S*: 150). It was decided to add $NaHCO_3$ on the 8th day because the cells need to grow first before lipid production is triggered. Algae biomass was harvested by gravity sedimentation for 4 days, so as to achieve a concentrated sludge and decant the water, before centrifugation at 2000 rpm for 30 min. This way, multiple rounds of centrifuging were avoided.

3.6.2. Lipid extraction: using Bligh and Dyer

Lipid extraction was performed for all experiments using a method adopted from Bligh and Dyer (1959). Other methods, such as Folch *et al*. (1957), are reported as being time-consuming and solvent-expensive.

The process was as follows: the late-exponential phase cells (after 12 days of growth) were centrifuged at 2000 rpm for 30 min. Thereafter, dry weight biomass of the pellet was determined after oven drying it at 50^{o}C for 8 h. This is the initial dry biomass weight (DW_i).

The biomass was homogenized in a chloroform: methanol (4 ml: 2 ml) solvent mixture, then centrifuged at 2000 rpm for 30 min and left overnight in order to extract total lipids. This mixture was filtered and the homogenate was collected in a centrifuge tube. Pure chloroform washings of the filter, mortar and pestle were collected in the same centrifuge tube. The residual biomass (DW_f) after filtration was dried at room temperature overnight and weighed.

What followed was the addition of 5 ml of NaCl (0.9%) to the homogenate mixture in the centrifuge tube, this was to allow the upper aqueous methanol layer and the lower lipid-containing chloroform layer to separate (Bligh & Dyer, 1959). This lower lipid-containing chloroform layer, which could not be dried to avoid lipid oxidation, was removed from the centrifuge tube and transferred to a sample vial sealed with parafilm before being stored in a cold room (4^{o}C) until transesterification.

Since the lipid-containing chloroform layer mentioned above could not be dried, it became more accurate to determine lipid content ($\%LC$) from the difference between initial and residual dry biomass weight, as shown in Eq. (6) below:

$$\%\boldsymbol{LC} = (\boldsymbol{DW_i} - \boldsymbol{DW_f}) \times \mathbf{100} \quad (6)$$

Where:

$\%LC$ = lipid content

DW_i = initial dry biomass weight ($g.L^{-1}$)

DW_f = residual dry biomass weight ($g.L^{-1}$)

Once the amount of lipid extract had been determined and the biomass productivity (*BP*) was known, the lipid productivity (*LP*) of the algae species was obtained by using Eq. (7) below (Griffiths, *et al*., 2012):

$$\boldsymbol{LP}\ (\mathbf{mg.L^{-1}.d^{-1}}) = \boldsymbol{BP} \times \boldsymbol{LC} \qquad (7)$$

Where:

LP = lipid productivity ($mg.L^{-1}.d^{-1}$)

BP = biomass productivity ($mg.L^{-1}.d^{-1}$)

LC = proportion of lipid content

3.6.3. Waste cooking oil

Sunflower waste cooking oil (WCO) (250 ml) was obtained from a household, to compare with the algae oil, because it is used as a biodiesel feedstock. It had been used twice to fry fish. Without any pre-treatment, WCO underwent the same procedures (transesterification and GC-MS analysis) as algae oil in this study.

3.7. Methyl ester derivation: using transesterification

This section details the approach adopted to produce FAMEs (*i.e.* biodiesel) from algae lipid.

Transesterification was carried out using a method outlined in Griffiths *et al*. (2010) because this approach was reported to lower free fatty acid (FFA) content. Thereby

preventing soap formation (Sharma, Singh, & Upadhyay, 2008). Samples (1 ml) were dissolved in glass test tubes containing 500 µl toluene.

Thereafter 100 µl of 2,2-dimethoxypropane (water scavenger) (Griffiths, *et al*., 2010) was added to the test tube samples to dehydrate the lipid extract (because water hydrolyzes lipids to free fatty acids that react with alkali catalyst to form soap) before they were placed in a water bath at 80^{o}C for 20 min, with shaking (by hand for 2 min) before and after. The samples were mixed with 1 ml of 50% (*m*/*v*) sodium methoxide (CH_3ONa) by shaking again briefly and incubated in the water bath again. They were then cooled for 5 min to room temperature.

Thereafter, 1 ml of 14% (*m*/*v*) boron trifluoride (BF_3) methanol was added to the samples, before repeating the water bath incubation to maintain the reaction temperature at 80^{o}C (Griffiths, *et al*., 2010). A volume of 400 µl distilled water (dH_2O) and 400 µl hexane (Griffiths, *et al*., 2010) were added to the samples and mixed by shaking again briefly, and allowing it to cool to room temperature. After 5 min of cooling, the samples were centrifuged at 2000 rpm for 2 min.

Finally 200 µl of the upper hexane-toluene layer, containing the FAME extract, was transferred to vials containing 20 ml of chloroform as a solvent for GC-MS analysis. The hexane-toluene layer containing the FAME extract was kept in a cold room (4^{o}C) in vials sealed with parafilm until GC-MS analysis.

3.8. FAME identification: using GC-MS

This section outlines the chromatographic method used to identify the type of FAMEs present in the esterified algae lipid. The results are reported in Chapter 5.

FAME identification was performed on a GC-MS-TQ8040 instrument (Shimadzu Corporation, Japan), fitted with a low-polarity fused silica column Rxi-5ms column (30 m length, 0.25 μm thickness and 0.25 mm diameter) (Restek Corporation, US) at a column flow of 2 $ml.min^{-1}$ (Helium gas). Components present in the vaporized sample interact differently with the column and thereby separate at different retention times. Water-washed samples (2 ml) were dissolved in chloroform (20 ml) solvent. Each sample (1 μL) was injected individually (no auto-sampler), at an injection temperature of 270 ^{o}C. The program was set as shown in Table 6 below.

Table 6: GC-MS program modified from Mandotra *et al*. (2016)

Rate ($^{o}C.min^{-1}$)	Temperature (^{o}C)	Hold time (min)
0	60	4
20	180	18
30	260	6

The total run time was 37 min. The detector temperature was set to 280^{o}C. A separated component enters the high-vacuum chamber of the detector (mass spectrometer), where it is fragmented into a number of ionized fragments that form a spectrum. This spectrum was then compared to both the NIST and Wiley Library Databases. The ionization energy (EI) was set to 70 eV. The scan range was 50-300 amu (m/z 50 to m/z 300), and one can

per second (1 s^{-1}). Finally, the ion source and interface temperatures were set to 200°C and 300°C (Mandotra, *et al*., 2016), respectively.

3.9. FAME quantification: theoretical estimation of $\%FAME_i$ from GC-MS area proportions

This section outlines the theoretical approach used to estimate the quantity of each FAME present in the esterified algae lipid. A theoretical estimation was conducted to avoid costs associated with the standard solutions required to do this sort of analysis. The results are seen in Chapter 5.

3.9.1. Conversion of area values to FAME concentrations (in $mg.ml^{-1}$)

All area proportions of the identified FAMEs obtained via GC-MS were converted to concentration values (in $mg.ml^{-1}$) by relating area to FAME concentration (Eq. 8) using values from Botineştean *et al*. (2012) shown in Table 7. Botineştean *et al*. (2012) used standard solutions to convert area proportions of three FAMEs: methyl palmitate (zero double bonds), methyl oleate (one double bond) and methyl linoleate (two double bonds).

Table 7: FAME concentrations from Botineştean *et al*. (2012)

FAME		Saturation	Area (%)	FAME conc. ($mg.ml^{-1}$)
IUPAC Name	Common Name			
Hexadecanoic acid, methyl ester (CAS)	Methyl palmitate	0*db*	13.5191	0.05
9-Octadecenoic acid (Z)-, methyl ester (CAS)	Methyl oleate	1*db*	18.85073	0.07
9,12-Octadecadienoic acid (Z,Z)-, methyl ester (CAS)	Methyl linoleate	2*db*	54.91247	1.34

All area proportions of saturated FAMEs (SFAs) were theoretically converted using the relationship of methyl palmitate (0*db*). Mono-unsaturated FAMEs (MUFAs) were converted using methyl oleate (1*db*). Poly-unsaturated FAMEs (PUFAs) were converted using methyl linoleate (2*db*). Area proportions (%) were converted to concentrations (mg.ml^{-1}) using Eq. (8) below:

$$\frac{\textbf{Area (Botineştean } \boldsymbol{et\ al.}\textbf{)}}{\textbf{Concentration (Botineştean } \boldsymbol{et\ al.}\textbf{)}} = \frac{\textbf{Area } (\boldsymbol{known})}{\textbf{Concentration } (\boldsymbol{unknown})} \qquad (8)$$

3.9.2. Conversion of FAME concentrations (in mg.ml^{-1}) to %FAME$_i$

FAME concentrations (in mg.ml^{-1}) were then represented as *%FAME* values using an average lipid density of 881.2 mg.ml^{-1} (for green microalgae) that was determined from algae lipid densities provided by Kumar *et al*. (2011).

3.10. Prediction of fuel properties: using *%FAME$_i$* values

This section outlines the equations used to predict fuel properties: saponification value (*SV*), iodine number (*IN*), cold-filter plugging point (*CFPP*), cetane number (*CN*) and viscosity (*V*). These equations require FAME carbon length (C*k*), molecular weight (*MW*) and quantity (*%FAME$_i$*) data. The *%FAME$_i$* values were used to predict the biodiesel properties of both algae species. A theoretical approach was chosen to avoid costs associated with the sophisticated equipment required to thoroughly perform this sort of investigation.

The methyl ester content ($\%FAME_m$) of each esterified algae lipid was summed up (by using Eq. (9) below) from the concentrations of individual FAMEs ($\%FAME_i$) identified in that algae lipid:

$$\%\boldsymbol{FAME_m} = \sum(\%\boldsymbol{FAME_i}) \quad (9)$$

Where:

$\%FAME_i$ = methyl ester content of an individual FAME molecule

$\%FAME_m$ = total methyl ester content in esterified algae lipid

The saponification value (SV), iodine number (IN) and cold-filter plugging point ($CFPP$) of the overall FAME mixture were estimated by using Eq. (10), (11), (12) and (13) below, as in Francisco *et al*. (2010):

$$\boldsymbol{SV} = \frac{\sum(\mathbf{560}\times\boldsymbol{FAME_i})}{\boldsymbol{MW}} \quad (10)$$

Where:

SV = saponification value of the overall FAME mixture (mg.KOH.g^{-1})

$FAME_i$ = proportion of the methyl ester content of an individual FAME molecule

MW = molecular weight of an individual FAME molecule (g.mol^{-1})

$$\boldsymbol{IN} = \frac{\sum(\mathbf{256}\times\boldsymbol{db}\times\boldsymbol{FAME_i})}{\boldsymbol{MW}} \quad (11)$$

Where:

IN = iodine number of the overall FAME mixture ($g.I_2.100\ g^{-1}$)

db = number of double bonds in the parent structure of an individual FAME molecule (*e.g.* 2*db* in methyl linolelaidate)

$FAME_i$ = proportion of methyl ester content of an individual FAME molecule

MW = molecular weight of an individual FAME molecule ($g.mol^{-1}$)

$$\boldsymbol{CFPP = (3.1417 \times LCSF) - 16.477} \quad (12)$$

$$\boldsymbol{LSF = (0.1 \times C16) + (0.5 \times C18) + (1 \times C20) + (1.5 \times C22) + (2 \times C24)} \quad (13)$$

Where:

CFPP = cold-filter plugging point of the overall FAME mixture (°C)

LCSF = long-chain saturated factor of the overall FAME mixture

Ck = number (*k*) of carbon atoms in the chain of an individual FAME molecule in the overall mixture

Lastly, the cetane number (CN_m) and viscosity (V_m) of the overall FAME mixture were estimated from the individual cetane numbers (CN_i) and viscosities (V_i) of the identified FAME molecules, by using Eq. (14) and (15) in Knothe *et al*. (2009) and Stansell *et al*. (2012) respectively:

$$\boldsymbol{CN_m = \sum FAME_i CN_i} \quad (14)$$

Where:

$FAME_i$ = proportion of an individual FAME molecule in the mixture

CN_i = cetane number of an individual FAME molecule

CN_m = cetane number of the overall FAME mixture

$$\boldsymbol{V_m = \sum FAME_i V_i} \quad (15)$$

Where:

$FAME_i$ = proportion of an individual FAME molecule in the mixture

V_i = viscosity of an individual FAME molecule ($mm^2.s^{-1}$)

V_m = viscosity of the overall FAME mixture ($mm^2.s^{-1}$)

The different individual cetane numbers (CN_i) and viscosities (V_i) of the FAMEs are tabulated in APPENDIX C.2.

CHAPTER FOUR

4. RESULTS AND DISCUSSION [ALGAE CULTIVATION]

This chapter addresses question one, that is, which algae species is more productive?

4.1. Cultivation conditions

In Chapter 3 it was mentioned that the CO_2 flow was kept constant at F = 20 ml.min^{-1} for 2 h for Condition 1 (I: 60; S: 250) to Condition 4 (I: 80; S: 100). There was no CO_2 fed under Condition 0 (I: 35; S: 150) as it was used as a baseline experiment. All experiments were kept at room temperature (T = 25^{o}C) and carried out in triplicates. The algae species investigated were: *Acutodesmus obliquus* (*AD*) and *Chlamydomonas CC125* (*CR*).

4.1.1. Growth curves

For all conditions tested, the growth patterns observed (curves shown below), maximum dry biomass weight (*DW*) and growth rate (μ) of *AD* and *CR* are discussed. The objective of this chapter is to identify a more robust algae species and condition which yield the highest dry weight and the fastest growth.

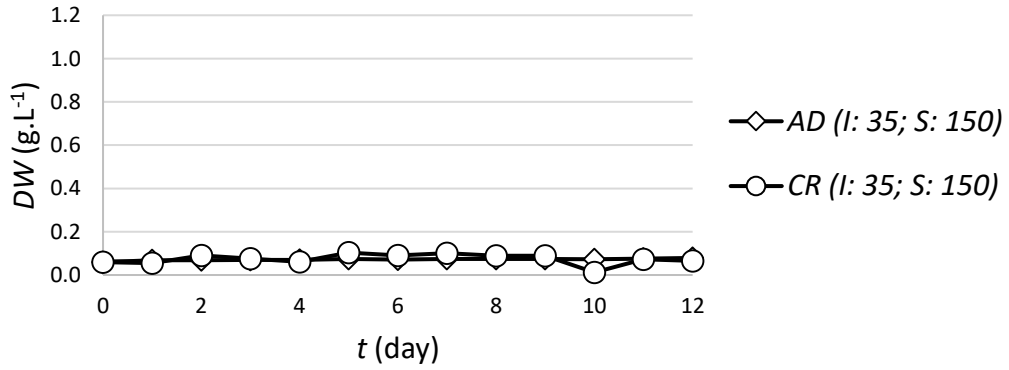


Figure 5. Dry weight of *A. obliquus* and *Chlamydomonas* under Condition 0 (*I*: 35; *S*: 150). Error bars represent *SD*.

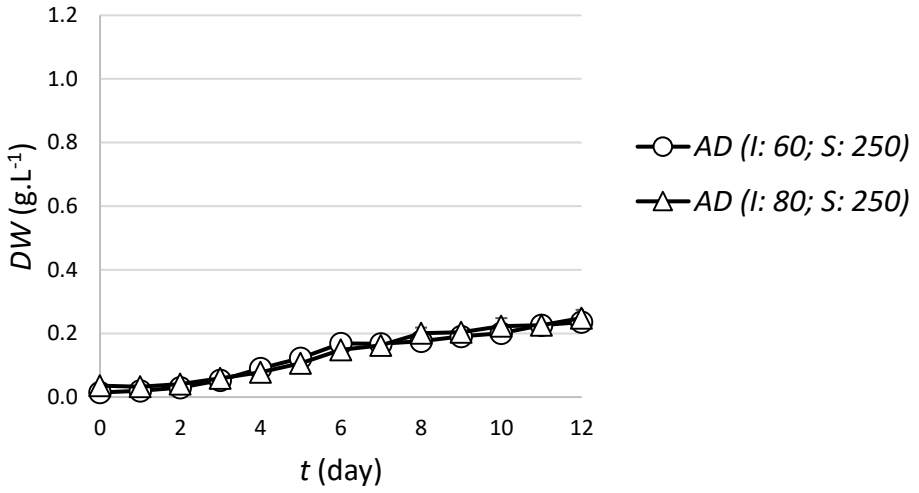


Figure 6. Dry weight of *A. obliquus* under two different light intensities and agitation of *S* = 250 rpm (Condition 1 & 3). Error bars represent *SD*.

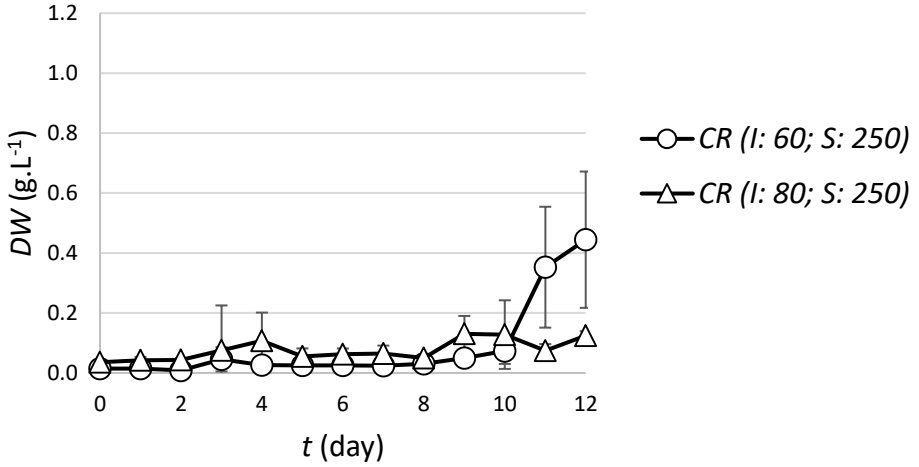


Figure 7. Dry weight of *Chlamydomonas* under two different light intensities and agitation of *S* = 250 rpm (Condition 1 & 3). Error bars represent *SD*.

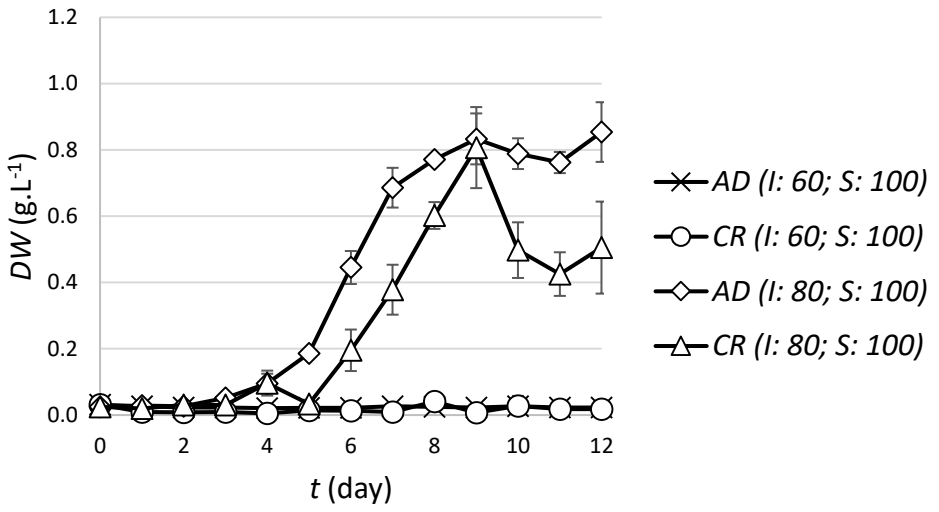


Figure 8. Dry weight of *A. obliquus* and *Chlamydomonas* under two different light intensities and agitation of *S* = 100 rpm (Condition 2 & 4). Error bars represent *SD*.

It can be observed that there is close to no net growth in both algae species after t = 12 days (Figure 5), although some growth occurs on the 1st and 4th day. This was expected because a light intensity of I = 35 μmol.m^{-2}.s^{-1} is relatively very low (it could be merely providing energy for cell maintenance) to what has previously been used in algae cultivation. It was a deliberate choice in establishing a baseline, for purposes of knowing the lowest conditions for growth. Nevertheless, as seen in Figure 5, *AD* and *CR* reached a maximum growth rate of μ = 0.136 d^{-1} and μ = 1.80 d^{-1} respectively. At a certain point within the 12 day growth period, *CR* still managed to reach faster growth than *AD* (Figure 5). This confirms that some negligible growth (less than 0.1 g.L^{-1}) occurred.

AD follows the same pattern under both intensities of light: 60 and 80 μmol.m^{-2}.s^{-1}. It experienced a maximum growth rate of μ = 0.56 d^{-1} (under 60 μmol.m^{-2}.s^{-1}) and μ = 0.38 d^{-1} (under 80 μmol.m^{-2}.s^{-1}). This is for the case of S = 250 rpm agitation. One could say that

the pattern of growth is a function of the agitation speed. However, when comparing with the case of *S* = 100 rpm (Figure 6), it is shown that this cannot be true. Microalgae, as observed even in the case of *CR*, do not follow the same growth pattern under an agitation of *S* = 100 rpm. This could be a phenomenon exclusive to an agitation of *S* = 250 rpm, as observed again in the case of *CR*. *CR* remains relatively unchanged in growth pattern under both 60 and 80 $\mu mol.m^{-2}.s^{-1}$ light intensities, until the 10^{th} day, where there begins a rapid exponential growth phase under Condition 1 (*I*: 60; *S*: 250), albeit with large error deviations, *e.g.* 57% (11^{th} day) and 51% (12^{th} day) of the average weight (Figure **7**). It can safely be said then that *CR*, like *AD* under *S* = 250 rpm, remains unchanged in growth pattern.

Neglecting the errors (*SD*), of significance is that *AD* grows more resilient as it reaches a higher maximum biomass weight than *CR* under an agitation of *S* = 250 rpm (Condition 1 & 3). Both algae maximum biomass weights do not exceed 0.25 $g.L^{-1}$. Nevertheless *AD* reaches higher biomass weights than *CR*, whereas *CR* reaches faster growth rates than *AD*.

There is close to zero growth observed for both species under Condition 2 (*I*: 60; *S*: 100) (Figure 8). This is the similar growth behavior observed under Condition 0 (*I*: 35; *S*: 150), and is a stark contrast to the growth observed under Condition 4 (*I*: 80; *S*: 100). Therefore Condition 2 is unsuitable for robust algae growth and resilience required in the biodiesel pipeline. This can be attributed to the low light intensity, as it is observed that under Condition 4 ($I = 80\ \mu mol.m^{-2}.s^{-1}$) a much higher growth occurred.

Under Condition 4 (*I*: 80; *S*: 100), *AD* reaches the stationary phase and a maximum biomass weight (0.85 $g.L^{-1}$) on the 12th day, although roughly the same dry weight (0.83 $g.L^{-1}$) is reached on the 9th day (Figure 8). *CR* reaches a maximum biomass weight (0.81 $g.L^{-1}$) on the 9th day, followed by a sharp decrease in growth, and then a stationary phase. The maximum biomass weight of both species after 12 days of growth under Condition 4 exceeds those obtained under faster stirring, *e.g. S* = 250 rpm. Both species exhibit their fastest growth under Condition 4 (compared to other core conditions), with *CR* growing faster (μ = 1.76 d^{-1}) than *AD* (μ = 0.88 d^{-1}) (Figure 9). Therefore Condition 4 appears to be the most suitable condition for the cultivation of algae biodiesel feed.

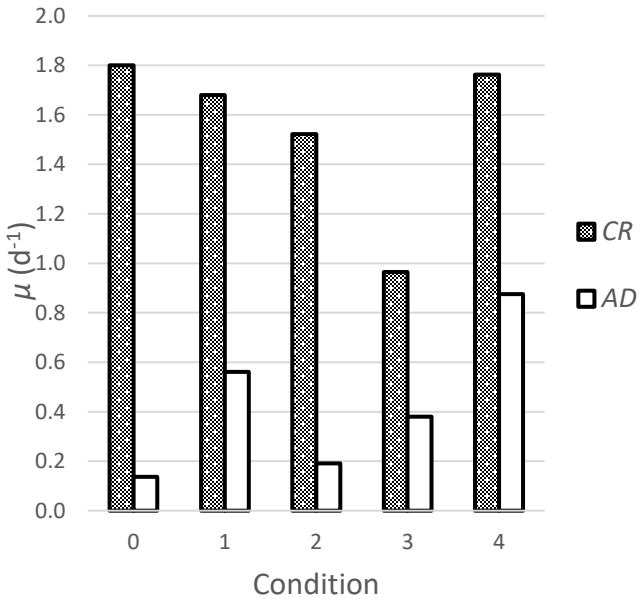


Figure 9. Maximum growth rate of *A. obliquus* and *Chlamydomonas* under different conditions (0, 1, 2, 3 & 4)

It can be said that a slower agitation coupled with a decent light intensity, *i.e.* higher than 35 and 60 $\mu mol.m^{-2}.s^{-1}$, can yield a more robust growth than faster agitation (as it was seen with the productivity achieved by Xia *et al*. 2015). Faster agitation can establish shear forces that are lethal for the algae cells (Christi, 2007). Although *CR* reaches faster growth rates than *AD* (Figure 9), *AD* grows more resilient and robust as it reaches higher maximum biomass weights. Robustness and higher growth rates are both desirable qualities for algae feedstock in biodiesel production.

4.1.2. Biomass productivities (BPs)

The maximum biomass productivity (*BP*) of *AD* and *CR* under the conditions tested is shown in this section. *BP* was used to determine the most productive algae species. It is a product of the growth rate (μ) and biomass weight (*DW*) (Eq. 5). Hence *BPs* resemble robustness and fastness in growth (Griffiths, van Hille, & Harrison, 2012).

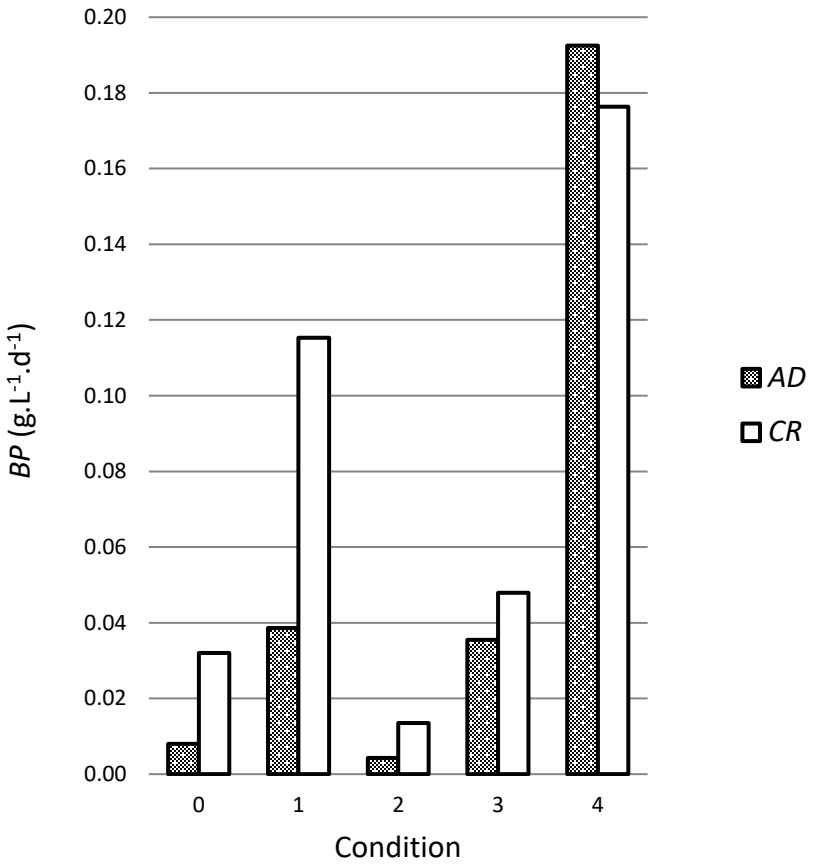


Figure 10. Maximum biomass productivity of *A. obliquus* and *Chlamydomonas* under different conditions (0, 1, 2, 3 & 4)

As seen in Figure 10 both algae were at their most productive under Condition 4. This confirms the highest growth rates and maximum weights observed on the growth curves in the previous section, as these occurred under Condition 4. *CR* reaches a productivity of 0.18 $g.L^{-1}.d^{-1}$. Nascimento *et al*. (2013) showed that *CR* can be more productive (0.33% more), by adding I = 60 $\mu mol.m^{-2}.s^{-1}$ of light intensity to Condition 4 and reducing the agitation speed to S = 90 rpm. *CR* reaches higher maximum *BPs* than *AD* in all the conditions, except Condition 4 (I = 80; S = 100).

AD reached a maximum *BP* that was more than 6 times that reached by Xia *et al*. (2015). *AD* is the most productive under Condition 4, therefore the most suitable candidate as lipid feed. Xia *et al*. (2015) showed that a type of *AD* species (*Desmodesmus* sp) has low productivity, $BP = 0.03\ g.L^{-1}.d^{-1}$, regardless of a high light intensity of $I = 184\ \mu mol.m^{-2}.s^{-1}$ during outdoor cultivation. This could have also been because of their faster agitation ($S = 150$ rpm), as it was seen in Section *4.1.1.*, that this can lower growth rates. Kativu *et al*. (2012) achieved a higher *BP* (135% higher) (Table 1), than *AD* under Condition 4, using *Desmodesmus* sp. exposed to $I = 81\ \mu mol.m^{-2}.s^{-1}$ and 100% CO_2 (similar to this study).

In addition to a high agitation speed and photoinhibiting light intensity, researchers (Table 1) confirm that a low intense light of $I = 36.3$ and 65 $\mu mol.m^{-2}.s^{-1}$, close to that of Condition 0 and 2 respectively, yields low productivity levels. Indeed, this is the case with algae cultivation under Condition 0 and 2 (Figure 10).

4.1.3. Dissolved oxygen

Dissolved oxygen (*DO*) affects algae growth because oxygen (O_2) is a product of photosynthesis (Eq. 1). Rate of oxygen production (RO_2) was used to assess the rate of photosynthesis of each algae species under the conditions tested. RO_2 informs the robustness of each algae species during growth, and the suitability of each condition. RO_2 was also used to understand the removal or build-up of O_2 pressure in the growth vessel. Pressure build-up is undesirable as it can cause an explosion in larger operations of algae cultivation and result in unnecessary costs (Pulz, 2001; Karemore, *et al*., 2015). However, an efficient stirring regime should avoid this and remove excess O_2 (Griffiths, *et al*., 2011).

It can be assumed that some O_2 was being removed from the growth vessel, since algae cultures were subjected to agitation (Pulz, 2001; Karemore, *et al.*, 2015), under the environmental conditions investigated. This being the case, one can then deduce that positive rates of O_2 production (Figure 11) suggest that O_2 is being produced faster than it was being removed ($+RO_2 > -RO_2$) and this is undesirable.

Both species grown under Condition 1 (I = 60; S = 250) and 3 (I = 80; S = 250) result in positive rates of production ($+RO_2$). This was also the case with Condition 0 (I = 35; S = 150). In the case of *AD*: O_2 was being produced the fastest under Condition 3 (1.4 $mg.L^{-1}.d^{-1}$), followed by Condition 0 (1.2 $mg.L^{-1}.d^{-1}$) and 1 (0.7 $mg.L^{-1}.d^{-1}$). In the case of *CR*: O_2 was being produced the fastest under both Condition 0 and 1 (0.9 $mg.L^{-1}.d^{-1}$), followed by Condition 3 (0.1 $mg.L^{-1}.d^{-1}$). Therefore *AD* and *CR* photosynthesize faster under Condition 3 and 1 respectively. Condition 0 is a reference point. Faster rates of O_2 production simply mean faster photosynthetic rates. The glucose from photosynthesis (Eq. 1) is assimilated in the production of biomass (Barsanti & Gualtieri, 2006). Hence the combination of a faster rate of photosynthesis ($+RO_2 > -RO_2$) and biomass productivity (Section *4.1.2.*) can shorten cultivation times or increase biomass weight (*DW*).

However, without efficient agitation, a faster $+RO_2$ causes increased O_2 levels and build-up in the cultivation vessel because O_2 is being produced faster ($+RO_2$) than it is being removed. As aforementioned, this is undesirable for enclosed large-scale algae cultivation necessary to provide lipid feed that can meet biodiesel demands.

Under Condition 2 (I = 60; S = 100) and 4 (I = 80; S = 100) a different phenomenon took place because negative rates of O_2 production ($-RO_2$) are observed (Figure 11). These suggest that O_2 was being removed faster than it was being produced ($+RO_2 < -RO_2$), which is a rather desirable than O_2 build-up. However one can argue that a negative rate ($-RO_2$) could suggest that photosynthesis has not occurred. This would mean that there was no growth (Section *4.1.1.*). Photosynthetic glucose molecules provide energy for cell maintenance and growth (Kiran, Kumar, & Deshmukh, 2014). Be that as it may, there was biomass production (BP) in both Condition 2 and 4, and therefore photosynthesis did occur under these conditions; although more productively under Condition 4 than 2. Hence $-RO_2$ means the rate of O_2 removal.

Furthermore, the opposite of photosynthesis (*i.e.* photorespiration), which consumes O_2 and yields CO_2 (Reece, *et al*., 2009), can be effectively eliminated by maintaining a high CO_2 concentration around the photosynthetic enzyme – RuBisCO (Cuellar-Bermudez, *et al*., 2013). In this study, algae were saturated with a high CO_2 concentration (100% CO_2 at F = 20 ml.min^{-1} for 2 h daily). This supports the notion that a net negative rate of O_2 production can be understood as a faster rate of O_2 removal ($-RO_2 > +RO_2$).

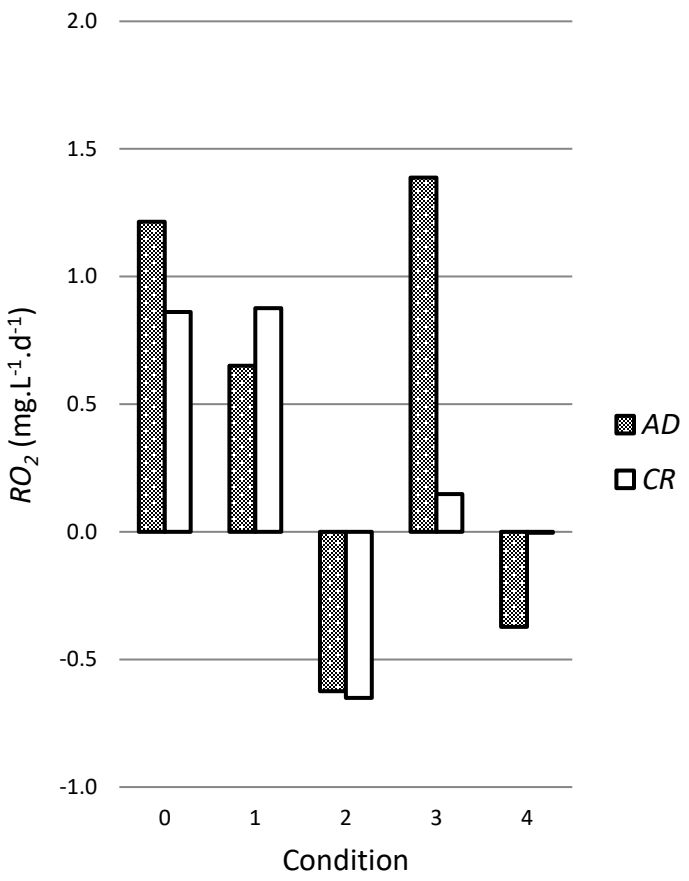


Figure 11. Maximum rate of O_2 production of *A. obliquus* and *Chlamydomonas* under different conditions (0, 1, 2, 3 & 4) (RO_2 = 0 is ideal)

Both algae cultures (*AD* & *CR*) experience their fastest rates of O_2 removal (0.6 and 0.7 mg.L^{-1}.d^{-1}) under Condition 2. As for Condition 4, the rate of production of O_2 in the *CR* culture equals the rate of removal ($+RO_2 = -RO_2$). Therefore equilibrium was reached, which suggests that the agitation speed (S = 100 rpm) employed was efficient in removing O_2 because it matched the photosynthetic rate ($+RO_2$) to avoid O_2 build-up. Therefore *CR* cultivated under Condition 4 (I = 80, S = 100) is the most desirable case with regards to photosynthetic O_2.

CHAPTER FIVE

This chapter states and discusses the outcomes related to algae lipid yield and the quality of the esterified algae oil (*i.e.* biodiesel).

5.1. Lipid extract yield

The lipid content (%*LC*) of *AD* and *CR* under all the conditions tested is shown and discussed in this section. The synergistic effect (e_{IS}) of light and agitation on %*LC* of algae is equal to the individual effects of light (e_I) and agitation (e_S). The ratios of these effects are all equal ($e_{IS}/e_I = e_{IS}/e_S = 1.001$). The effects are directly proportional to %*LC* ($e \rightarrow \%LC$). See APPENDIX C.1.

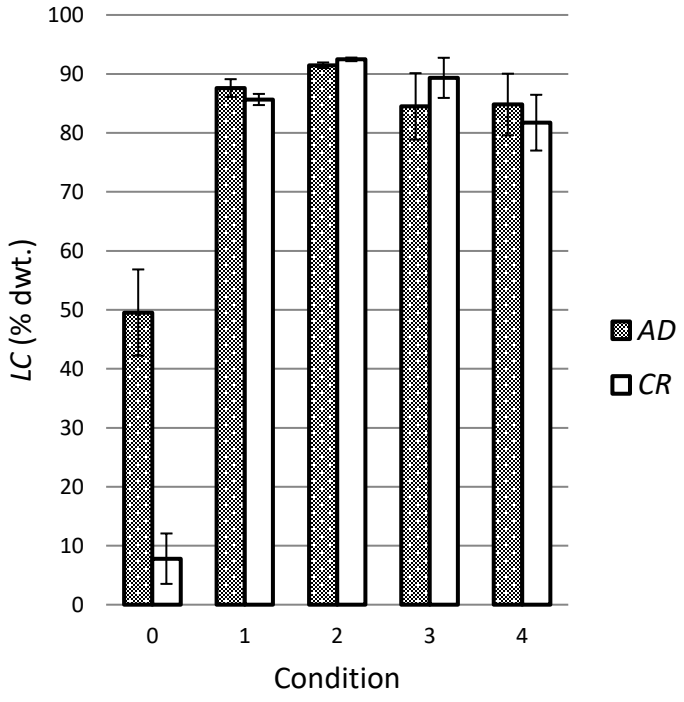


Figure 12. Percentage lipid extracts of *A. obliquus* and *Chlamydomonas* under different conditions (0, 1, 2, 3 & 4). Error bars represent *SD*.

As seen in Figure 12 both species have high extract yields, *i.e.* 65% dwt. and above, under all the core conditions (1, 2, 3 & 4) investigated. These lipid yields are higher than all those found by Griffiths *et al*. (2009) when studying 55 algae species. Condition 2 (I = 60; S = 100) produced the highest extract yields, 91 and 92% dwt. for *AD* and *CR* respectively. Whereas Condition 0 (I = 35; S = 150), as the baseline condition, produced the lowest extract yields, 50 and 8% dwt. for *AD* and *CR* respectively (Figure 12), because no net growth occurred. Photosynthetic growth must occur to provide the metabolite glyceraldehyde 3-phosphate (G3P), necessary for lipid biosynthesis (Lenka, et al., 2016). Therefore, the lipid yields observed under Condition 0 are lipids that were already present in the algae inoculum of both species. These could be representative of membrane lipids, because no deliberate triggering of TAGs was implemented (zero $NaHCO_3$ addition). These are unsuitable as biodiesel feed, because they can contain phosphorus, which inhibits the esterification reaction; and sulfur (*e.g.* sulfoquinovosyldiacylglycerol – SQDG), which pollutes the air upon combustion (Sharma, Singh, & Upadhyay, 2008). TAGs are often said to be the most desirable substrate to produce biodiesel (Christi, 2007; Hu *et al*., 2008).

High lipid content, has been reported close to 40-45% dwt. (Table 3), extracted using the Bligh and Dyer chloroform/methanol (2:1) solvent mixture for oleaginous microalgae (Singh & Mallick, 2014; Cancela, *et al*., 2016; Martínez, *et al*., 2017). However, algae investigated in this study accumulated extracts between 82-92% dwt. (Figure 12). Xia *et al*. (2015) used $NaHCO_3$ to trigger lipid storage, and extracted 41% dwt. total lipid from *Desmodesmus* sp., 18% of which were TAGs. In this study, $NaHCO_3$ was added on the 8th day to obtain higher extract yields (Figure 12) than Xia *et al*. (2015). This could mean that

AD and *CR* are oleaginous algae, like *B. braunii* (Nagaraja, *et al*., 2014). These values are higher than those of other authors (Table 3).

It could also be explained by the presence of membrane lipids, as already attributed to Condition 0. If lipids were detected for Condition 0, as seen in Figure 12, then the Bligh and Dyer method extracts other lipids in addition to TAGs (storage lipids). It could be that the high lipid content extracted in each of the core conditions, includes other lipids that were pre-existing in the algae cells prior to the storage of lipids (Mutanda, *et al*., 2011) which was triggered on the 8th day by adding $NaHCO_3$. Lipid productivities (*LP*s) can be used to assess whether storage lipid accumulation occurred or not (Griffiths & Harrison, 2009).

Many authors agree that TAGs accumulate during the stationary phase of growth (Lombardi & Wangersky, 1995; Lòpez Alonso *et al*., 1998; Hu *et al*., 2008). A closer look at the growth curves of each condition (Section *4.1.1.*) shows that both algae species experience a stationary phase under Condition 4 (I = 80; S = 100) only. This means that other conditions tested are unlikely to have stored lipids. In the next section, *LPs* of algae are discussed in relation to the accumulation of TAGs, and the pre-existence of lipids.

5.2. Lipid productivities

The lipid productivities (*LPs*) of *AD* and *CR* under all the conditions tested are shown in this section. *LP* was used to further understand the accumulation of storage lipids (TAGs). It is a product of the lipid content (%*LC*) and growth rate (μ) (see Eq. 7). *LPs*, together with biomass productivities (*BPs*), are important parameters of algae feed for biodiesel to be commercially viable. Lipid production via alkaline pH stress ($NaHCO_3$ addition) was the most efficient stage, because 81.52% of biomass carbon was assimilated into lipid.

As seen in Figure 13, there was relatively no lipid production for both algae species under Condition 0 (I = 35; S = 150) and 2 (I = 60; S = 100), and this confirms that the extract yield of *AD* and *CR* grown under these conditions does not represent stored lipid, *e.g.* TAGs. This is especially the case for Condition 2, even though both algae species contained the highest lipid extracts under Condition 2. Thus, the observed lipid extract yields represent membrane lipids, lipids other than TAGs (Athenstaedt & Daum, 2006).

AD is the most productive algae species for lipids (Figure 13). It was most productive (LP = 295 $mg.L^{-1}.d^{-1}$) under Condition 4 (I = 80; S = 100) (Figure 13). This is followed by Condition 1 (I = 80; S = 100) and 3. On the other hand, *CR* produces lipid under Condition 1 at a similar rate (97% similar) as when cultivated under Condition 4, with a mere 3 $mg.L^{-1}.d^{-1}$ difference in productivity. Thus, Condition 1 and 4 can be said to be the most suitable conditions for lipid production, with *AD* being the fastest storage lipid producing algae species between the two.

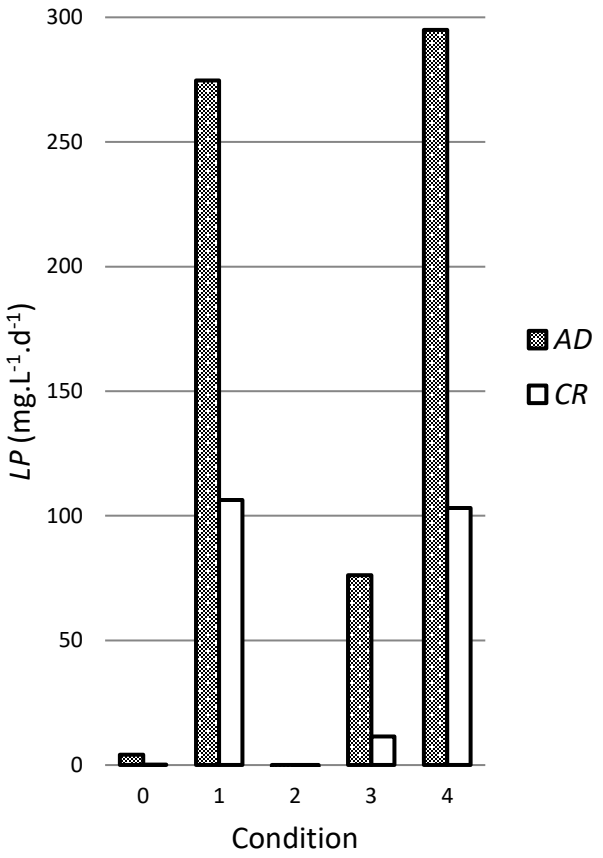


Figure 13. Maximum lipid productivities of *A. obliquus* and *Chlamydomonas* under different conditions (0, 1, 2, 3 & 4)

Under Condition 1 and 4, *AD* produces lipid faster than other freshwater chlorophytes: *Ankistrodesmus falcatus* (109 $mg.L^{-1}.d^{-1}$), *S. obliquus* (25 $mg.L^{-1}.d^{-1}$) and *C. vulgaris* (28 $mg.L^{-1}.d^{-1}$) (Becker, 1994). *CR*, under Condition 1 and 4, produces lipid at a similar rate (97.3% and 94.5%) to that of *A. falcatus* (Sheehan, *et al*., 1998). However, as mentioned above (Section 5.1.), TAGs accumulate during stationary phase of growth (Lombardi & Wangersky, 1995; Lòpez Alonso *et al*., 1998; Hu *et al*., 2008). Therefore, under Condition 1, these lipids are unlikely to be TAGs because no clear stationary phase was observed. Therefore, Condition 4 is suitable for high lipid productivities, and is thereby economically advantageous over the other conditions (Griffiths & Harrison, 2009).

Moreover, lipid production usually decreases biomass production because these biological processes occur inversely ($LP = 1/BP$) (Roopnarain, Sym, & Gray, 2014). This is not the case with Condition 4. Under this condition, both algae species remain highly productive in biomass, although they have a high lipid production rate. Therefore Condition 4 is more desirable.

5.3. FAME profile of esterified lipid

FAMEs were derived from the lipid extract via the reaction of transesterification using methanol as a reagent. FAMEs are an ester form of the parent FAs found in the lipid extract (Figure 3). The presence of a particular FAME in the profile of any algae species denotes the existence of its parent FA molecule in the lipid extract. That is, unlike the cultivation conditions, transesterification should not alter the type of FAs found in the extracted lipids (Stansell, Sym, & Gray, 2012). The FAME profile of both algae species grown under all the conditions tested is discussed in this section.

According to Knothe (2008), the ideal biodiesel contains methyl myristate (myristic acid), methyl palmitoleate (palmitoleic acid) and methyl oleate (oleic acid). This is a combination of saturated (SFAs) and mono-unsaturated FAMEs (MUFAs). Poly-unsaturated FAMEs (PUFAs) are unsuitable for biodiesel purposes (Popovich, *et al*., 2011). All conditions did not have algae species produce methyl myristate and palmitoleate (Table 8). However, under Condition 3 ($I = 80$; $S = 250$) and Condition 4 ($I = 80$; $S = 100$) *trans*-oleic acid (methyl elaidate) was produced by: both algae (Condition 3) and only *CR* (Condition 4).

Furthermore, under Condition 0 (I = 35; S = 150) *AD* also produced oleic acid (methyl oleate). Other conditions did not show any oleic acid production by algae, despite this FAME (together with palmitic and linoleic) being quite common in microalgae. *AD* produced palmitic acid under Condition 1 and 3; and *CR* under Condition 3. No linoleic acid was produced under Condition 1 (Table 8). It is not necessarily the presence of one of these FAMEs (myristic, palmitoleic or oleic) that is suitable, but rather the combination of these, which is a combination of one type of SFA and two types of MUFAs (ratio 1:2). In this study, no myristic and palmitoleic was produced, and a 1:1 ratio (SFA: MUFA) was obtained under Condition 1 and 3.

Additionally as per Table 8, the algae species cultivated under Condition 2 (I = 60; S = 100) did not produce any SFAs and MUFAs. It only produced a variety of PUFAs. Condition 4 (I = 80; S = 100) algae also produced a variety of PUFAs. Both conditions had an agitation speed of S = 100 rpm. Furthermore, under Condition 1 (I = 60; S = 250) and Condition 3 both algae only produced one type of PUFA each (Table 8). Both conditions had an agitation speed of S = 250 rpm. This may suggest that agitation increases or decrease the variety of PUFAs in the lipid extract (Aslanbay & Imamoglu, 2016).

Furthermore, Condition 0 (I = 35; S = 150) produced a lesser variety of PUFAs than Condition 2 (I = 60; S = 100) and Condition 4 (I = 80; S = 100), for both species, under an agitation speed of S = 150 rpm (Table 8). That is, only one type of PUFA by *AD* and two types of PUFA by *CR*. With two types of PUFA produced by *CR*, Condition 0 was more variable in PUFA than Condition 3 (I = 80; S = 250). This further supports the observation

that agitation could alter the variety (and possibly the concentration) of PUFAs ($S \rightarrow N_{PUFA}$) and FAMEs in general. Mixing algae culture exposes cells to different degrees of light which then influence the FA profile (Hu, *et al*., 2008; Ho, *et al*., 2012).

It can be seen in Table 8 that *CR* did not produce FAMEs under Condition 1 (I = 60; S = 250). One might think that this was due to the light intensity under Condition 1, because *CR* did produce FAMEs under Condition 3 (I = 80; S = 250); but *CR* also produced FAMEs under Condition 0 (I = 35; S = 150), which had the lowest light intensity. However, Condition 0 had a lower agitation speed (S = 150 rpm) than S = 250 rpm (Condition 1 & 3). This could mean that it was not solely the lower light intensity that was responsible for zero FAMEs in *CR* under Condition 1, but rather the combined effect (e_{IS}) of the lower light intensity and a higher agitation speed. Therefore for *CR* to produce FAMEs, a lower light intensity requires a lower agitation speed (as observed under Condition 0); or a higher agitation speed requires a higher light intensity (as observed under Condition 3).

With less variety in PUFA content and more in SFAs and MUFAs, Condition 1 (I = 60; S = 250) and Condition 3 (I = 80; S = 250) produced the most desirable FAME profile, although *CR* cannot produce any FAMEs under Condition 1.

Table 8: FAME identities of esterified algae oil from all conditions (0, 1, 2, 3 & 4)

FAME	Condition				
	0	**1**	**2**	**3**	**4**
			Saturated FAMEs (SFAs)		
Methyl palmitate	-	*AD*	-	*AD* & *CR*	-
Methyl stearate	*AD*	*AD*	-	*AD* & *CR*	*AD*
			Mono-unsaturated FAMEs (MUFAs)		
Methyl 10-undecenoate	-	-	-	*AD*	-
11,13-Dihydroxy-tetradec-5-ynoic acid, methyl ester	-	*AD*	-	-	-
Methyl oleate	*AD*	-	-	-	-
Methyl elaidate (*trans*-oleic acid)	-	-	-	*AD* & *CR*	*CR*
Methyl ricinoleate	-	-	-	*CR*	-
9-Octadecenoic acid, (2-phenyl-1,3-dioxolan-4-yl)methyl ester, *cis*-	-	*AD*	-	-	-
Methyl 10-octadecenoate	-	-	-	-	*AD*
			Poly-unsaturated FAMEs (PUFAs)		
[2H(4)]-Methyl 9-oxonona-5Z,7E-dienoate	-	*AD*	-	-	-
Methyl linoleate	*AD*	-	*AD* & *CR*	*AD* & *CR*	*CR*
Methyl linolelaidate		-	*CR*	-	*AD* & *CR*
Methyl isolinoleate	*CR*	-	*AD* & *CR*	-	*AD* & *CR*
Methyl 9,12-octadecadienoate	*CR*	-	*AD*	-	-
Methyl 11,14-eicosadienoate	-	-	*AD*	-	-

Thus, Condition 3 can be said to be more desirable than Condition 1 because both *AD* and *CR* produced a suitable combination of FAMEs, whereas *CR* produced no FAMEs under Condition 1 (therefore a comparison between the two microalgae cannot be done). However, Condition 3 does not provide the biomass and TAG productivity observed in both algae species under Condition 4. This is discussed in the next section.

Finally, having produced only PUFAs, Condition 2 (I = 60; S = 100) has the most undesirable FAME profile, with no SFAs and MUFAs produced.

5.4. Selection of the most suitable cultivation condition based on: biomass and lipid production

In this section, biomass productivity (*BP*), lipid productivity (*LP*) and lipid content (%*LC*) are considered together with other growth and lipid parameters in selecting the most desirable environmental condition to cultivate algae as biodiesel feedstock.

According to Griffiths and Harrison (2009), productivities (*BP* and *LP*) are the most important parameters to focus on, with *BP* being considered first. The highest *BP* and *LP* were achieved by both algae species under Condition 4 (I = 80; S = 100). This makes Condition 4 the most promising environmental candidate for algae cultivation for biodiesel purposes. Condition 1 produced the second-highest *LP*. Condition 1 (I = 80; S = 100), however, resulted in the lowest *BP*, even lower than Condition 0 (I = 35; S = 150). As mentioned in Section 5.2., the storage of lipids is inversely proportional to the production of biomass ($LP = 1/BP$) (Huerlimann, de Nys, & Heimann, 2010).

Lipid accumulation causes the cessation of algae growth (Roopnarain, Sym, & Gray, 2014). Hence a high *LP* would result in a low *BP (*Rodolfi*, et al., 2009;* Huerlimann, de Nys, & Heimann, 2010). This was not the case for Condition 4 and this is desirable.

Another important parameter to consider after *BP* and *LP* is the *%LC.* Under the core conditions (1, 2, 3 & 4) both species accumulated high percentages of lipid (> 40% dwt.). Therefore all these conditions produced desirable percentage extracts. Condition 2 (I = 60; S = 100) resulted in the highest percentage extracts from both species; but it also had the lowest *LP*s, and this is undesirable in the development of the algae biodiesel process (Griffiths & Harrison, 2009).

As a consequence of the considerations above, Condition 4 (I = 80; S = 100) was chosen as the most suitable. It produced the highest *BPs* and *LPs* for *AD* and *CR*.

5.5. Theoretical prediction of biodiesel properties: using $\%FAME_m$ values from Condition 4 (I = 80; S = 100)

In this section, the properties of the FAME mixture (*i.e.* biodiesel): saponification value (*SV*), iodine number (*IN*), cold-filter plugging point (*CFPP*), cetane number (*CN*) and viscosity (*V*) of the concerned feedstock were theoretically predicted from $\%FAME_m$ values (total of the $\%FAME_i$ concentrations) as outlined in Section 3.11. FAME concentrations are an important determining factor in investigating biodiesel fuel properties (Ramos, *et al*., 2009). These predicted fuel properties are discussed relative to the American (ASTM D6751-08**)** and European (EN 14214) standards, to

determine the quality of the FAME mixture produced under Condition 4 (I = 80; S = 100) – as this was selected as the most suitable condition (Section 5.4.) of all tested.

Firstly, the $\%FAME_i$ concentrations of both algae species are compared with each other, and then with those of the WCO fuel (Figure 14), because WCO has been reported as a favorable biodiesel feedstock option (Piker, *et al*., 2016; Sinha & Murugavelh, 2016; Bala, Misra, & Chidambaram, 2017).

The algae species with the most suitable biodiesel quality is further discussed in relation to literature findings (Section *5.5.5.*).

5.5.1. FAME concentration: comparison between A. obliquus and Chlamydomonas

It can be seen in Figure 14 that, methyl linolelaidate constitutes the largest proportion (94% and 67%) of FAME content ($\%FAME$) in *AD* and *CR* respectively. This is followed by methyl isolinoleate (5% and 26%). Yun *et al*. (2016) also found that *AD* produces methyl linolelaidate ($\%FAME_i$ = 3.7%), although under 14% CO_2. In the case of *CR*, it also produced methyl linoleate (5%). This FAME was not present in *AD*. These were the major FAMEs present, the remaining were below 2% of FAME content. None of these FAMEs were included in the ratio suggested by Knothe (2008) concerning an ideal biodiesel. One would then expect a poor biodiesel quality from these FAMEs, although *CR* also produced a stereoisomer of oleic acid: methyl elaidate (C18:1). Oleic acid is a desirable FAME (Knothe, 2008). On a basis of $\%FAME_m$ = 100%, *AD* and *CR* produced 98.9% and 98.1% PUFAs, respectively. *AD* fuel has more FAME content (35% more) than *CR* fuel.

The total FAME concentration of *AD* and *CR* is $\%FAME_m$ = 0.0410% and 0.0303% respectively. Having more FAME content is desirable because the European standard EN14214 requires a minimum of $\%FAME_m$ = 96.5% or more (Table 9).

5.5.2. FAME concentration: comparison between A. obliquus and waste cooking oil

WCO fuel had methyl palmitate (1.4%) and oleate (13%) but lacked myristate. As aforementioned, *AD* fuel (Figure 14) lacked all three of these FAMEs. Methyl linolelaidate constitutes the largest proportion (71%) of FAME content (*%FAME*) in WCO fuel, as is the case with *AD* fuel. This is followed by methyl oleate, and then methyl isolinoleate (7%) (Figure 14). WCO fuel (Figure 14) also had a variety of other methyl esters than *AD*. This clearly includes, in addition to palmitic- and oleic acid, hexadecadienoic acid (C16:2), which constitutes close to 5% of FAME content. All other FAMEs, such as methyl arachidate (C20:4), constitute less than 2% of content each. On a basis of $\%FAME_m$ = 100%, WCO produced 3.1% SFAs, 2.44% more than *AD*. *A. braunii* produced 78% SFAs and the biodiesel had V = 4.19 $mm^2 s^{-1}$ (meets standards) (Haik, *et al.*, 2011). The effect of *%FAME* of the algae species and WCO on biodiesel quality can be seen in Table 9.

5.5.3. Biodiesel quality: comparison between A. obliquus and Chlamydomonas

From the previous section, one would expect *AD* biodiesel to have suitable fuel properties than *CR* biodiesel because it is higher in *%FAME* (by 35%). Other than *CFPP*, which is equal across all feedstock investigated (Table 9), *AD* fuel has a higher *CN* (4054% more), *IN* (4036% more) and *V* (11363% more) than *CR* fuel. This suggests a short delay time in ignition, and a more unsaturated and viscous fuel (Stansell, Sym, & Gray, 2012).

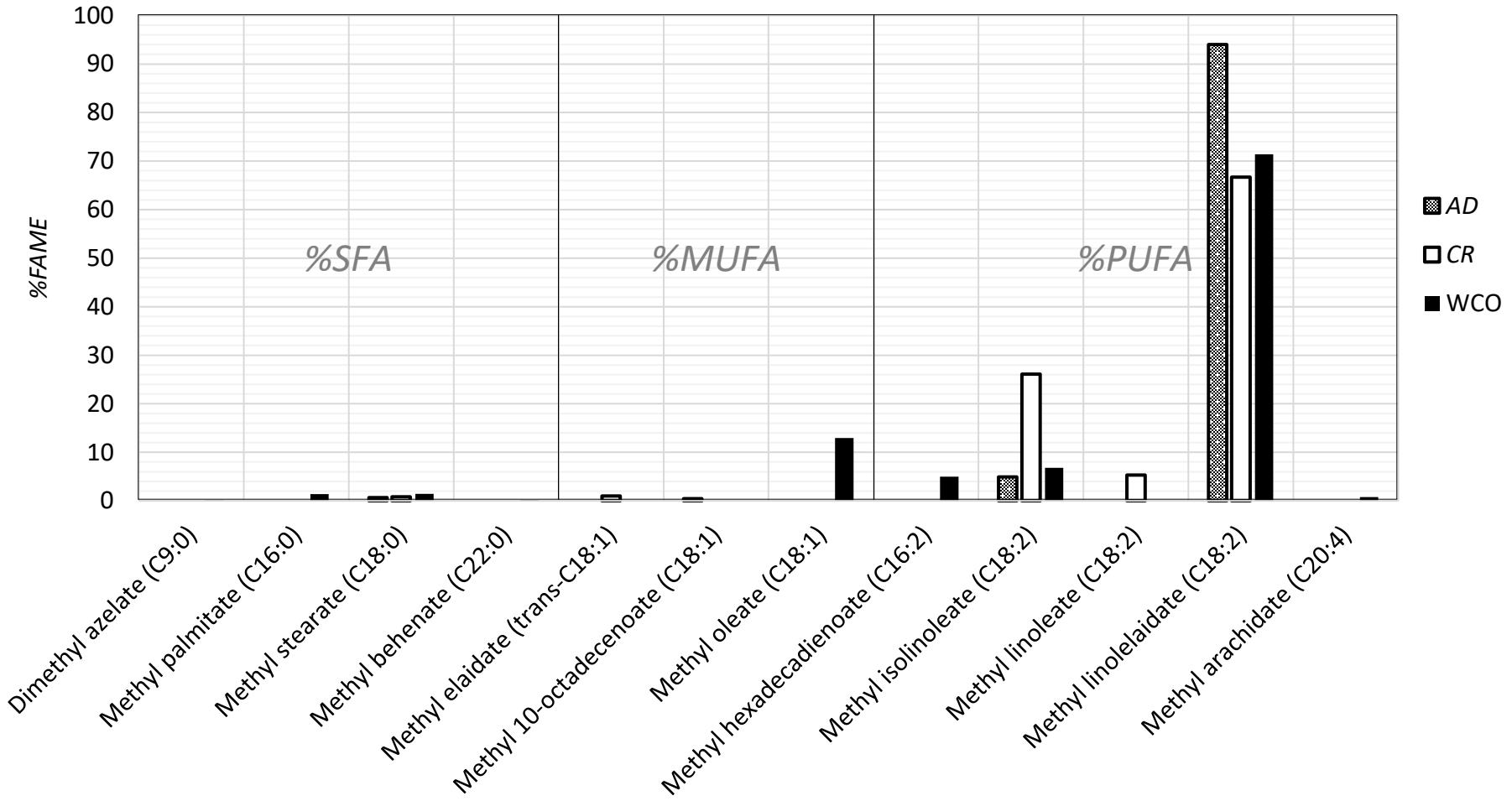


Figure 14. *%FAME* composition of microalgae and waste cooking oil under Condition 4 (*I* = 80; *S* = 100). The most common area value amongst a triplicate set (*n* = 3) was used to determine *%FAME* (Section *3.9.1.*)

AD fuel is more suitable than *CR* fuel because its *CN* and *V* are closer, by 1.12% and 2.45% respectively, to the lowest minimum limits (American standard). It is for this reason that the fuel quality of WCO is compared with that of *AD* fuel.

Table 9: Biodiesel quality from microalgae and waste cooking oil under Condition 4 (*I* = 80; *S* = 100)

Biodiesel property:	Condition 4		WCO	ASTM D6751-08 (American Standard)	EN 14214 (European Standard)
	AD	***CR***			
FAME concentration (*%FAME*)	0.0410	0.0303	0.0706	-	96.5 (min.)
Cetane number (*CN*)	0.54	0.013	0.030	47 (min.)	51 (min.)
Saponification value (*SV*) (mg KOH g^{-1}) (*also* acid value)	0.00078	0.00058	0.0013	0.50 (max.)	0.50 (max.)
Iodine number (*IN*) (g I_2 100 g^{-1})	0.0213	0.000515	0.00103	-	120 (max.)
Kinematic viscosity (*V*); 40°C (mm^2 s^{-1})	0.047	0.00041	0.0026	1.9-6.0	3.5-5.0
***CFPP* (°C)**	-17	-17	-17	0 (summer max.) -15 (winter max.)	-

5.5.4. Biodiesel quality: comparison between A. obliquus and waste cooking oil

As it can be seen in Table 9, the *CN* of WCO fuel is lower (by 94%) than that of *AD* fuel; although Islam *et al*. (2015) found microalgae (*C. cohnii*) to have a lower *CN* (20.7% lower) than WCO. Fuels with low *CN* tend to increase gaseous and particulate exhaust emissions because of incomplete combustion (Ramírez-Verduzco *et al*., 2012). This suggests a longer ignition delay time and thus a potentially slower combustion. The *SV* of the WCO fuel is

higher (by 67%), and its *IN* is lower (by 95%) than that of *AD* fuel, meaning that the WCO fuel is more acidic and saturated than the biodiesel produced from the *AD* algae species. Nevertheless, the *SVs* and *INs* of both fuels do not exceed the maximum standard limits, thereby being suitable with regards to acidity and unsaturation. Moreover, both fuels have a *CFPP* = -17°C, and this is advantageous because they meet the summer and winter cold-flow requirements. They are able to flow at -17°C and temperatures above; whereas Francisco *et al*. (2010) showed that *S. obliquus* (freshwater green microalgae, *CFPP* = 21°C) does not meet both summer and winter standard limits.

5.5.5. A. obliquus in relation to reported values

Several studies reported in literature (Table 4) meet the minimum limit of FAME concentration (%*FAME* = 96.5%) required in esterified algae oil. In this study, *AD* fuel contains %*FAME* = 0.0410%. This is 96.459% lower than the EN 14214 standard requirement. Only 0.001% of lipids produced by *AD* were converted to FAMEs (Figure 15 – Refer to APPENDIX C.2. for equations used in calculation). This means that slightly over 99% of lipids were not converted to FAMEs. The low *%FAME* may be the reason why *AD* fuel does not meet the standard *CN* and *V* minimum limits and range, because the non-FAME converted or unconverted lipid content could contain the essential biodiesel fatty acids (FAs): myristic (C14:0), palmitoleic (C16:1) and oleic (C18:1), said to be important as feed for the production of quality biodiesel fuel (Knothe, 2008).

The non-FAME content of *AD* under Condition 4, identified via GC-MS technique, is composed of alkanes and alkenes (Refer to APPENDIX B for complete list of compounds

identified). Other than linolelaidic acid, no FAs were identified in this non-FAME content. FAs have to be volatilized to be suitable for GC-MS identification. This is why the esterification reaction is necessary to produce FAMEs. Therefore, GC-MS analysis is likely to identify FAMEs than FAs. This means that if there were unconverted FAs present in the algae lipid extract, they were unidentified by GC-MS technique. In the case of *AD* under Condition 4, 48% of lipid content (*%LC*) was not identified. This could be unconverted FA content and possibly other less volatile compounds. Even so, *AD* remains the most suitable option amongst the feedstock investigated in this study (Section *5.5.3.* & *5.5.4.*).

The conversion of FAs to FAMEs was carried out via the transesterification reaction. This means a low $\%FAME_m$ or the presence of unconverted FA could have been the result of inefficient transesterification. Transesterification also affects *CN* and *V* because these are functions of the FAME content of individual FAMEs ($\%FAME_i$). In this study, sodium methoxide (CH_3ONa) was used as a catalyst under a 1:1 oil to alcohol ratio, and $T = 80^oC$ to yield $\%FAME_m = 0.041\%$ from *AD* oil extract. Stirring (S_t) was done briefly ($t = 0.033$ h) by handshaking before and after the reaction. Zeng *et al*. (2017) shows that an oil to alcohol ratio of 1:23, $T = 250^oC$ and $S_t = 50$ rpm yields $\%FAME_m = 97\%$ from soybean oil (Table 4), under the same catalyst and reaction time as in this study. Other researchers (Table 4) also reacted a higher alcohol volume relative to that of the oil and this has been reported to increase reaction efficiency (Sharma, Singh, & Upadhyay, 2008; Ehimen, Sun, & Carrington, 2010).

Even with an increased oil to alcohol ratio of 1:15 and direct transesterification (DT), Kim *et al*. (2014) yielded only $\%FAME_m$ = 55% from *Scenedesmus* sp. oil. Like this study, this also does not meet the EN14214 minimum limit. This could be the long reaction time (t = 10 h) (Table 4), because Silitonga *et al*. (2016) yielded more (30% more) in a shorter (75% shorter) reaction time than that of Kim *et al*. (2014), although this was from rubber oil extract. However, Silitonga *et al*. (2016) used S_t = 1000 rpm. A shorter reaction time, such as the one used in this study (t = 0.33 h), could require a faster stirring speed, such as that used by Silitonga *et al*. (2016). In this study, there was no stirring (S_t = 0 rpm) during esterification. This, together with a 1:1 oil to alcohol ratio, could have been contributing factors to the FAME yield of $\%FAME_m$ = 0.041% in the biodiesel.

CN, *V* and *IN* are also affected by the type of FAME produced during transesterification, unlike *SV*, which is not. In this study, no myristic and palmitoleic FAMEs were produced. In this work, both *AD* and *CR* were exposed to a 12:12 light-dark cycle at I = 80 and T = 25^{o}C for 12 days (100% CO_2) (Condition 4). In addition to unconverted FAs (as already suggested above), it could have been that myristic and palmitoleic FAs were not synthesized by both *AD* and *CR*. Yeo *et al*. (2011) found that a species of *Chlamydomonas* (*C. moewusii*) does not produce myristic and palmitoleic after a 2-week cultivation period under a 16:8 light-dark cycle at I = 70 and T = 28^{o}C (0.04% CO_2). Moreover, Gumbi *et al*. (2016) produced zero total FAMEs using a strain of *Chlamydomonas* (*Chlamydomonas* U2), although a low light intensity of I = 37 (similar to that of Condition 0) was employed. A lack of a particular FA in the FAME profile must be a result of the environmental conditions applied during lipid production (Krzeminska, *et al*., 2014), such as light

intensity, and thereby agitation (*S*). CO_2 concentration may also influence FAME profile (Cuellar-Bermudez, *et al*., 2015), as briefly discussed next.

Few studies (Yun, *et al*., 2015) have specifically investigated *AD* for biodiesel purposes, especially under high CO_2 conditions. *CR* (together with other green freshwater microalgae), is used to understand *AD* behavior because it is a model organism (Kim, *et al*., 2016). Other researchers showed that these algae types (green freshwater microalgae) produce myristic and palmitoleic FAMEs. Hu *et al*. (2014) and Wu & Miao (2014) found that *C. vulgaris* (grown under 15% CO_2) and *S. obliquus* (a type of *AD*) produced myristic and palmitoleic, at I = 81 and T = 25°C, during a cultivation period of 7 and 14 days respectively. Ho *et al*. (2015) showed that a 2-fold increase in light intensity produces and increases (by 1%) palmitoleic acid in *Chlamydomonas* sp. JSC4 (grown under 2% CO_2).

These suggest that a doubled light intensity, and a 15% CO_2 concentration or lower (although not lower than 2%) during FA synthesis, promote the production of myristic and palmitoleic acid; and thereby meet standard *CN*, *V*, and *IN* values. The rate of CO_2 fixation is dependent on the light intensity (Rodolfi, *et al*., 2009; Ho, *et al*., 2012). These are in synergy. Therefore, high CO_2 cultivation conditions, in turn, demand a high light intensity to provide ideal FAMEs for quality biodiesel.

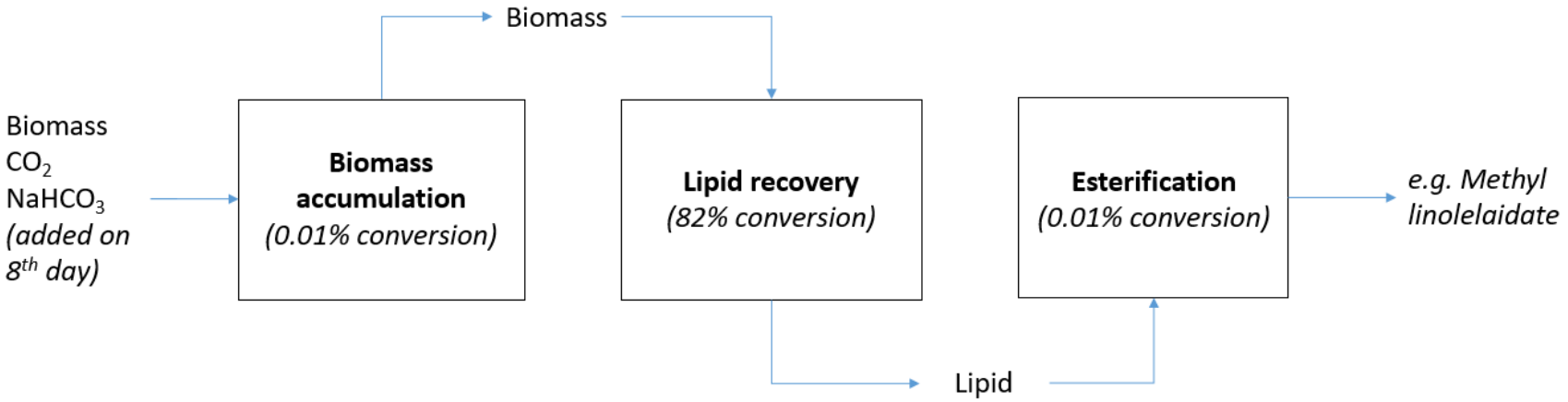


Figure 15. Summary of the carbon flow through the processes involved in studying *A. obliquus* FAMEs under Condition 4 (*I* = 80; *S* = 100)

CHAPTER SIX

6. CONCLUSIONS AND RECOMMENDATIONS

6.1. Conclusions

The growth parameters (growth rate, biomass productivity and dissolved oxygen), lipid productivities (*LP*s), and finally, FAME identity profiles and composition ($\%FAME_i$) of *Acutodesmus obliquus* (*AD*) and *Chlamydomonas* CC125 *(CR)* were investigated under $NaHCO_3$-fed and pure CO_2 conditions to answer the questions in Chapter 1:

1) Which algae species (*A. obliquus* or *Chlamydomonas*) is more productive in biomass and lipids? Under which condition?

Condition 4 (I = 80; S = 100) was the most suitable condition amongst those investigated for the cultivation of algae as biodiesel feedstock. Both algae species were most productive (robust) in biomass (*BP*) and lipid (*LP*) under this condition. *A. obliquus* was the more productive species, both in terms of biomass and lipid.

2) How much lipid can be extracted from $NaHCO_3$-fed algae?

A. obliquus and *Chlamydomonas* were confirmed as oleaginous algae species as they have shown to produce lipid yields as high as 82-92% dwt. With the stationary phase (lipid accumulation phase) clearly observed under Condition 4 only, storage lipids (*i.e.* TAGs) were produced by *A. obliquus* and *Chlamydomonas* cultivated under this condition. Lipid production, via alkaline pH stress ($NaHCO_3$ addition), was the most efficient stage involved in this study, with a carbon conversion of 82%.

3) What is the synergistic effect of light and agitation on lipid content (%*LC*)?

It was shown that the synergistic effect (e_{IS}) of light and agitation on the lipid content (%*LC*) of algae is the same as the individual effects of light (e_I) and agitation (e_S). The ratios of these effects are all equal ($e_{IS}/e_I = e_{IS}/e_S = 1.001$). The effects are directly proportional to the lipid content ($e \rightarrow \%LC$). The greater the effect, the more the content of lipid.

4) What type of fatty acid methyl esters (FAMEs) are present in the extract and how do these compare with those present in waste cooking oil (WCO)?

Regarding the FAME analysis, *A. obliquus* produced more linoelaidic- and isolinoleic acid than *Chlamydomonas*. Methyl linolelaidate and methyl isolinoleate were the dominant FAMEs produced by both *A. obliquus* and *Chlamydomonas*, and this was also found to be the case in the WCO fuel. *A. obliquus* fuel had more FAME content than *Chlamydomonas.*

5) What quality of biodiesel can be expected from these FAMEs?

Furthermore, *A. obliquus* produced the most suitable biodiesel than *Chlamydomonas* and WCO. Although *A. obliquus* biodiesel cetane number (*CN*) and kinematic viscosity (*V*) were found to be below the standard limits set by the American Society for Testing and Materials (ASTM D6751-08**)** and Européen de Normalisation (EN 14214), these remain the closest to the standard limits, relative to those of *Chlamydomonas* and WCO fuel. That is, *A. obliquus* fuel has the potential to burn faster and be more viscous than *Chlamydomonas* and WCO fuel. All feedstock (*AD*, *CR*, & WCO) met the saponification value (*SV*), iodine number (*IN*), and cold-flow plugging point (*CFPP*) limits – both the winter and summer limits. They had acceptable levels of acidity and unsaturation, and cold-flow properties.

This work confirms that: *A. obliquus* and *Chlamydomonas* can accumulate biomass under pure CO_2 conditions, although only under a suitable combination of light and agitation (*i.e.* Condition 4). The agitation speed, S = 100 rpm, is effective in establishing a stirring regime than can remove dissolved oxygen (*DO*) to avoid pressure build-up. Finally, alkaline pH stress (via the addition of $NaHCO_3$) can trigger the accumulation of lipid in algae (thereby confirming the work of Nascimento *et al*. (2013)).

6.2. Recommendations

The main goal of this research project was to explore the suitability of freshwater green microalgae, *A. obliquus* and *Chlamydomonas* CC125, as lipid feedstock for biodiesel, through a FAME profile that was used to estimate fuel quality. For this purpose, bench-scale experiments were more appropriate and feasible.

However, the cultivation of algae as lipid feedstock requires a large-scale approach to meet future biodiesel demand. With this in mind, the following should be considered:

1) Cultivate algae feedstock using sunlight (during midday), because it has an intensity (above I = 200 $\mu mol.m^{-2}.s^{-1}$) higher than lab-scale cool white light tubes, and it is provided at no cost. However, this would require a reactor specifically designed to maximize sunlight capture by the algae cells. Various configurations are available. Zero accumulation of *DO*, in the reactor, can be attained by *Chlamydomonas* (as shown Figure 11). Higher light intensity may also improve carbon conversion.

2) Large-scale cultivation of algae would require large volumes of water and nutrients. "Dirty" water resources containing the necessary growth nutrients should be investigated and incorporated into the algae cultivation stage. This may reduce costs associated with nutrients.

3) *A. obliquus* and *Chlamydomonas* produce fatty alcohols (*e.g.* 1-dodecanol – Condition 3 – APPENDIX B). These are typically used in the production of detergents and surfactants, and could form part of the biodiesel process to promote its economic viability. A techno-economic analysis could be performed on this.

4) Direct (*in situ*) transesterification could be performed rather than the two-stage approach (lipid extraction followed by transesterification). Chloroform is an effective but hazardous solvent. In this work, lipid extraction was performed in order to determine how much lipid *(%LC*) was accumulated by the algae species. Otherwise *in situ* transesterification could be a safer and less time-consuming approach.

Ultimately, future studies (*e.g.* PhD work) will be conducted, to improve the carbon conversions of algae cultivation and transesterification of lipid extract (Figure 15). The relationship between light- and CO_2- related parameters, will be thoroughly studied; together with the relationship between transesterification reaction conditions and *%FAME*, as these questions were beyond the scope proposed in this work.

REFERENCES

Amini, Z., Ong, H. C., Harrison, M. D., Kusumo, F., Mazaheri, H., & Ilham, Z. (2017). Biodiesel production by lipase-catalyzed transesterification of *Ocimum basilicum* L. (sweet basil) seed oil. *Energy Conversion and Management, 132*, 82-90.

Antizar-Ladislao, B., & Turrion-Gomez, J. L. (2008). Second-generation biofuels and local bioenergy systems. *Biofuels, Bioproducts and Biorefining, 4*, 455-469.

Aslanbay, B., Demirel, Z., & Imamoglu, E. (2016). Evaluation of air flow rate on the growth of *Haematococcus pluvialis*. *International Journal of Chemical, Environmental & Biological Sciences, 4*(1), 2320-4087.

Athenstaedt, K., & Daum, G. (2006). The life cycle of neutral lipids: Synthesis, storage and degradation. *Cellular and Molecular Life Sciences , 63*, 1355-1369.

Bala, D. D., Misra, M., & Chidambaram, D. (2017). Solid-acid catalyzed biodiesel production, part I: Biodiesel synthesis from low quality feedstock. *Journal of Cleaner Production, 142*, 4169-4177.

Bamgboye, A., & Hansen, A. (2008). Prediction of cetane number of biodiesel fuel from the fatty acid methyl ester (FAME) composition. *International Agrophysics, 22*(1), 21-29.

Banerjee, A., Sharma, R., Christi, Y., & Banerjee, U. C. (2002). *Botryococcus braunii*: A renewable source of hydrocarbons and other chemicals. *Critical Reviews in Biotechnology, 22*(3), 245-279.

Barsanti, L., & Gualtieri, P. (2006). *Algae: Anatomy, biochemistry, and biotechnology*. Boca Raton, FL: CRC Press.

Becker, E.W. (1994). *Microalgae: Biotechnology and Microbiology*, Cambridge, UK: Cambridge University Press.

Bellou, S., Baeshen, M. N., Elazzay, A. M., Aggeli., D., Fotoon, S., & Aggells, G. (2014). *Microalgal lipids biochemistry and biotechnological perspectives, 32*(8), 1476-1493.

Bligh, E. G., & Dyer, W. J. (1959). A rapid method of total lipid extraction and purification. *Canadian Journal of Biochemistry and Physiology, 37*(8), 911-917.

Breuer, G., Evers, W. A., de Vree, J. H., Kleinegris, D. M., Martens, D. E., Wijffels, R. H., & Lamers, P. P. (2013). Analysis of fatty acid content and composition in microalgae. *Journal of Visualized Experiments*.

Botineştean, C., Hădărugă, N. G., Hădărugă, D. I., & Jianu, I. (2012). Fatty acids composition by gas chromatography – mass spectrometry (GC-MS) and most

important physicalchemicals parameters of tomato seed oil. *Journal of Agroalimentary Processes and Technologies, 18* (1), 89-94.

Cai, T., Park, S. Y., & Li, Y. (2013). Nutrient recovery from wastewater streams by microalgae: Status and prospects. *Renewable and Sustainable Energy Reviews, 19*, 360-369.

Campbell, M. K., & Farrell, S. O. (2012). *Biochemistry* (7th ed.). Boston: Brooks/Cole Centage Learning.

Cancela, A., Maceiras, R., Garcia, B., Alfonsin, V., & Sanchez, A. (2016). Harvesting and lipids extraction of *Pavlova Lutheri*. *Environmental Progress & Sustainable Energy*.

Carvalho, A. K., da Conceição, L. R., Silva, J. P., Perez, V. H., & de Castro, H. F. (2017). Biodiesel production from *Mucor circinelloides* using ethanol and heteropolyacid in one and two-step transesterification. *Fuel, 202*, 503-511.

Christi, Y. (2007). Biodiesel from microalgae. *Biotechnology Advances , 25*, 294-306.

Cronan, J. E., & Waldrop, G. L. (2002). Multi-subunit acetyl-CoA carboxylases. *Progress in Lipid Research, 41*(5), 407-435.

Cuellar-Bermudez, S. P., Garcia-Perez, J. S., Rittmann, B. E., & Parra-Saldivar, R. (2015). Photosynthetic bioenergy utilizing CO_2: An approach on flue gases utilization for third generation biofuels. *Journal of Cleaner Production, 98*, 53-65.

Damiani, C. M., Popovich, C. A., Constenla, D., & Leonardi, P. I. (2010). Lipid analysis in *Haematococcus pluvialis* to assess its potential. *Bioresource Technology, 101*, 3801-3807.

Demirbas, A. H. (2009). Inexpensive oil and fats feedstocks for production of biodiesel. *Energy Education Science and Technology Part A, 23*, 1-13.

Demirbas, A., & Demirbas, M. F. (2011). Importance of algae oil as a source of biodiesel. *Energy Conservation and Management, 52*(1), 163-170.

Demirbas, M. F. (2011). Biofuels from algae for sustainable development. *Applied Energy, 88*(10), 3473-3480.

Dharma, S., Masjuki, H., Ong, H. C., Sebayang, A., Silitonga, A., Kusumo, F., & Mahlia, T. (2016). Optimization of biodiesel production process for mixed *Jatropha curcas–Ceiba pentandra* biodiesel using response surface methodology. *Energy Conversion and Management, 115*, 178-190.

Dunn, R., & Bagby, M. (1995). Low-temperature properties of triglyceride-based diesel fuels: Transesterified methyl esters and petroleum middle distillate/ester blends. *Journal of the American Oil Chemists' Society, 72*(8), 895-904.

Ehimen, E., Sun, Z., & Carrington, C. (2010). Variables affecting the in situ transesterification of microalgae lipids. *Fuel, 89*(3), 677-684.

ExxonMobil. (2017). *Outlook for Energy: Journey to 2040*. Retrieved February 2017, from http://corporate.exxonmobil.com/en/energy/energy-outlook/highlights

Fakhry, E. M., & El Maghraby, D. M. (2013). Fatty acids composition and biodiesel characterization of *Dunaliella salina. Journal of Water Resource and Protection, 5*, 894-899.

Folch, J., Lees, M., & Stanley, G. (1957). A simple method for the isolation and purification of total lipids from animal tissues. *The Journal of Biological Chemistry, 226*(1), 497-509.

Francisco, É. C., Neves, D. B., Jacob-Lopes, E., & Franco, T. T. (2010). Microalgae as feedstock for biodiesel production: Carbon dioxide sequestration, lipid production and biofuel quality. *Journal of Chemical Technology and Biotechnology, 85*(3), 395-403.

Fukuda, H., Kondo, A., & Noda, H. (2001). Biodiesel fuel production by transesterification of oils. *Journal of Bioscience and Bioengineering, 92*(5), 405-416.

Gardner, R., Peters, P., Peyton, B., & Cooksey, K. E. (2011). Medium pH and nitrate concentration effects on accumulation of triacylglycerol in two members of the Chlorophyta. *Journal of Applied Phycology, 23*, 1005-1016.

Griffiths, M. J., & Harrison, S. T. (2009). Lipid productivity as a key characteristic for choosing algal species for biodiesel production. *Journal of Applied Phycology, 21*, 493-507.

Griffiths, M. J., van Hille, R. P., & Harrison, S. T. (2010). Selection of direct transesterification as the preferred method for assay of fatty acid content of microalgae. *Lipids, 45*, 1053-1060.

Griffiths, M. J., van Hille, R. P., & Harrison, S. T. (2012). Lipid productivity, settling potential and fatty acid profile of 11 microalgal species grown under nitrogen replete and limited conditions. *Journal of Applied Phycology, 24*, 989-1001.

Guldhe, A., Singh, B., Rawat, I., Ramluckan, K., & Bux, F. (2014). Efficacy of drying and cell disruption techniques on lipid recovery from microalgae for biodiesel production. *Fuel, 128*, 46-52.

Gumbi, S. T., Majeke, B. M., Olaniran, A. O., & Mutanda, T. (2017) Isolation, identification and high-throughput screening of neutral lipid producing indigenous microalgae from South African aquatic habitats. *Applied Biochemistry and Biotechnology, 182* (1), 382-399.

Haik, Y., Selim, M. Y. E., Abdulrehman, T. (2011). Combustion of algae oil methyl ester in an indirect injection diesel engine. *Energy, 36*(3), 1827-1835.

Halim, R., Danquah, M. K., & Webley, P. A. (2012). Extraction of oil from microalgae for biodiesel production: A review. *Biotechnology Advances, 30*(3), 709-732.

Halim, R., Gladman, B., Danquah, M. K., & Webley, P. A. (2011). Oil extraction from microalgae for biodiesel production. *Bioresource Technology, 102*(1), 178-185.

Hanagata, N., Takeuchi, T., Fukuju, Y., Barnes, D. J., & Karube, I. (1992). Tolerance of microalgae to high CO_2 and high temperature. *Phytochemistry, 31*(10), 3345-3348.

Harding, K. G., Dennis, J. S., von Blottnitz, H., & Harrison, S. T. (2008). A life-cycle comparison between inorganic and biological catalysis for the production of biodiesel . *Journal of Cleaner Production, 16*, 1368-1378.

Ho, S. H., Chen, C. Y., & Chang, J. S. (2012). Effect of light intensity and nitrogen starvation on CO_2 fixation and lipid/carbohydrate production of an indigenous microalga *Scenedesmus obliquus* CNW-N. *Bioresource Technology*, 244-252.

Ho, S. H., Huang, S. W., Chen, C. Y., Hasunuma, T., Kondo, A., & Chang, J. S. (2013). Characterization and optimization of carbohydrate production from an indigenous microalga *Chlorella vulgaris* FSP-E. *Bioresource Technology, 135*, 157-165.

Ho, S., Nakanishi, A., Ye, X., Chang, J., Chen, C., Hasunuma, T., & Kondo, A. (2015). Dynamic metabolic profiling of the marine microalga *Chlamydomonas* sp. JSC4 and enhancing its oil production by optimizing light intensity. *Biotechnology for Biofuels, 8*, 48.

Hu, Q., Sommerfield, M., Jarvis, E., Ghirardi, M., Posewitz, M., Seiber, M., & Darzins, A. (2008). Microalgal triacylglycerols as feedstocks for biofuel production: Perspectives and advances. *The Plant Journal, 54*, 621-639.

Hu, Q., Zeng, R., Zhang, S.-X., Yang, Z.-H., & Huang, H. (2014). Production of microalgal lipids as biodiesel feedstock with fixation of CO_2 by *Chlorella vulgaris*. *Food Technology and Biotechnology, 52*(3), 285-291.

Huerlimann, R., de Nys, R., & Heimann, K. (2010). Growth, lipid content, productivity and fatty-acid composition of tropical microalgae for scale-up production. *Biotechnology and Bioengineering , 107*(2), 245-257.

Islam, M. A., Rahman, M. M., Heimann, K., Nabi, M. N., Ristovski, Z. D., Dowell, A., Thomas, G., Feng, B., von Alvensleben, N., & Brown, R. J. (2015).Combustion analysis of microalgae methyl ester in a common rail direct injection diesel engine. *Fuel, 143*, 351-360.

Jaworski, J., & Cahoon, E. B. (2003). Industrial oils from transgenic plants. *Current Opinion in Plant Biology, 6*(2), 178-184.

Joyard, J., Ferro, M., Masselon, C., Seigneurin-Berny, D., Salvi, D., Garin, J., & Rolland, Norbert. (2010). Chloroplast proteomics highlights the subcellular compartmentation of lipid metabolism. *Progress in Lipid Research, 49*(2), 128-158.

Karemore, A., Ramalingam, D., Yadav, G., Subramanian, G., & Sen, R. (2015). Photobioreactors for improved algal biomass production: Analysis and design considerations. In D. Das (Ed.), *Algal Biorefinery: An Integrated Approach* (pp. 103-124). Capital Publishing Company.

Kativu, E., Hildebrandt, D., Matambo, T., & Glasser, D. (2012). Effects of CO_2 on South African freshwater microalgae growth. *Environmental Progress & Sustainable Energy, 31*(1), 24-28.

Kim, E. J., Jung, W., Lim, S., Kim, S., Han, S. J., & Choi, H.-G. (2016). Growth and lipid content at low temperature of Arctic alga *Chlamydomonas* sp. KNM0029C. *Bioprocess and Biosystems Engineering, 39*, 151-157.

Kim, G. V., Choi, W., Kang, D., Lee, S., & Lee, H. (2014). Enhancement of biodiesel production from marine alga, *Scenedesmus* sp. through *in situ* transesterification process. *BioMed Research International*.

Kiran, B., Kumar, R., & Deshmukh, D. (2014). Perspectives of microalgal biofuels as a renewable source of energy. *Energy Conversion and Management, 88*, 1228-1244.

Kishimoto, M., Okakura, T., Nagashima, H., Minowa, T., Yokoyama, S.-Y., & Yamaberi, K. (1994). CO_2 fixation and oil production using micro-algae. *Journal of Fermentation and Bioengineering, 78*(6), 479-482.

Knothe, G. (2005). Dependence of biodiesel fuel properties on the structure of fatty acid alkyl esters. *Fuel Process Technology, 86*, 1059-1070.

Knothe, G. (2008). "Designer" biodiesel: Optimizing fatty ester composition to improve fuel properties. *Energy Fuels, 22*(2), 1358-1364.

Knothe, G. (2009). Improving biodiesel fuel properties by modifying fatty ester composition. *Energy and Environmental Science , 2*(7), 759-766.

Knothe, G., & Steidley, K. R. (2005). Kinematic viscosity of biodiesel fuel components and related compounds. Influence of compound structure and comparison to petrodiesel fuel components. *Fuel, 84*, 1059-1065.

Krzeminska, I., Pawlik-Skowronska, B., Trzcinska, M., & Tys, J. (2014). Influence of photoperiods on the growth rate and biomass productivity of green microalgae. *Bioprocess and Biosystems Engineering , 37*, 735-741.

Kumar, P., Suseela, M. R., & Toppo, K. (2011). Physico-chemical characterization of algal oil: A potential biofuel. *Asian Journal of Experimental Biological Science, 2*(3), 493-487.

Kumar, V. R., & Melchias, G. (2014). Effect of temperature on the lipid content in *Nannochloropsis oculata*, *Dunaliella salina* and *Isochrysis galbana* for biodiesel production. *International Journal of Pharma and Bio Sciences, 5*(4), 499-506.

Kunst, L., & Samuels, L. (2009). Plant cuticles shine: Advances in wax biosynthesis and export. *Current Opinion in Plant Biology, 12*(6), 721-727.

Lee, S., Go, S., Jeong, G., & Kim, S. (2011). Oil production from five marine microalgae for the production of biodiesel. *Biotechnology and Bioprocess Engineering , 16*(3), 561-566.

Leite, G. B., Abdelaziz, A. E., & Hallenback, P. C. (2013). Algal biofuels: Challenges and opportunities. *Bioresource Technology, 145*, 134-141.

Lenka, S. K., Carbonaro, N., Park, R., Miller, S. M., Thorpe, I., & Li, Y. (2016). Current advances in molecular, biochemical, and computational modeling analysis of microalgal triacylglycerol biosynthesis. *Biotechnology Advances, 34*(5), 1046-1063.

Li-Beisson, Y., Shorrosh, B., Beisson, F., Andersson, M. X., Arondel, V., Bates, P. D., Baud, S., Bird, D., DeBono, A., Durrett, T. P., Franke, R. B., Graham, I. A., Katayama, K., Kelly, A. A., Larson, T., Markham, J. E., Miquel, M., Molina, I., Nishida, I., Rowland, O., Samuels, L., Schimd, K. M., Wada, H., Welti, R., Xu, C., Zallot, R., & Ohlrogge, J. (2013). Acyl-lipid metabolism. *The Arabidopsis Book, 9*, 161.

Lin, C.-Y., & Lin, B.-Y. (2015). Fatty acid characteristics of *Isochrysis galbana* lipids extracted using a microwave-assisted method. *Energies, 8*, 1154-1165.

Liu, Z. Y., Wang, G. C., & Zhou, B. C. (2008). Effect of iron on growth and lipid accumulation in *Chlorella vulgaris*. *Bioresource Technology, 99*, 4717-4722.

Livne, A., & Sukenik, A. (1992). Lipid synthesis and abundance of Acetyl CoA Carboxylase in *Isochrysis galbana* (Prymnesiophyceae) following nitrogen starvation. *Plant and Cell Physiology, 33*(8), 1175-1181.

Lombardi, A. T., & Wangersky, P. J. (1995). Particulate lipid class composition of three marine phytoplankters *Chaetoceros gracilis*, *Isochrysis galbana* (Tahiti) and *Dunaliella tertiolecta* grown in batch culture. *Hydrobiologia, 306*, 1-6.

Lopes, J. C. A., Boros, L., Krähenbühl, M. A., Meirelles, A. J. A, Daridon, J. L., Pauly, J., Marrucho, I. M., & Coutinho, J. A. P. (2013). Prediction of cloud points of biodiesel. *Energy Fuels, 22*(2), 747-752.

López Alonso, D., Belarbi, E. H., Rodríguez-Ruiz, J., Segura, C. I., Jiménez, A. (1998). Acyl lipids of three microalgae. *Phytochemistry, 47*, 1473-1481.

Ma, F., & Hanna, M. A. (1999). Biodiesel prodcution: A review. *Bioresource Technology, 70*(1), 1-15.

Maeda, K., Owada, M., Kimura, N., Omata, K., & Karube, I. (1995). CO_2 fixation from the flue gas on coal fired thermal power plant by microalgae. *Energy Conversion and Management, 36*, 717-720.

Maity, J. P., Bundschuh, J., Chen, C.-Y., & Bhattacharya, P. (2014). Microalgae for third generation biofuel production, mitigation of greenhouse gas emissions and wastewater treatment: Present and future perspectives – A mini review. *Energy, 78*, 104-113.

Mandotra, S. L., Kumar, P., Suseela, M., Nayaka, S., & Ramteke, P. W. (2016). Evaluation of fatty acid profile and biodiesel properties of microalga *Scenedesmus abundans* under the influence of phosphorus, pH and light intensities. *Bioresource Technology , 201*, 222-229.

Martínez, N., Callejas, N., Morais, E. G., Costa, J. A., Jachmanián, I., & Vieitez, I. (2017). Obtaining biodiesel from microalgae oil using ultrasound-assisted *in-situ* alkaline transesterification. *Fuel, 202*, 512-519.

Mata, T. M., Martins, A. A., & Caetano, N. S. (2010). Microalgae for biodiesel production and other applications: A review. *Renewable and Sustainable Energy Reviews, 14*(1), 217-232.

Mercer, P., & Armenta, R. E. (2011). Developments in oil extraction from microalgae. *European Journal of Life Science and Technology , 113*(5), 539-547.

Meher, L., Vidyasagar, D., & Naik, S. (2006). Technical aspects of biodiesel production by transesterification – A review. *Renewable and Sustainable Energy Reviews*, *10*(3), 248-268.

Metzger, P., & Largeau, C. (2005). *Botryococcus braunii*: A rich source for hydrocarbons and related ether lipids. *Applied Microbiology and Biotechnology, 66*(5), 486-496.

Miao, X., & Wu, Q. (2006). Biodiesel production from heterotrophic microalgal oil. *Bioresource Technology, 97*(6), 841-846.

Miao, X., Wu, Q., & Yang, C. (2004). Fast pyrolysis of microalgae to produce renewable fuels. *Journal of Analytical and Applied Pyrolysis, 71*(2), 855-863.

Mohsenpour, S. F., & Willoughby, N. (2013). Luminescent photobioreactor design for improved algal growth and photosynthetic pigment production through spectral conversion of light. *Bioresource Technology, 142*, 147-153.

Mutanda, T., Desikan, R., Karthikeyan, S., & Bux, F. (2011). Bioprospecting for hyper-lipid producing microalgal strains for sustainable biofuel production. *Bioresource Technology , 102*(1), 57-70.

Myers, R. H., Montgomery, D. C., & Anderson-Cook, C. M. (2009). *Response Surface Methodology* (3rd ed.). Hoboken, New Jersey: Wiley & Sons.

Nagaraja, Y., Biradar, C., Manasa, K., & Venkatesh, H. (2014). Production of biofuel by using microalgae (*Botryococcus braunii*). *International Journal of Current Microbiology and Applied Sciences, 3*(4), 851-860.

Narula, V., Thakur, A., Uniyal, A., Kalra, S., & Jain, S. (2017). Process parameter optimization of low temperature transesterification of algae-*Jatropha Curcas* oil blend. *Energy, 119*, 983-988.

Nascimento, I. A., Marques, S. S., Cabanelas, I. T., Pereira, S. A., Druzian, J. I., de Souza, C. O., . . . Nascimento, M. A. (2013). Screening microalgae strains for biodiesel production: lipid productivity and estimation of fuel quality based on fatty acids profiles as selective criteria. *Bioenergy Research, 6*, 1-13.

NOAA. (2016). *National Ocean Service*. Retrieved February 2017, from http://oceanservice.noaa.gov/facts/oceanwater.html

Nongbe, M. C., Ekou, T., Ekou, L., Yao, K. B., Le Grognec, E., & Felpin, F.-X. (2017). Biodiesel production from palm oil using sulfonated graphene catalyst. *Renewable Energy, 106*, 135-141.

NTNU. (2015). *Phys.org*. Retrieved October 9, 2017, from https://phys.org/news/2015-05-downside-biodiesel-fuel.html

Ohlrogge, J., & Browse, J. (1995). Lipid biosynthesis, *The Plant Cell, 7*, 957-970.

O'Neil, G. W., Knothe, G., Williams, J. R., Burlow, N. P., Culler, A. R., Corliss, J. M., . . . Reddy, C. M. (2014). Synthesis and analysis of an alkenone-free biodiesel from *Isochrysis* sp. *Energy & Fuels, 28*, 2677-2683.

Onukwuli, D. O., Emembolu, L. N., Ude, C. N., Aliozo, S. O., & Menkiti, M. C. (2017). Optimization of biodiesel production from refined cotton seed oil and its characterization. *Egyptian Journal of Petroleum, 26*, 103-110.

Pandey, R. K., Rehman, A., & Sarviya, R. M. (2012). Impact of alternative fuel properties on fuel spray behavior and atomization. *Renewable and Sustainable Energy Reviews, 16*(3), 1762-1778.

Patel, R. L., & Sankhavara, C. (2017). Biodiesel production from Karanja oil and its use in diesel engine: A review. *Renewable and Sustainable Energy Reviews, 71*, 464-474.

Peña, M. R. D. (2007). Cell growth and nutritive value of the tropical benthic diatom, *Amphora* sp., at varying levels of nutrients and light intensity, and different culture locations. *Journal of Applied Phycology, 19*(6), 647-655.

Piker, A., Tabah, B., Perkas, N., & Gedanken, A. (2016). A green and low-cost room temperature biodiesel production method from waste oil using egg shells as catalyst. *Fuel, 182*, 34-41.

Popovich, C. A., Damiani, C., Constenla, D., Martínez, A. M., Freije, H., Giovanardi, M., . . . Leonardi, P. I. (2012). *Neochloris oleoabundans* grown in enriched natural seawater for biodiesel feedstock: Evaluation of its growth and biochemical composition. *Bioresource Technology, 114*, 287-293.

Popovich, C. A., Damiani, C., Costenla, D., & Leonardi, P. I. (2011). Lipid quality of the diatoms *Skeletonema costatum* and *Navicula gregaria* from the South Atlantic Coast (Argentina): Evaluation of its suitability as biodiesel feedstock. *Journal of Applied Phycology, 24*, 1-10.

Pulz, O. (2001). Photobioreactors: Production systems for phototrophic microorganisms. *Applied Microbiology and Biotechnology, 57*(3), 287-293.

Pulz, O., & Gross, W. (2004). Valuable products from biotechnology of microalgae. *Applied Microbiology and Biotechnology, 65*(6), 635-648.

Ramírez-Verduzco, L.F., Rodríguez-Rodríguez, J.E., Jaramillo-Jacob, A.D.R. (2012). Predicting cetane number, kinematic viscosity, density and higher heating value of biodiesel from its fatty acid methyl ester composition. *Fuel, 91*, 102–111.

Ramos, M. J., Fernández, C. M., Casas, A., Rodríguez, L., & Pérez, A. (2009). Influence of fatty acid composition of raw materials on biodiesel properties. *Bioresource Technology, 100*(1), 261-268.

Rawat, I., Kumar, R., Mutanda, T., & Bux, F. (2013). Biodiesel from microalgae: A critical evaluation from laboratory to large scale production. *Applied Energy, 103*, 444-467.

Reece, J. B., Urry, L. A., Cain, M. L., Wasserman, S. A., Minorsky, P. V., & Jackson, R. B. (2009). *Campbell Biology* (9th ed.). Benjamin Cummings.

Regan, D., & Gartside, G. (1983). *Liquid fuels from micro-algae in Australia.* Melbourne: CSIRO.

Richmond, A. (2004). *Handbook of microalgal culture: Biotechnology and applied phycology.* Blackwell Science Ltd.

Rodolfi, L., Zittelli, G. C., Bassi, N., Padovani, G., Biondi, N., Bonini, G., Tredici, M. R. (2009). Microalgae for oil: Strain selection, induction of lipid synthesis and outdoor

mass cultivation in a low-cost photobioreactor. *Biotechnology and Bioengineering, 102*, 100–112.

Rogelj, J., Nabel, J., Chen, C., Hare, W., Markmann, K., Meinshausen, M., . . . Höhne, N. (2010). Copenhagen Accord pledges are paltry. *Nature, 464*(7292), 1126-1128.

Roopnarain, A., Sym, S. D., & Gray, V. M. (2014). Effect of nitrogenous resource on growth, biochemical composition and ultrastructure of *Isochrysis galbana* (Isochrysidales Haptophyta). *Phycological Research, 63*(1), 43-50.

Sáncheza, Á., Maceiras, R., Cancela, Á., & Péreza, A. (2013). Culture aspects of *Isochrysis galbana* for biodiesel production. *Applied Energy , 101*, 192-197.

Santin, C. M., Michelin, S., Scherer, R. P., Valério, A., di Luccio, M., Oliveira, D., & Oliveira, J. V. (2017). Comparison of macauba and soybean oils as substrates for the enzymatic biodiesel production in ultrasound-assisted system. *Ultrasonics Sonochemistry, 35*, 525-528.

Scott, S. A., Davey, M. P., Dennis, J. S., Horst, I., Howe, C. J., Lea-Smith, D. J., & Smith, A. G. (2010). Biodiesel from algae: Challenges and prospects. *Current Opinion in Biotechnology, 21*, 277-286.

Sharma, Y., Singh, B., & Upadhyay, S. (2008). Advancements in development and characterization of biodiesel: A review. *Fuel, 87*, 2355-2373.

Shay, E. G. (1993). Diesel fuel from vegetable oils: Status and opportunities. *Biomass and Bioenergy, 4*(4), 227-242.

Sheehan, J., Dunahay, T., Benemann, J., & Roessler, P. (1998). *A look back at the U.S. Department of Energy's aquatic species program: Biodiesel from algae.* USA: National Renewable Energy Laboratory (NREL/TP-580-24190).

Shenk, P. M., Thomas-Hall, S. R., Stephens, E., Marx, U. C., Mussgnug J. H., Posten, C., Kruse, O., Hankamer, B. (2008). Second generation biofuels: High-efficiency microalgae for biodiesel production. *BioEnergy Research, 1*(1), 20-43.

Shirazi, H. M., Karimi-Sabet, J., & Ghotbi, C. (2017). Biodiesel production from *Spirulina* microalgae feedstock using direct transesterification near supercritical methanol condition. *Bioresource Technology, 239*, 378-386.

Shubert, E. (2011). *Encyclopedia of Life*. Retrieved February 2017, from http://eol.org/pages/908262/details

Siaut, M., Cuinhu , S., Cagnon, C., Fessler, B., Nguyen, M., Carrier, P., Belyl, A., Beisson, F., Triantaphylides, C., Li-Beisson, Y. H., Peltier, G. (2011). Oil accumulation in the model green alga *Chlamydomonas reinhardtii*: Characterization, variability between

common laboratory strains and relationship with starch reserves. *BMC Biotechnology, 11*, 7.

Silitonga, A., Masjuki, H., Ong, H. C., Yusaf, T., Kusumo, F., & Mahlia, T. (2016). Synthesis and optimization of *Hevea brasiliensis* and *Ricinus communisas* feedstock for biodiesel production: A comparative study. *Industrial Crops and Products, 85*, 274-286.

Singh, D. K., & Mallick, N. (2014). Accumulation potential of lipids and analysis of fatty acid profile of few. *Journal of Microbiology and Biotechnology Research, 4*(1), 37-44.

Sinha, D., & Murugavelh, S. (2016). Biodiesel production from waste cottonseed oil using low cost catalyst: Engine performance and emission characteristics. *Perspectives in Science, 8*, 237-240.

Soares, A. T., da Costa, D. C., Silva, B. F., Lopes, R. G., Derner, R. B., & Filho, N. R. (2014). Comparative analysis of the fatty acid composition of microalgae obtained by different oil extraction methods and direct biomass transesterification. *BioEnergy Research, 7*(3), 1035-1044.

Solovchenko, A., Lukyanov, A., Solovchenko, O., Didi-Cohen, S., Boussiba, S., & Khozin-Goldberg, I. (2014). Interactive effects of salinity, high light, and nitrogen starvation on fatty acid and carotenoid profiles in *Nannochloropsis oceanica* CCALA 804. *European Journal of Lipid Science and Technology , 116*, 635-644.

Spolaore, P., Joannis-Cassan, C., Duran, E., & Isambert, A. (2006). Commercial applications of microalgae . *Journal of Bioscience and Bioengineering, 101*(10), 87-96.

Stansell, G. R., Sym, S. D., & Gray, V. (2012). Microalgal fatty acid composition: Implications for biodiesel quality. *Journal of Applied Phycology, 24*(4), 1-11.

Taher, H., Al-Zuhair, S., Al-Marzouqi, A. H., Haik, Y., & Farid, M. (2014). Effective extraction of microalgae lipids from wet biomass for biodiesel production. *Biomass and Bioenergy, 66*, 159-167.

Tong, D., Hu, C., Jiang, K., & Li, Y. (2010). Cetane number prediction of biodiesel from the composition of fatty acid methyl esters. *Journal of the American Oil Chemists' Society, 88*(3), 415-423.

Tsukahara, K., & Sawayama, S. (2005). Liquid fuel production using microalgae. *Journal of the Japan Petroleum Institute , 48*(5), 251-259.

Ullah, K., Ahmad, M., Sofia, Sharma, V. K., Lu, P., Harvey, A., . . . CN. (2014). Algal biomass as a global source of transport fuels: Overview. *Progress in Natural Science: Materials International*, 329-339.

Um, B. H., & Kim, Y. S. (2009). Review: A chance for Korea to advance algal-biodiesel technology. *Journal of Industrial and Engineering Chemistry, 15*, 1-7.

Uprety, B. K., Chaiwong, W., Ewelike, C., & Rakshit, S. K. (2016). Biodiesel production using heterogeneous catalysts including wood ash and the importance of enhancing byproduct glycerol purity. *Energy Conversion and Management, 115*, 191-199.

Verma, P., & Sharma, M. (2016). Comparative analysis of effect of methanol and ethanol on Karanja biodiesel production and its optimisation. *Fuel, 180*, 164-174.

Wahidin, S., Idris, A., & Shaleh, S. R. (2013). The influence of light intensity and photoperiod on the growth and lipid content of microalgae *Nannochloropsis* sp. *Bioresource Technology, 129*, 7-11.

Wang, B., Li, Y., Wu, N., & Lan, C. Q. (2008). CO_2 bio-mitigation using microalgae. *Applied Microbiology and Biotechnology, 79*(5), 707-718.

Wu, H., & Miao, X. (2014). Biodiesel quality and biochemical changes of microalgae *Chlorella pyrenoidosa* and *Scenedesmus obliquus* in response to nitrate levels. *Bioresource Technology, 170*, 421-427.

Wu, L. F., Chen, P. C., Huang, A. P., & Lee, C. M. (2012). The feasibility of biodiesel production by microalgae using industrial wastewater. *Bioresource Technology, 113*, 14-18.

Wu, L., Xu, L., & Hu, C. (2015). Screening and characterization of oleaginous microalgal species from Northern Xinjiang. *Journal of Microbiology and Biotechnology, 25*(6), 910-917.

Xia, L., Yang, H., He, Q., & Hu, C. (2015). Physiological responses of freshwater oleaginous microalgae *Desmodesmus* sp. NMX451 under nitrogen deficiency and alkaline pH-induced lipid accumulation. *Journal of Applied Phycology, 27*, 649-659.

Yang, H., He, Q., & Hu, C. (2015). Lipid accumulation by NaCl induction at different growth stages and concentrations in photoautotrophic two-step cultivation of *Monoraphidium dybowskii* LB50. *Bioresource Technology, 187*.

Yeo, I., Jeong, J., Cho, Y., Hong, J., Yoon, H. S., Kim, S. H., & Kim, S. (2011). Characterization and comparison of biodiesels made from Korean freshwater algae. *Bulletin- Korean Chemical Society, 32*(8), 2830-2832.

Yun, H. S., Ji, M. K., Park, Y. T., Salama, E. S., & Choi, J. (2016). Microalga, *Acutodesmus obliquus* KGE 30 as a potential candidate for CO_2 mitigation and biodiesel production. *Environmental Science and Pollution Research, 23*, 17831-17839.

Zeng, D., Yang, L., & Fang, T. (2017). Process optimization, kinetic and thermodynamic studies on biodiesel production by supercritical methanol transesterification with CH_3ONa. *Fuel, 203*, 739-748.

Zhang, Y., He, M., Zou, S., Fei, C., Yan, Y., Zheng, S., . . . Wang, C. (2016). Breeding of high biomass and lipid producing *Desmodesmus* sp. by ethylmethane sulfonate-induced mutation. *Bioresource Technology, 207*, 268-275.

Zhu, S., Wang, Y., Shang, C., Wang, Z., Xu, J., & Yuan, Z. (2015). Characterization of lipid and fatty acids composition of *Chlorella zofingiensis* in response to nitrogen starvation. *Journal of Bioscience and Bioengineering, 120*(2), 205-209.

APPENDICES

APPENDIX A: Algae cultivation

A.1. Beijerinck medium recipe

Optimized Beijerinck medium was prepared by mixing 100 ml of stock solution 1, 40 ml of stock solution 2, 60 ml of stock solution 3 and 1ml of micronutrients with 749 ml of distilled water in an Erlenmeyer flask. The stock solutions and micronutrients were composed as follows:

Stock solution 1	*Concentration*	*Units*
NH_4Cl	0.68	$g.L^{-1}$
KNO_3	2.23	$g.L^{-1}$
K_2HPO_4	0.2	$g.L^{-1}$
$MgSO_4.7H_2O$	0.2	$g.L^{-1}$
$CaCl_2.2H_2O$	0.1	$g.L^{-1}$
Stock solution 2		
KH_2PO_4	4.535	$g.L^{-1}$
Stock solution 3		
K_2HPO_4	5.535	$g.L^{-1}$
Micronutrients		
H_3BO_3	1.0	$g.100\ ml^{-1}$
$CuSO_4.5H_2O$	0.15	$g.100\ ml^{-1}$
EDTA	5.0	$g.100\ ml^{-1}$
$ZnSO_4.7H_2O$	2.2	$g.100\ ml^{-1}$
$MnCl_2.4H_2O$	0.5	$g.100\ ml^{-1}$
$FeSO_4\ .7H_2O$	0.5	$g.100\ ml^{-1}$
$CoCl_2.6H_2O$	0.15	$g.100\ ml^{-1}$
$(NH_4)_6Mo_7O_{24}.4H_2O$	0.10	$g.100\ ml^{-1}$

A.2. Calibration curves

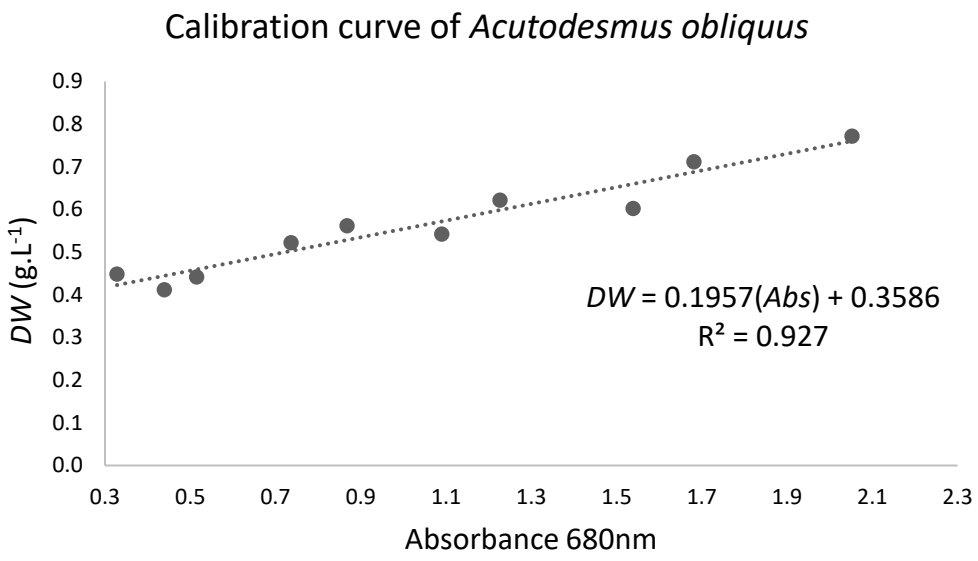


Figure A1. Calibration curve of absorbance (λ = 680 nm) and *AD* dry weight

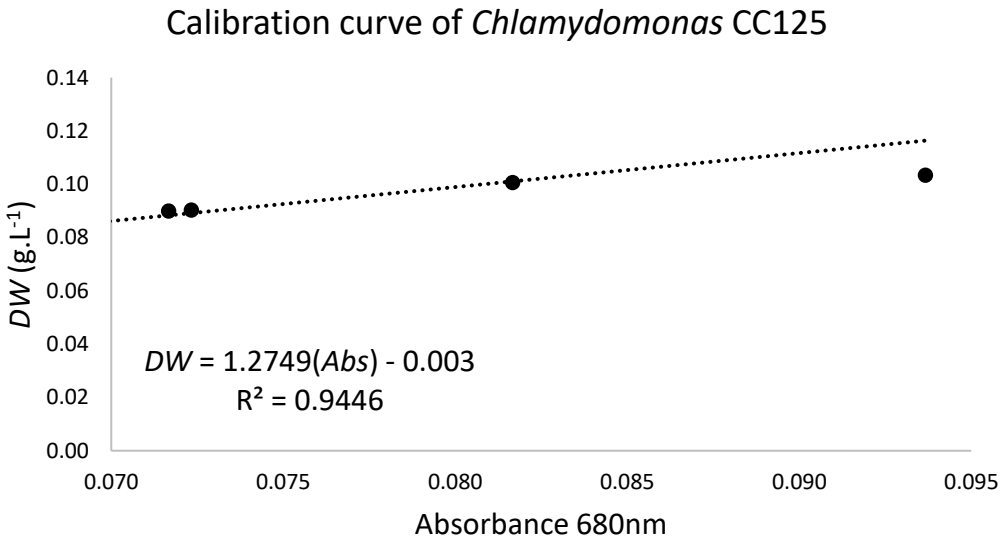


Figure A2. Calibration curve of absorbance (λ = 680 nm) and *CR* dry weight

APPENDIX B: GC-MS compound tables and chromatograms

These are all the compounds identified in all the cultivation conditions tested. The area total represents the percentage of identified compounds. The remaining percentage difference represents unidentified compounds (*i.e.* those that cannot be identified via GC-MS). This study was interested in FAMEs, and these are commonly identified via GC-MS technique (Botineştean, *et al*., 2012).

B.1. Condition 0 (I = 35; S = 150)

Table B1: Complete list of compounds identified in *A. obliquus*

Retention time (min)	Area (%)	Compound
2.026	1.28	Trichloromethane
2.258	56.87	Toluene
8.533	0.07	1-Dodecanol
10.216	0.11	1-Tetradecene
10.270	0.22	Tetradecene
	0.33	**Total Tetradecene**
10.990	0.19	Heptadecane
11.720	0.23	Heptadecane
12.576	0.08	Heptadecane
	0.50	**Total Heptadecane**
11.189	0.10	2,4-Di-*tert*-butylphenol
11.668	0.14	1-Pentadecanol
13.589	0.11	*n*-Nonadecanol-1
16.601	0.10	*n*-Tetracosanol-1
19.285	0.09	1-Heptacosanol
21.488	0.11	1-Heptacosanol
	0.20	**Total Heptacosanol**
22.496	0.90	Hexatriacontane
23.410	1.66	Hexatriacontane
24.394	1.23	Hexatriacontane
25.533	2.23	Hexatriacontane
	6.02	**Total Hexatriacontane**
25.992	1.92	Squalene
26.878	1.94	Triacontane, 1-iodo-
30.085	0.20	9,12-Octadecadienoic acid (Z,Z)-, methyl ester

Retention time (min)	Area (%)	Compound
30.155	1.37	9-Octadecenoic acid (Z)-, methyl ester
30.467	0.06	Methyl stearate
	Total: 71.21	

Table B2: Complete list of compounds identified in *Chlamydomonas*

Retention time (min)	Area (%)	Compound
2.030	0.94	1-Bromo-2,2-dichloro-ethane
2.388	66.19	Toluene
7.637	0.14	Dodecane
8.660	0.17	Dodecane
	0.31	**Total Dodecane**
8.588	0.08	1-Tetradecene
10.282	0.11	1-Tetradecene
	0.19	**Total Tetradecene**
9.538	0.21	Tridecane
10.339	0.17	Heptadecane (CAS)
11.227	0.17	Pentadecane (CAS)
12.278	0.12	1-Pentadecane (CAS)
	0.29	**Total Pentadecane**
15.993	0.16	Cetene
29.421	0.34	9,12-Octadecadienoic acid, methyl ester
30.282	0.40	9,11-Octadecadienoic acid, methyl ester, (E,E)-
	0.74	**Total Octadecadienoic acid methyl ester**
	Total: 69.20	

B.2. Condition 1 (I = 60; S = 250)

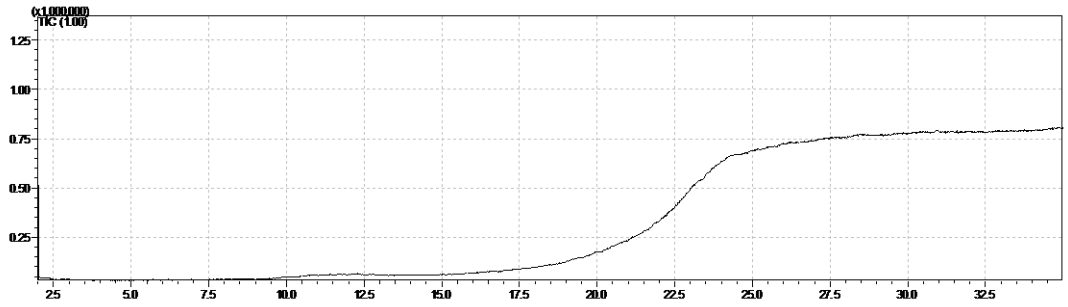


Figure B1. Chromatogram (Abundance vs Retention time) of *A. obliquus* under Condition 1

Table B3: Complete list of compounds identified in *A. obliquus*

Retention time (min)	Area (%)	Compound
2.192	0.08	2,5-Dimethyl-4-methoxyphenol
2.211	0.05	Benzene, 1,1'-(fluorocyclopropylidene)bis- (CAS)
25.404	14.33	Tetracosamethylcyclododecasiloxane
28.912	0.23	Cyclohexanamine, N-nitro-
28.935	0.18	1(2H)-Naphthalenone, 6-acetyloctahydro-8a-methyl-, (4a.alpha.,7.beta.,8a.beta.)- (CAS)
28.977	0.35	Silane, trimethyl[5-methyl-2-(1-methylethyl)phenoxy]- (CAS)
29.050	0.34	Trimer from Isobutyroylpyrazine
29.100	0.31	Hexadecanoic acid, 2-hydroxy-1,3-propanediyl ester (CAS)
29.140	0.82	Cyclododecanecarboxylic-acid-
29.184	0.38	Sclerediol
29.266	0.40	(-)-Isopulegol
29.361	0.41	1(2H)-Naphthalenone, 4-ethoxyoctahydro-8-methyl- (CAS)
29.470	0.32	Octadecanoic acid (CAS) (*added* as methyl stearate)
29.536	0.28	Quercetin 7,3',4'-trimethoxy
29.571	0.23	Tetradecanenitrile
29.849	0.69	[2H(4)]-Methyl 9-oxonona-5Z,7E-dienoate
29.938	0.27	Hexadecanoic acid, 2-hydroxy-1,3-propanediyl ester (CAS)
30.062	0.26	(1R*,2R*,3aR*)-2-Benzyltetrahydro-6',6'-dimethylspiro[cyclobutane-1,2'(3'H)-pyrrolo[1,2-b]isoxazole]
30.196	0.45	Adamantane-1-(3,3-dichloropropyn-1-yl)
30.308	0.18	3-Azabicyclo[3.3.1]nonane, 9.alpha.-methoxy-3-methyl- (CAS)
30.520	0.34	Octanoic acid (5-azepan-1-yl-furan-2-ylmethylene)-hydrazide
30.696	0.18	Octadecanoic acid, ethyl ester (CAS)
30.744	0.23	4-Fluorophenyl 4-(4-Propylcyclohexyl)cyclohexanecarboxylate
30.920	0.48	2,5-Dichloro-N-cyclohexylbenzenesulfonamide

Retention time (min)	Area (%)	Compound
30.959	0.24	9-Octadecenoic acid, (2-phenyl-1,3-dioxolan-4-yl)methyl ester, cis- (CAS)
31.187	1.14	Hexacontane
31.226	0.79	Hexacontane
	1.93	**Total Hexacontane**
31.274	0.25	Hexadecanoic acid (CAS) (*added* as methyl palmitate)
31.318	0.32	Selinane
31.355	0.19	11,13-Dihydroxy-tetradec-5-ynoic acid, methyl ester
31.397	0.20	9,12-Octadecadienoic acid (Z,Z)-, 2-[(trimethylsilyl)oxy]-1-[[(trimethylsilyl)oxy]methyl]ethyl ester (CAS)
31.503	0.29	Trimethylsilyl derivative of 2-Monoolein
31.577	0.85	6-Methoxy-4-[2-[(methoxymethyl)oxy]phenyl]-5-methyl-2-phenylpyridine-3-carboxylic Acid
31.599	0.16	d,l-Xylitol, 1-O-undec-10-enoyl-
31.787	0.52	Heneicosane, 11-cyclopentyl- (CAS)
31.831	0.21	Eicosanoic acid, 2-[(1-oxohexadecyl)oxy]-1-[[(1-oxohexadecyl)oxy]methyl]ethyl ester (CAS)
31.878	0.24	Ethyl cis-4-octenoate
31.959	0.29	Stearic acid, 2-hydroxy-1-methylpropyl ester (CAS)
32.081	0.13	Cyclopropaneoctanal, 2-octyl- (CAS)
32.105	0.18	Oxo - eicosa - triene
32.160	0.33	.alpha.-D-Xylofuranose, cyclic 1,2:3,5-bis(butylboronate) (CAS)
32.224	0.22	Mebutamate
32.266	0.15	9,10-Secocholesta-5,7,10(19)-triene-1,3-diol, 25-[(trimethylsilyl)oxy]-, (3.beta.,5Z,7E)- (CAS)
32.284	0.31	9-Octadecenoic acid (Z)-, ethyl ester
32.404	0.17	Ethanone, 1-[3-methyl-3-(4-methyl-3-pentenyl)oxiranyl]- (CAS)
32.449	0.16	Fructopyranose, 1,2:4,5-di-O-isopropylidene-, .alpha.-D- (CAS)
32.497	0.08	Decanal (CAS)
32.567	0.18	4,4-Dimethyl-2-(1-hydroxycyclohexyl)-2-penten-3-ol
32.615	0.10	Z5-Decenylacetate
32.636	0.11	5-Methyl-2-ethylamino-2-thiazoline
	Total: 29.60	

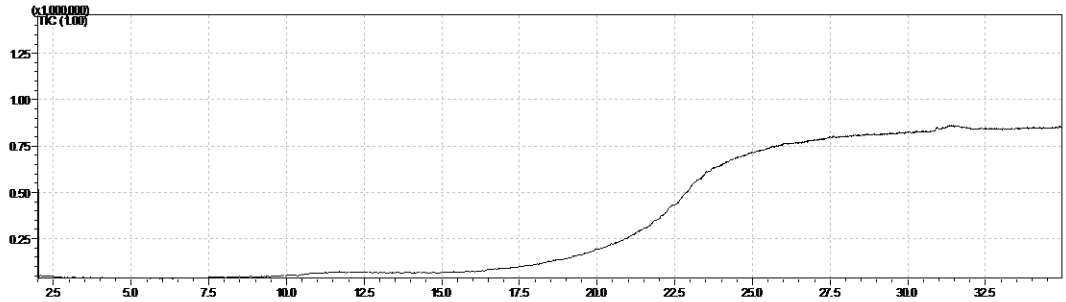


Figure B2. Chromatogram (Abundance vs Retention time) of *Chlamydomonas* under Condition 1

Table B4: Complete list of compounds identified in *Chlamydomonas*

Retention time (min)	Area (%)	Compound
2.145	0.10	5,6,8-Tri-o-acetyl-2,4,3,7-dianhydro-1-deoxy-2-2-C-methyl-D-glycero-D-ido-octitol
2.304	0.20	2-Chloro-9-oxabicyclo[3.3.1]nonane
10.325	0.41	Disulfide, diphenyl (CAS)
12.225	0.07	Cyclononasiloxane, octadecamethyl-
16.107	0.09	Tetrapentacontane
29.040	0.78	Tetrapentacontane
29.435	0.97	Tetrapentacontane
29.923	0.39	Tetrapentacontane
32.091	0.29	Tetrapentacontane
	2.52	**Total Tetrapentacontane**
28.906	0.42	6-methyl-8-deutero-pyrimido[5,4-e][1.2.4]triazine-5,7-dione
29.020	0.31	10-Methyl-2,5
29.103	0.20	2-Propen-1-ol, 3-(2,6,6-trimethyl-1-cyclohexen-1-yl)-(CAS)
30.987	0.40	Tetracosamethylcyclododecasiloxane
33.285	1.12	Tetracosamethylcyclododecasiloxane
	1.52	**Total Tetracosamethylcyclododecasiloxane**
31.488	0.13	2,6-Di-*tert*-butyloctahydroazulene-3a,8-diol
31.517	0.34	c18-Juvenile hormone
31.586	0.17	Tetradecane, 4-methyl- (CAS)
31.688	0.19	1-Naphthalenepropanol, .alpha.-ethenyldecahydro-4-hydroxy-.alpha.,5,5,8a-tetramethyl-2-methylene-, [1S-[1.alpha.(R*),4.beta.,4a
32.062	0.19	1-(1-Phenylthiocyclopropyl)-2,2-dimethyl-1-propanol
	Total: 6.77	

B.3. Condition 2 (I = 60; S = 100)

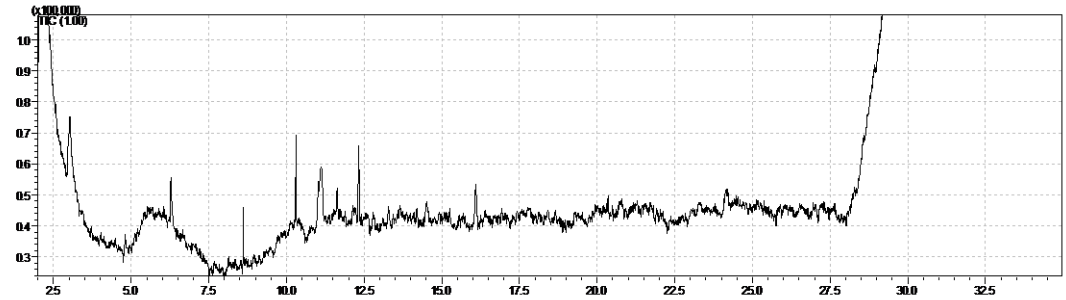


Figure B3. Chromatogram (Abundance vs Retention time) of *A. obliquus* under Condition 2

Table B5: Complete list of compounds identified in *A. obliquus*

Retention time (min)	Area (%)	Compound
2.031	0.76	1-Bromo-2,2-dichloro-ethane
8.578	0.05	1-Dodecene
10.303	0.13	1-Tetradecene
11.631	0.18	Phenol, 3,5-bis(1,1-dimethylethyl)
12.324	0.16	Cetene
16.089	0.09	Cetene
	0.25	**Total Cetene**
29.519	0.93	9,12-Octadecadienoic acid (Z,Z)-, methyl ester (CAS)
29.789	1.21	9,12-Octadecadienoic acid, methyl ester
30.344	2.45	9,11-Octadecadienoic acid, methyl ester, (E,E)-
30.660	3.85	9,12-Octadecadienoic acid, methyl ester
32.300	3.78	9,12-Octadecadienoic acid (Z,Z)-(CAS)
	12.22	**Total Octadecadienoic acid methyl ester**
30.857	2.63	Hexadecadienoic acid, methyl ester (CAS)
31.997	3.37	11,14-Eicosadienoic acid, methyl ester
	Total: 19.59	

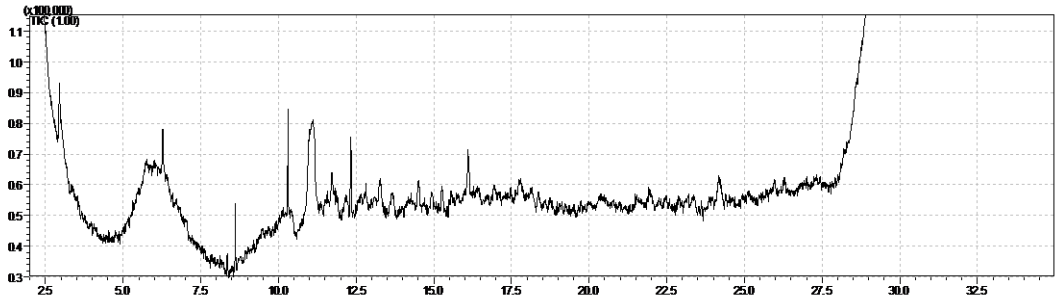


Figure B4. Chromatogram (Abundance vs Retention time) of *Chlamydomonas* under Condition 2

Table B6: Complete list of compounds identified in *Chlamydomonas*

Retention time (min)	Area (%)	Compound
2.029	0.29	Chloroform
10.308	0.06	1-Pentadecene
12.329	0.06	1-Hexadecene (CAS)
16.104	0.06	1-Hexadecene (CAS)
	0.12	**Total Hexadecene**
29.700	1.00	9,12-Octadecadienoic acid, methyl ester, (E,E)-
30.351	1.87	9,11-Octadecadienoic acid, methyl ester, (E,E)-
30.668	3.55	9,11-Octadecadienoic acid, methyl ester, (E,E)-(CAS)
31.245	23.61	9,12-Octadecadienoic acid, methyl ester, (Z,Z)-
	30.03	**Total Octadecadienoic acid methyl ester**
32.007	3.01	9,12-Octadecadien-1-ol, (Z,Z)-
33.085	1.51	Linolelaidic acid (*added* into methyl linolelaidate)
	Total: 34.67	

B.4. Condition 3 (I = 80; S = 250)

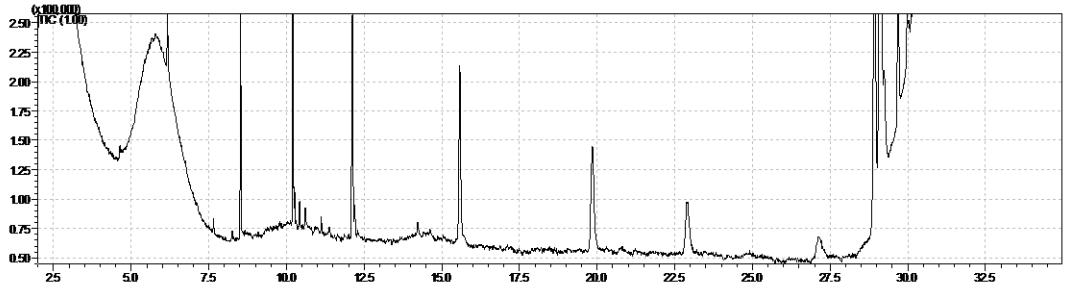


Figure B5. Chromatogram (Abundance vs Retention time) of *A. obliquus* under Condition 3

Table B7: Complete list of compounds identified in *A. obliquus*

Retention time (min)	Area (%)	Compound
2.033	4.54	Chloroform
2.311	21.02	Toluene
6.162	0.38	Cyclopropane, nonyl-
7.647	0.02	Nonanal (CAS)
8.517	0.18	1-Dodecanol
10.203	0.36	1-Pentadecene
10.260	0.14	Tetradecane (CAS)
10.415	0.16	10-Undecenoic acid, methyl ester
11.119	0.17	Pentadecane (CAS)
11.410	0.34	Phenol, 2,4-bis(1,1-dimethylethyl)-
12.114	0.45	1-Heptadecene
12.195	0.15	Heptadecane
14.203	0.49	1-Dodecanol, 3,7,11-trimethyl-
15.578	0.40	*n*-Nonadecanol-1
19.851	0.34	Hexadecanoic acid, methyl ester (CAS)
28.935	0.69	9,12-Octadecadienoic acid (Z,Z)-, methyl ester
31.102	5.38	9,12-Octadecadienoic acid (Z,Z)-
	6.07	**Total Octadecadienoic acid methyl ester**
29.121	1.48	9-Octadecenoic acid, methyl ester, (E)-

Retention time (min)	Area (%)	Compound
29.687	0.58	Octadecanoic acid, methyl ester
30.256	9.65	9-Octadecen-1-ol, (Z)-
30.574	2.07	Octacosanol
31.682	3.13	Stigmasta-5,22-dien-3-ol, acetate, (3.beta.,22Z)- (CAS)
32.664	2.08	9-Hexacosene
	Total: 54.20	

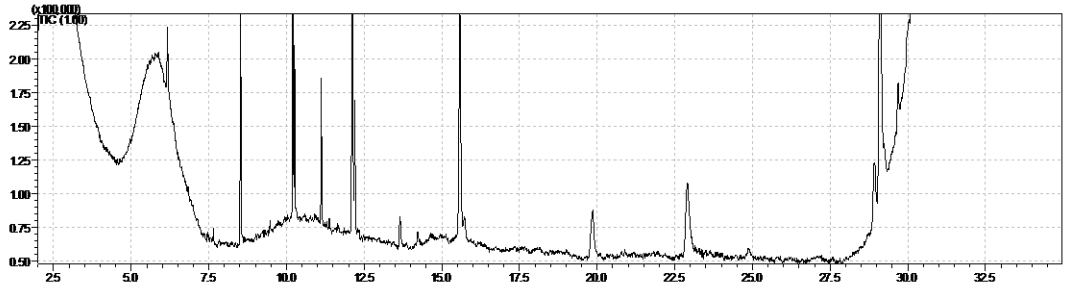


Figure B6. Chromatogram (Abundance vs Retention time) of *Chlamydomonas* under Condition 3

Table B8: Complete list of compounds identified in *Chlamydomonas*

Retention time (min)	Area (%)	Compound
2.028	5.89	Chloroform
2.305	11.97	Toluene
6.162	0.35	1-Decene
7.648	0.03	Nonanal (CAS)
8.518	0.21	1-Dodecanol
10.204	0.39	1-Pentadecene
10.260	0.28	Tetradecane (CAS)
11.119	0.21	Pentadecane (CAS)
12.116	0.48	*n*-Heptadecanol-1
12.195	0.18	Heptadecane
13.654	0.12	Heptadecane
	0.30	**Total Heptadecane**
14.203	0.41	1-Dodecanol, 3,7,11-trimethyl-
15.581	0.41	*n*-Nonadecanol-1

Retention time (min)	Area (%)	Compound
19.865	0.17	Hexadecanoic acid, methyl ester (CAS)
28.942	0.36	9,12-Octadecadienoic acid (Z,Z)-, methyl ester
31.182	13.62	9,12-Octadecadienoic acid (Z,Z)-, methyl ester
	13.98	**Total Octadecadienoic acid methyl ester**
29.111	1.34	9-Octadecenoic acid, methyl ester, (E)-
31.878	2.53	9-Octadecenoic acid, 12-hydroxy-, methyl ester, (Z)-
	3.87	**Total Octadecenoic acid methyl ester**
29.698	0.72	Methyl stearate
30.753	9.16	Linoleic acid, ethyl ester
32.663	3.34	1-Heptacosanol
	Total: 52.17	

B.5. Condition 4 (I = 80; S = 100)

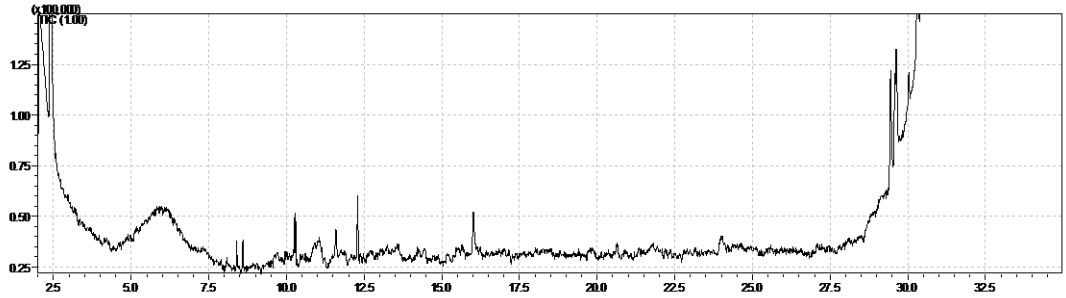


Figure B7. Chromatogram (Abundance vs Retention time) of *A. obliquus* under Condition 4

Table B9: Complete list of compounds identified in *A. obliquus*

Retention time (min)	Area (%)	Compound
2.031	1.57	1-Bromo-2,2-dichloro-ethane
2.383	32.50	Toluene
8.595	0.07	1-Dodecene
10.289	0.11	1-Tetradecene

Retention time (min)	Area (%)	Compound
11.585	0.12	Phenol, 3,5-bis(1,1-dimethylethyl)- (CAS)
12.294	0.15	1-Hexadecene (CAS)
16.020	0.17	1-Nonadecene
29.453	0.47	9,12-Octadecadienoic acid, methyl ester, (E,E)-
30.300	0.73	9,11-Octadecadienoic acid, methyl ester, (E,E)-
	1.20	**Total Octadecadienoic acid methyl ester**
29.582	0.43	10-Octadecenoic acid, methyl ester
30.034	0.65	Octadecanoic acid, methyl ester (CAS)
30.812	1.85	Oxirane, tetradecyl-
31.178	13.45	Linoelaidic acid (*added* into methyl linolelaidate)
	Total: 52.27	

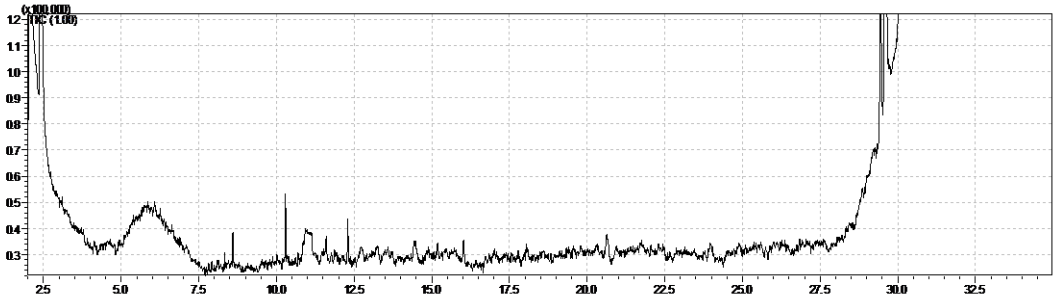


Figure B8. Chromatogram (Abundance vs Retention time) of *Chlamydomonas* under Condition 4

Table B10: Complete list of compounds identified in *Chlamydomonas*

Retention time (min)	Area (%)	Compound
2.031	0.80	1-Bromo-2,2-dichloro-ethane
2.388	22.90	Toluene
8.335	0.06	2-Nonenal, (E)-
8.594	0.08	1-Dodecene
10.289	0.12	1-Pentadecene
12.292	0.09	1-Hexadecene (CAS)
16.027	0.10	Cetene

Retention time (min)	Area (%)	Compound
29.450	0.56	9,12-Octadecadienoic acid, methyl ester, (E,E)- (CAS)
29.632	0.58	9,12-Octadecadienoic acid (Z,Z)-, methyl ester (CAS)
30.300	1.32	9,11-Octadecadienoic acid, methyl ester, (E,E)-
30.617	1.54	9,11-Octadecadienoic acid, methyl ester, (E,E)- (CAS)
	4.00	**Total Octadecadienoic acid methyl ester**
29.587	0.69	9-Octadecenoic acid, methyl ester, (E)-
30.036	0.60	Octadecanoic acid, methyl ester (CAS)
31.125	6.75	Linolelaidic acid (*added* into methyl linolelaidate)
	Total: 36.19	

B.6. Waste cooking oil

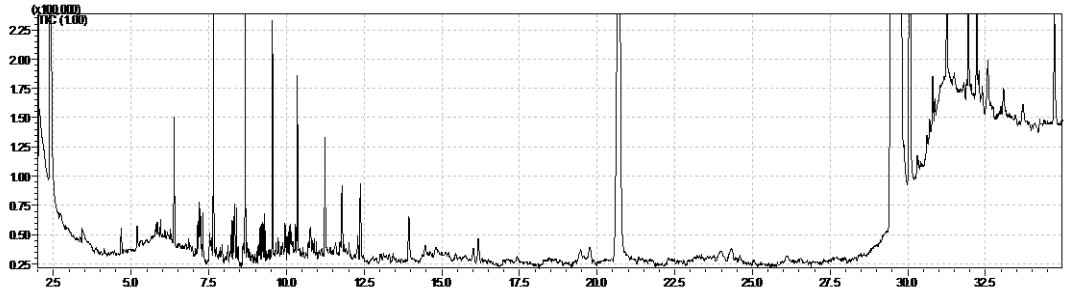


Figure B9. Chromatogram (Abundance vs Retention time) of waste cooking oil – which underwent the same transesterification procedure as algae oil (Section *3.6.3.*)

Table B11: Complete list of compounds identified in waste cooking oil

Retention time (min)	Area (%)	Compound
2.031	0.59	1-Bromo-2,2-dichloro-ethane
2.389	23.30	Toluene
8.617	0.08	1-Dodecene
10.288	0.08	1-Tetradecene
11.788	0.26	Nonanedioic acid, dimethyl ester (CAS)
12.297	0.11	1-Hexadecene (CAS)

Retention time (min)	Area (%)	Compound
12.401	0.14	Dodecanal dimethylacetal
16.023	0.10	1-Nonadecene
20.683	2.41	Hexadecanoic acid, methyl ester (CAS)
29.521	19.00	9,12-Octadecadienoic acid, methyl ester, (E,E)-
30.297	0.72	9,11-Octadecadienoic acid, methyl ester, (E,E)-
30.613	1.09	9,11-Octadecadienoic acid, methyl ester, (E,E)-
	20.81	**Total Octadecadienoic acid methyl ester**
29.656	22.68	9-Octadecenoic acid (Z)-, methyl ester (CAS)
30.050	2.50	Octadecanoic acid, methyl ester (CAS)
30.806	1.32	Hexadecadienoic acid, methyl ester (CAS)
31.954	1.80	9,12-Octadecadienoyl chloride, (Z,Z)-
32.232	1.36	Eicosanoic acid, methyl ester
34.732	0.27	Docosanoic acid, methyl ester
	Total: 77.81	

APPENDIX C: Calculations

C.1. Effects of cultivation on algae lipid yield

The effect of light intensity (e_I), agitation speed (e_S), and the synergistic effect (e_{IS}) of both these parameters on the quantity of lipid content ($\%LC$) were calculated using Eq. (C.1.), (C.2.), and (C.3.) below derived by Myers *et al*. (2009) for a 2^k factorial experimental design.

The effect of light intensity:

$$\boldsymbol{e_I = \frac{1}{2} n\,(i \times s + i - s - 1)} \qquad \text{(C.1.)}$$

The effect of agitation speed:

$$\boldsymbol{e_S = \frac{1}{2} n\,(i \times s + s - i - 1)} \qquad \text{(C.2.)}$$

The synergistic effect of both light and agitation:

$$\boldsymbol{e_{IS} = \frac{1}{2} n\,(i \times s + 1 - i - s)} \qquad \text{(C.3.)}$$

Where:

n = number of replicates in each condition

s = total sum of the lipid content (%LC) of replicates under Condition 1

1 = total sum of the lipid content (%LC) of replicates under Condition 2

i x s = total sum of the lipid content (%LC) of replicates under Condition 3

i = total sum of the lipid content (%LC) of replicates under Condition 4

The total sum values (s, 1, i x s & i) required by the equations shown above are tabulated below (Table C1).

Table C1: Total sum values for calculation of the effect of algae cultivation on lipid yield

	%LC				
				Total	
Condition	**Replicate 1**	**Replicate 2**	**Replicate 3**	**Symbol**	**Value (%)**
1	86.2	89.2	87.4	*s*	262.8
2	91.1	92.0	91.3	*1*	274.4
3	87.8	87.7	78.0	*i* x *s*	253.5
4	87.3	78.8	88.4	*i*	254.4

C.2. Cetane number and viscosity of biodiesel

The cetane number (CN_i) and viscosity (V_i) of each individual FAME identified were used to calculate the cetane number (CN_m) and viscosity (V_m) of the overall biodiesel. All CN_i and V_i values were obtained or averaged from Bamgboye and Hansen (2008) and Knothe and Steidley (2005) respectively, and are shown below (Table C2).

Table C2: Cetane number and viscosity values of individual FAME molecules identified

FAME	Cetane number (CN_i)	Viscosity (V_i); 40°C mm^2s^{-1}
Methyl behenate	125	7.33
Methyl arachidate	112	7.2097
Methyl stearate	101	5.85
Methyl palmitate	85.9	4.38
11,13-Dihydroxy-tetradec-5-ynoic acid, methyl ester	72	2.73
Dimethyl azelate	61.4	2.43
Methyl elaidate	57.15	5.86
Methyl oleate	56.66	4.51
9-Octadecenoic acid, (2-phenyl-1,3-dioxolan-4-yl)methyl ester, *cis*-	56.66	4.51
Methyl 10-octadecenoate	53.9	5.41
Methyl 11,14-eicosadienoate	49	5.77
Methyl 10-undecenoate	47.9	1.71
Methyl linolelaidate	43	3.65
Methyl linoleate	38.2	3.65
Methyl isolinoleate	38.2	5.33
Methyl ricinoleate	37.38	15.44
[2H(4)]-Methyl 9-oxonona-5Z,7E-dienoate	33.6	1.44
Hexadecadienoic acid, methyl ester	32	3.67
Methyl 9,12-octadecadienoate	40.6	4.49

C.3. Carbon mass analysis

The carbon conversions stipulated in Figure 15 were calculated using the Principle of Mass Conservation (Eq. (C.4.)):

$$\sum \boldsymbol{M_{carbon\ input}} = \sum \boldsymbol{M_{carbon\ output}} \qquad \text{(C.4.)}$$

Where:

$M_{carbon\ input}$ = mass of carbon coming into the overall process (g)

$M_{carbon\ output}$ = mass of carbon going out of the overall process (g)

The mass% of carbon in each compound was determined from the quotient of the molecular weight (*MW*) of carbon and that of the compound, as in Eq. (C.5.) below:

$$\%\boldsymbol{M_{carbon}} = \frac{\boldsymbol{MW_{carbon}}}{\boldsymbol{MW_{compound}}} \times \mathbf{100} \qquad \text{(C.5.)}$$

Where:

$\%M_{carbon}$ = mass% of carbon in the whole compound

MW_{carbon} = molecular weight of carbon ($g.mol^{-1}$)

$MW_{compound}$ = molecular weight of the whole carbon compound ($g.mol^{-1}$)

The mass% of any other element or compound was determined using the same principle as Eq. (C.5.).